UNIVERSITY OF BARCELONA

Faculty of Medicine

Department of Physiological Sciences I

TIME COURSE OF BIOCHEMICAL, BIOMECHANICAL AND HISTOLOGICAL CHANGES FOR THE ASSESSMENT OF INFLAMMATION AND REMODELLING IN A BLEOMYCIN-INDUCED MURINE MODEL OF LUNG INJURY

DISSERTATION

submitted in partial fulfilment of the requirements for the degree of

DOCTOR OF PHILOSOPHY

by

Mariona Pinart Gilberga

Supervisors: Dr. Pablo V. Romero Colomer (Bellvitge Hospital)

Dr. Patricia Rieken Macedo Rocco (Federal University of Rio de Janeiro)

Tutor: Dr. Daniel Navajas

"Biopathology in medicine" doctorate program (2004-2006)

The author of this thesis has been supported by grants from:

- Fundació August Pi i Sunyer - Red RESPIRA (03/RED-020), Spain (Year 2004);

- Institut d'Investigacions Biomèdiques de Bellvitge (06/IDB-001) during the years 2005-2007.

The studies have been funded by:

- Red Respira (ISCiii RTIC 03/011), Spain (Year 2004);

- Fondo de Investigaciones Sanitarias (FISS) grant PI 04/0671, Ministerio de Sanidad, Spain (Year 2004);

- Centres of Excellence Program (PRONEX-FAPERJ), Brazilian Council for Scientific and Technological Development (CNPq), Carlos Chagas Filho, Rio de Janeiro State Research Supporting Foundation (FAPERJ), Brazil (Year 2005).

"Quando o homem aprender a respeitar o menor ser da Criação, seja animal ou vegetal, ninguém precisará ensiná-lo a amar seu semelhante"

Albert Schurveitzer

To the people I love

INDEX

ABBREVIATIONS

η	hysteresivity
Ψ	Young elastic modulus
AECs	alveolar epithelial cells
ARDS	acute respiratory distress syndrome
AT-1	type-1 pneumocytes cells
AT-2	type-2 pneumocytes cells
BAL	bronchoalveolar lavage
BLM	bleomycin
E	elastance
ECM	extracellular matrix
EGF	epidermal growth factor
EMT	epithelial-mesenchymal transition
FGF	fibroblast growth factor
G	tissue damping
H	elastic modulus
HP	hidroxyproline
i.p	intraperitoneal
i.v	intravenous
IL	interleukins
IIP	idiopathic interstitial pneumonias
IPF	idiopathic pulmonary fibrosis
LI	lung index
MMPs	matrix metalloproteinases
MPO	myeloperoxidase
NGF	nerve growth factor
PARP	poly-(ADP-ribose) polymerase
PDGF	platelet-derived growth factor
PF	pulmonary fibrosis
PGE	prostaglandin
PMN	polymorphonuclear leukocytes
R	resistance
RD	repeat dose
RNS	reactive nitrogen species

ROS	reactive oxygen species
s.c	subcutaneous
SD	single dose
TGF	transforming growth factor
TIMPs	tissue inhibitors of metalloproteinases
TNF	tumor necrosis factor
UIP	usual interstitial pneumonia
Z	lung impedance

I. INTRODUCTION

I.1. MECHANISMS OF LUNG TISSUE REPAIR: SEQUENCE OF EVENTS OCCURING DURING WOUND HEALING

The epithelial surface of the alveoli is composed of alveolar epithelial cells (AECs) such as: type I and type II cells. Type 1 cells comprise more than 90% of the alveolar surface area. These cells cells are extremely thin, thus, minimizing diffusion distance between the alveolar air space and pulmonary capillary blood. Type 2 cells, morphologically appearing as large rounded cells, are distributed in the corners of alveoli and are in close proximity to mesenchymal cells lying beneath them. They are multifunctional cells that synthesize and secrete pulmonary surfactant, serve as progenitor cells for type 1 pneumocytes and participate in the effector phase of the immune response by producing molecules involved in innate host defense. In normal human lungs there are numerous contacts between AECs and lung fibroblasts. These contacts occur at holes in the epithelial basal lamina that seem to be highly organised to maintain communication (**Sirianni et al., 2003**).

Alveolar epithelial damage is an important initial event in pulmonary fibrosis (PF). Epithelial cell damage and cell death during alveolitis induce the formation of gaps in the epithelial basement membranes. The migration of fibroblasts through these gaps into the alveolar space may lead to intra-alveolar fibrosis (**Kuwano et al., 2004**) even though, when the degree of lung injury is mild, damaged tissue will normally be repaired (**Kuwano et al., 2004**).

Wound healing is a complex and dynamic process that comprises an ordered sequence of inflammatory reactions, matrix deposition and resolution. Physiologically, there is a balance between matrix formation and degradation. This balance is impaired in fibrosis. Thus, in pulmonary fibrotic diseases, fibroblast proliferation, matrix synthesis and accumulation continue, thereby resulting in progressive destruction of the normal lung parenchyma, and eventual impairment of normal pulmonary functions. In pulmonary fibrosis, matrix synthesis often continues despite the apparent resolution of initial triggering and/or inflammatory events (Fig. 1).

Wound healing is a consequence of complex interactions among the fibroblasts, cytokines/growth factors, proteases and extracellular matrix (ECM) proteins. It is the persistent activation of genes encoding for matrix proteins that distinguishes controlled wound repair from uncontrolled connective tissue deposition, leading to pathological

fibrosis. Epidermal growth factor (EGF) is mitogenic for epithelial cells and fibroblasts (**Marikovsky et al., 1993**), while platelet-derived growth factor (PDGF) plays a key regulatory role in the proliferation and migration of fibroblasts and myofibroblasts during wound healing (**Seppa et al., 1982**). Fibroblast growth factor (FGF) and vascular endothelial growth factor (VEGF) control endothelial cell function during angiogenesis (**Nissen et al., 1998; Tonnesen et al., 2000**), and transforming growth factor-β (TGF-β) regulates matrix turnover (**Takehara et al., 2000**), thus contributing to the healing process. During wound healing there is rapid synthesis and degradation of connective tissue proteins, a process often referred to as *remodelling*. The stimulation of collagen synthesis exceeds that of extracellular collagen degradation so that the total amount of collagen continues to increase during this phase of scar formation. The final process in normal wound healing is *resolution* of the scar.

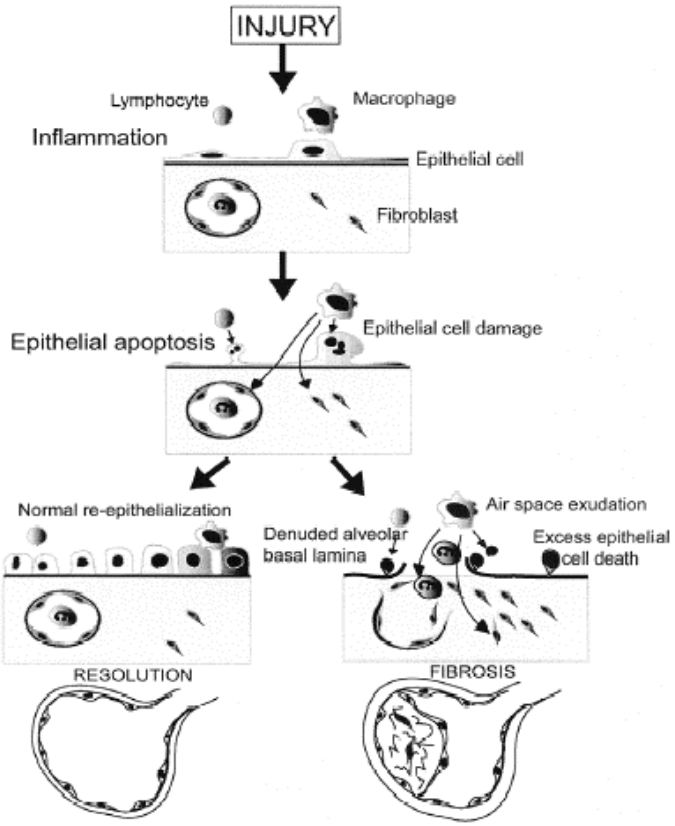

Figure 1. Epithelial cell death and an imbalance between pro- and anti-apoptotic factors may participate in the pathogenesis of PF (**Kuwano et al., 2004**).

The excessive accumulation of matrix proteins, mainly produced by fibroblasts and myofibroblasts, is responsible for the derangement of alveolar walls, loss of elasticity

and development of rigid lung. The progression of pulmonary fibrosis results in the widening of interstitial matrix, eventual compressions and destruction of normal lung parenchyma, with resultant damage to the capillaries leading to ventilatory insufficiency. The process and progression of pulmonary fibrosis can be broadly divided into three phases (Fig. 2) and/or events (**Razzaque and Taguchi, 2003**):

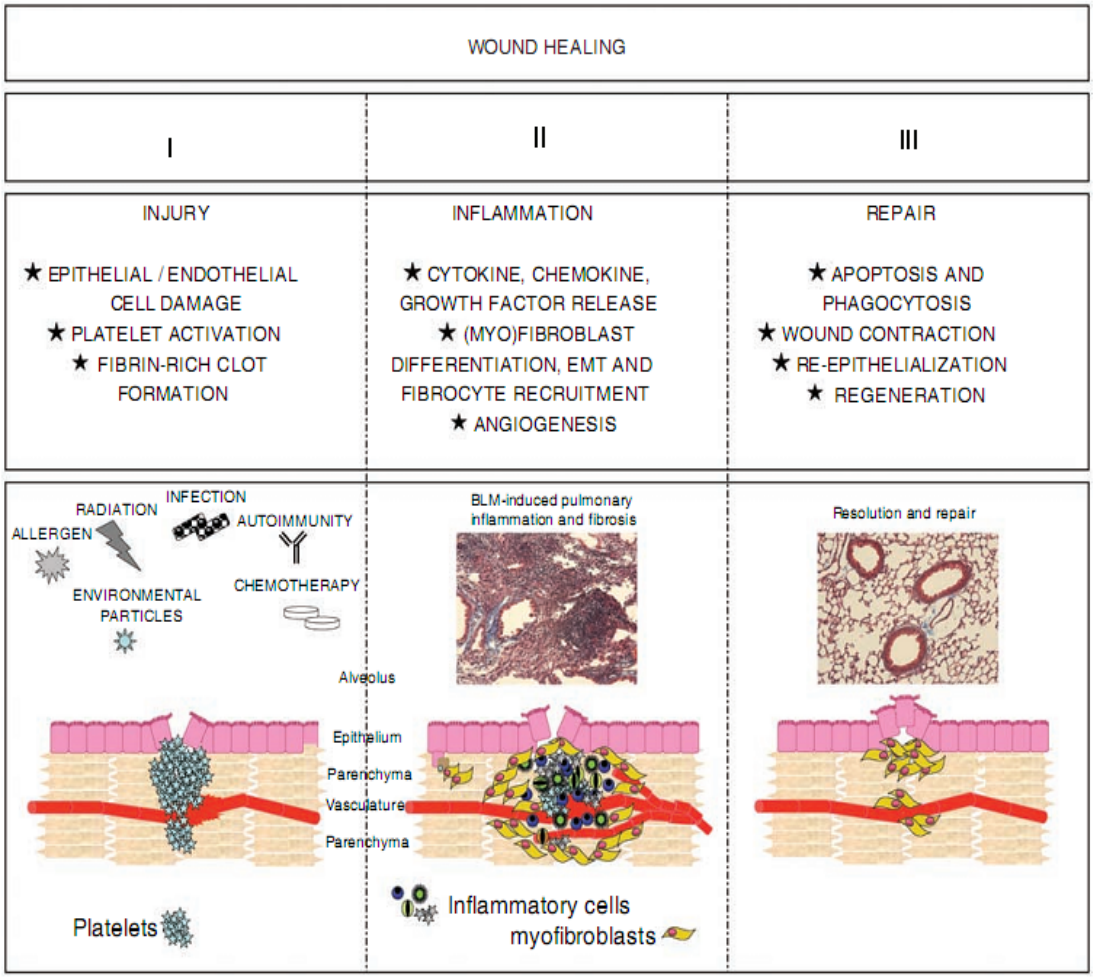

Figure 2. Representative view of phases of injury and wound healing with successful response (**Wilson and Wynn, 2009**).

I.1.1. Injury: initial triggering events

Pulmonary fibrosis is triggered by diverse known and yet to be identified factors, including drugs and exposure to inorganic dusts or radiation. However, not all exposed individuals develop fibrosis, which may suggest a genetic predisposition (**Lympany and du Bois, 1997**). In addition, whether the response of resident cells to exogenous stimuli differ in various forms of interstitial pneumonias, for example, the recruitment of

inflammatory cells and subsequent inflammatory responses, might help us to understand the variability in the prognosis of various forms of interstitial pneumonias. The nature of the initial insult to the lung is not always known. A number of causative agents, factors or disorders that are known to cause interstitial lung diseases might act as initial triggering factors for the activation or injury of alveolar epithelial cells, leading to inflammatory reactions in the interstitium. The induction of various mitogenic and fibrogenic factors by inflammatory cells and resident cells acts on interstitial cells causing their proliferation, differentiation and production of collagen or scar tissue in response to this damage.

Epithelial cells have been demonstrated to release chemotactic factors and, along with macrophages, control the type of inflammatory cell influx into the lung. Thus, AECs have emerged as a key site of initial injury as well as a major determinant of repair. The mechanisms of AEC apoptosis in patients developing Acute Respiratory Distress Syndrome (ARDS) or Usual Interstitial Pneumonia (UIP) are still unclear, but recent evidence suggests the role of the extrinsic Fas/Fas ligand pathway (**Wang et al., 1999; Albertine et al., 2002; Kuwano et al., 2002**). The implication that AEC apoptosis in an early event is an important concept since it can explain the breakdown of barrier function. Moreover, the activation of the Fas signaling cascade culminating in apoptosis can also lead to the release of pro-inflammatory mediators, which in turn, result in inflammation (**Chen et al., 1998**). IL-8 expression and neutrophilic inflammation occur as a consequence of Fas activation in macrophages (**Park et al., 2003**). Apoptosis or programmed cell death, inflammation, and matrix remodelling in the lung appear intricately linked.

Apoptotic cells undergo well ordered morphologic and molecular alterations, including cytoskeletal rearrangement, nuclear membrane collapse, chromatin condensation, DNA fragmentation, cell shrinkage, plasma membrane blebbing, and formation of apoptotic bodies (**Lu et al., 2005**). Conversely, necrotic cells swell and lyse, thereby releasing intracellular contents into the interstitium, which lead to an inflammatory response (**Lu et al., 2005**). Apoptosis is important in developmental biology, in remodelling of tissues during repair, as well as in the progression of some diseases. Polymorphonuclear leukocytes (PMN) undergo apoptosis and are phagocyted by macrophages phagocytose apoptotic. It has been suggested that enhanced PMN apoptosis may overt inflammation (**Savill et al., 1992**) and also that the lack of PMN apoptosis may prolong inflammatory responses and predispose the patients to ARDS after acute lung injury (**Matute-Bello et al., 1997**). Epithelial apoptosis and necrosis

are increased in lungs of patients with idiopathic pulmonary fibrosis (IPF). Apoptosis has been thought to be a non-inflammatory means of removing injurious cells thus facilitating lung repair. However, there is increasing evidence that Fas/Fas L-mediated lung epithelial apoptosis induces release of proinflammatory cytokines (i.e. TNF-α and TGF-β1), leading to inflammation and progression from ARDS to fibrosis (**Chapman et al., 1999**).

I.1.2. Inflammatory events

The lung has evolved intricate defense systems to preserve homeostasis and protect itself from injury. The first line of defense against microbial pathogens and pollutants is the innate immune response, which, in turn, is highly effective. The innate immune system of the lung is diverse and includes structural cells such as epithelial cells and fibroblasts as well as itinerant leukocytes as: neutrophils, monocytes, and macrophages. Dendritic cells and mast cells, although of hematopoietic origin, are resident in the lung and help sense and orchestrate immune responses in the lung. Cells of the innate immune system secrete various soluble factors that are directly or indirectly microbicidal and/or modulate the inflammatory response. Among these soluble factors, proteinases and anti-proteinases factor prominently and exert both physiological and pathological effects on the function of diverse cell types in the lung (**Suzuki et al., 2008**).

As above mentioned, the triggering events are usually followed by inflammatory events where damaged alveolar epithelial cells and other resident cells release inflammatory mediators to promote the recruitment of inflammatory cells (Fig. 3a). Extravasations of blood components lead to haemostasis, with platelet aggregation and clot formation. Within minutes of injury, surrounding blood vessels constrict, reducing the extent of haemorrhage. Therefore, agents released from activated platelets cause vasodilatation and increased permeability of nearby blood vessels. Stimulation of the clotting cascade results in the cleavage of fibrinogen by thrombin to form a fibrin plug, which associated with fibronectin, holds damaged tissues together and provides a provisional matrix for the recruitment of inflammatory cells. Agents from blood and injured or dead parenchymal cells induce inflammatory cells to adhere to blood vessel walls and pass between endothelial cells lining these vessels towards the site of injury by chemotaxis (**Mutsaers et al., 1997**).

Accumulation of neutrophils, eosinophils, lymphocytes, mast cells, monocytes and alveolar macrophages is a consistent histological feature of the early stage of various pulmonary fibrotic diseases. Neutrophils are the most abundant cells in the early stages of healing. As they degranulate and die, macrophages predominate. If the macrophage infiltration is prevented, healing is impaired. They act in concert with neutrophils to phagocyte debris and invading pathogenic microorganisms. Moreover, macrophages secrete PDGF, and TGF-β1 can directly activate fibroblasts and myofibroblasts to produce various matrix proteins (**Khalil et al., 1989; Nagaoka et al., 1990**). Increased accumulation and local proliferation of macrophages are important events during chronic inflammation and PF (Fig. 3b). Increased numbers of both $CD4^+$ and $CD8^+$ T cells have been detected in diseases associated with PF (**Gruber et al., 1996**), and counts of T-cell subpopulations are good predictors of outcome of PF (**Fireman et al., 1998**).

Interleukine (IL-4) is known to activate mononuclear cells as well as fibroblasts, and has a stimulatory effect on collagen synthesis, which is important in the pathogenesis of PF as demonstrated in a murine model of bleomycin-induced PF in which IL-4-expressing cells were identified as mononuclear cells and macrophages localized to areas of active fibrosis by *in situ* hybridisation and inmunohistochemistry (**Gharaee-Kermani et al., 2001**). Furthermore, IL-4 may play an important role in PF by amplifying the inflammatory responses and by stimulating collagen synthesis in fibroblasts, thereby contributing to the progression of fibrosis and end-stage lung disease. Therefore, the release of certain chemokines, monocyte chemotractant protein-1, cytokines (IL-1, IL-4 and IL-8), and growth factors (PDGF, TGF-β1 and TNF-α) by inflammatory cells and activated resident cells could intensify both the inflammatory and fibrotic events in the lung (**Gutiérrez-Ruíz et al., 2002; Gharaee-Kermani and Phan, 2005; Laurent et al., 2007**).

In addition, reactive oxygen species (ROS) play an important role in the pathogenesis of PF as the anti-oxidant defense system is thought to be impaired during fibrogenesis. Alveolar macrophages isolated from patients with PF and experimental fibrotic models generate ROS. Furthermore, recent studies suggest that structural cells of lung, in particular activated myofibroblasts, produce significant concentrations of extracellular ROS that are sufficient to induce injury/apoptosis of adjacent epithelial cells (**Waghray et al., 2005**). ROS have also been implicated in mediating fibroblast proliferation (**Murrell et al., 1990**). Also high levels of myeloperoxidase and low levels of glutathione, an important antioxidant, have been detected in the alveolar epithelial

lining fluid patients with IPF (**Cantin et al., 1987a; Cantin et al., 1987b**), suggesting the role of oxidant-mediated injury in PF.

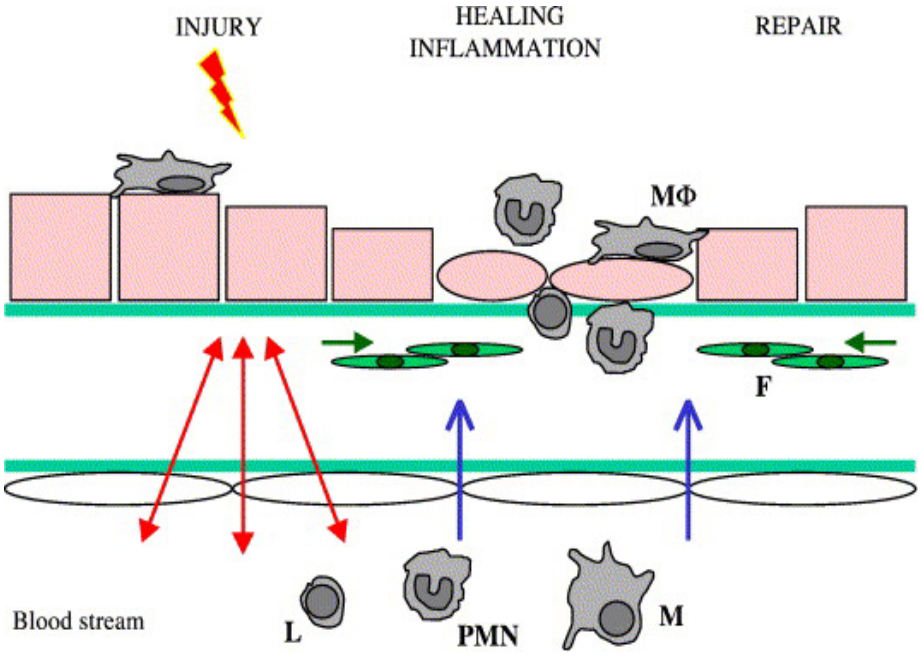

Figure 3a) Representative view of the sequence of events occurring from cell damage to tissue repair. Following injury, cytokines and chemokines are released from blood, injured tissues, or parenchymal cells (red arrowheads). This production rapidly stimulates leukocyte extravasations and migration into tissues (blue arrows). The first blood cell members to appear are PMNs (the most abundant are neutrophils), followed by monocytes (M) that differentiate into macrophages (MΦ). Finally, the immune response is completed with the immigration of lymphocytes (L). The production of cytokines and of a variety of growth factors also triggers the migration of resident cells and fibroblasts (F) to restore tissue integrity (**Chanson et al., 2005**).

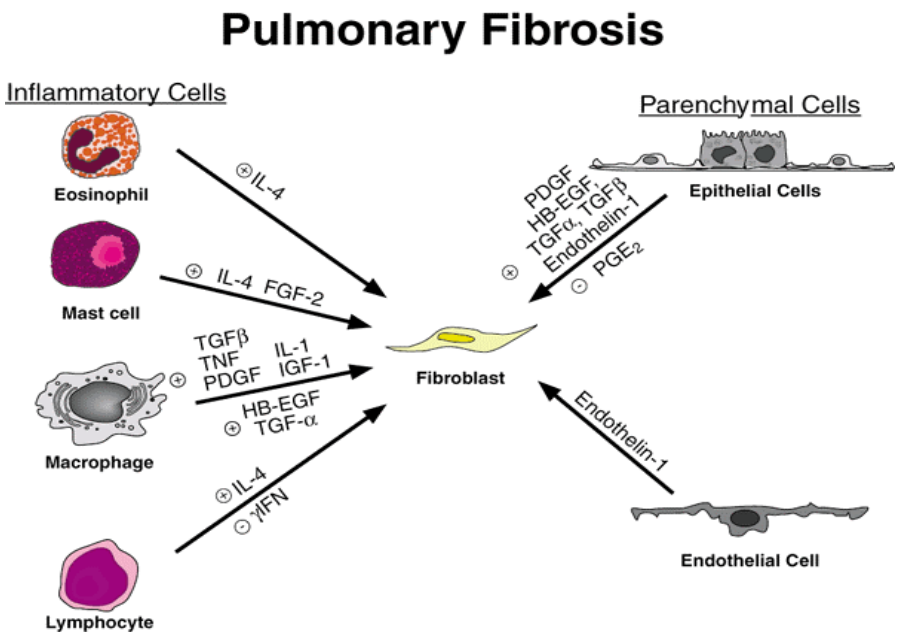

Figure 3b) Inflammatory events in the development of PF. Pathogenesis of PF. Abbreviations: IL-4 (interleukin-4); FGF-2 (fibroblast growth factor-2); TGF-β (transforming growth factor-beta); TNF-α (tumor necrosis factor-alpha); PDGF (platelet-derived growth factor); IL-1 (interleukin-1); IGF-1 (insulin-like growth factor-1); HB-EGF (heparin binding epidermal-like growth factor); γIFN (gamma interferon); PGE2 (prostaglandin E2) (**Mason et al., 1999**).

I.1.3. Reparative processes: remodelling and resolution/fibrosis

After injury, the alveolar epithelium must initiate a wound healing process to restore its barrier integrity. One important step is the rapid re-epithelialization of the denuded area through epithelial cell migration, proliferation, and differentiation (**Selman et al., 2001**). During wound healing, tissue injury causes disruption of blood vessels and extravasation of blood constituents into the wound (**Singer et al., 1999**). This step reestablishes hemostasis and provides a provisional ECM in which the repair process can begin. Loss of homeostatic matrix regulation with concomitant alterations in synthesis and degradation quickly results in the disproportionate deposition of lung connective and its adverse consequences (**Chua et al., 2005a**). The actions of initiators and inhibitors of the coagulation cascade tightly regulate the amount of fibrin present at sites of injury. Usually, the fibrynolitic system, required to cleave a path for cell migration, is active during repair processes that restore injured tissues to normal

(Martin, 1997). During normal wound healing, epithelial cells have to dissolve the fibrin barrier to migrate throughout the denuded wound surface (**Martin, 1997**).

Early in this century, Selman *et al*. (**Selman et al., 2001**) proposed the concept of inflammation-independent PF, and emphasized the role of alveolar epithelial injury and formation of fibroblast-myofibroblast foci as a basis for fibrogenesis. Importantly, altered alveolar type 2 cells synthesize a variety of enzymes, such as matrix metalloproteinases (MMPs), cytokines and growth factors, suggesting that the contribution of the epithelium in the ECM remodelling is greater than commonly thought. In addition, type 1 AECs are highly vulnerable to injury, whereas the type 2 AECs are more resistant and can therefore function as progenitor cells for regeneration of the alveolar epithelium after injury. These cells proliferate and migrate to recover the denuded basement membrane by forming a layer of cuboidal epithelial cells. Afterwards, they should differentiate to reestablish both type 1 and type 2 pneumocytes into a functional alveolar epithelium.

In IPF, the capacity of type 2 alveolar epithelial cells to restore damaged type 1 cells is seriously altered, resulting in the presence of transitional reactive phenotypes, abnormalities in pulmonary surfactant and alveolar collapse (**Kasper and Haroske, 1996; Geiser, 2003**). In fact, during the development of IPF, alveolar epithelial cells appear to be responsible for the expression and release of most, if not all, the profibrotic cytokines and growth factors that have usually been associated with inflammatory cells, primarily alveolar macrophages. In the later stages of fibrosis, basement membranes are frequently wavy and disrupted, and fibroblasts migrate through gaps in the epithelial basement membranes and continue proliferating and producing ECM in the alveolar spaces (**Selman and Pardo, 2002**). The imbalance between the production of newly synthesized matrix proteins and their inadequate removal, degradation or clearance results in excessive accumulation of matrix proteins, and the net effect is the alteration of the structure and function of the involved tissue organs. The generation of ECM is predominantly achieved through the production of collagenous and non-collagenous proteins, whereas degradation of ECM is predominantly achieved by various proteolytic enzymes, such as MMPs.

Lung injury leads to vasodilatation, with the subsequent leakage of plasma proteins into interstitial and alveolar spaces, activation of the coagulation cascade and deposition of fibrin. The key protein involved in fibrin resorption is plasmin which in turn, activates several metalloproteinases such as MMP-1 and MMP-9. Activation of MMPs provokes

ECM degradation that, together with fibrin removal, results in the clearance of alveolar spaces. In contrast, the persistence of fibrin and inappropriate regulation of plasmin promotes fibrosis. Essentially, the balance between procoagulant, fibrynolitic and anti-fibrinolitic systems determines whether fibrin will be deposited or reabsorbed. In this context, increased local procoagulant and antifibrinolytic activities have been found in patients with IPF, suggesting that fibrin matrix removal is slow in them and, as a consequence, fibroblast migration, ECM deposition and the magnitude of the fibrotic response is increased (**Kotani et al., 1995; Imokawa et al., 1997; Selman and Pardo, 2002**).

Fibroblasts produce and deposit large quantities of matrix proteins, predominantly types I and III collagen, which increases the tensile strength of the wound. After a variable period of time, which mainly depends on the vascularity and innervation of the tissue affected, mesenchymal cells (myofibroblasts) contract, reduce and bring the wound margins closer together. The nature of the matrix components in wounds changes with time. In the earliest stage, excessive type III collagen deposition is seen but later type I collagen predominates. Although in this intermediate stage the wound appears to be healed, chemical and structural changes continue. Collagen fibrils become tightly packed and stabilized by the formation of inter- and intra-molecular cross-links (**Yamauchi and Mechanic, 1988**). This series of events occurs in most tissues including skin, lung, heart and bone. The final process in normal wound healing is *resolution* of the scar as described in Fig. 4.

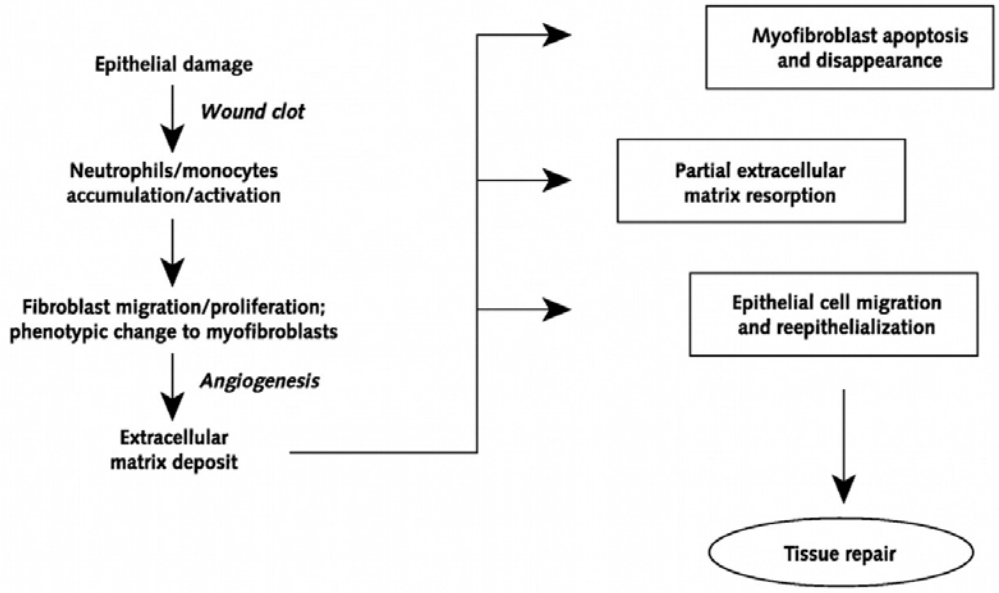

Figure 4. The normal wound healing model (**Selman et al., 2001**).

The degradation of wound collagen and other matrix proteins is controlled by a variety of collagenase enzymes and other metalloproteinases from granulocytes, macrophages, epidermal cells and fibroblasts, which degrade scar tissue altering its texture over a period of many months (**Mignatti et al., 1996**). Evidence suggests that matrix metalloproteinase levels or activity in chronic scarring states may be reduced thus preventing attenuation of scar tissue size (**McGrouther et al., 1994**).

Excessive accumulation of interstitial collagens destroys lung architecture, and subsequently leads to respiratory failure. It has been suggested that the injured epithelium in IPF releases a number of cytokines and growth factors, which control fibroblast proliferation, differentiation, chemotaxis and matrix production. Type II alveolar epithelial cells are one of the main sources of these fibrogenic factors. In the fibrotic phase, the activated resident and transformed interstitial matrix-producing cells synthesize an excessive amount of matrix proteins, which are deposited in the interstitial space, and gradually develop to form irreversible PF. Accumulation of various types of collagen fibres has been described in fibrotic lesions in the lung (**Zhang et al., 1994; Specks et al., 1995; Razzaque and Taguchi, 1999**). The three major histopathological features of this disease are the influx of inflammatory cells, proliferation of type II pneumocytes and the accumulation of collagen fibres.

I.2. REGULATION OF LUNG MATRIX REMODELLING

The complex process of normal lung repair after injury requires on one hand, epithelial cell migration, proliferation and differentiation, and on the other hand, fibroblast migration and proliferation, their transformation into myofibroblasts, and myofibroblast apoptosis. Thus, impaired apoptosis of myofibroblasts may result in a persistent and deregulated repair process that culminates in tissue fibrosis (**Thannickal and Horowitz, 2006**). Epithelial cells are the primary source of mediators capable of inducing fibroblast migration, proliferation, and activation as well as ECM accumulation in fibrotic diseases suchlike IPF. These include platelet-derived growth factor, TGF-β, TNF-α, endothelin-1, connective tissue growth factor, and osteopontin, all important in the development of PF (**Selman et al., 2004; Pardo et al., 2005**). Injured epithelium not only provides activation signals to mesenchymal cells but it also seems to lose its ability to provide its normal and homeostatic fibroblast-suppressive function, primarily mediated by prostaglandin-2 (PGE-2). A growing body of evidence indicates that under physiologic conditions AECs suppress fibroblast migration, proliferation, and activation, including collagen synthesis, through the action of PGE-2 (**Pan et al., 2001; Kohyama et al., 2001; Lama et al., 2002**).

I.2.1. The role of the fibroblasts

Evidence suggests that the earliest, and possibly the only, morphologic change associated with subsequent progression to dense fibrosis are the presence and extent of fibroblastic foci in the injured lung (**Kuhn et al., 1989; Kuhn and McDonald, 1991**; **Katzenstein and Myers, 1998**). Fibroblasts within these foci continually modify their interactions with the microenvironment. Fibroblasts assume first a migratory phenotype, second a proliferative phenotype, and finally a profibrotic phenotype, during which they produce abundant ECM components. Most cells in the fibroblast foci are myofibroblasts aligned in parallel to one another and thus probably contribute to active concentration and distorted architecture (**Kuhn and McDonald, 1991**).

Myofibroblasts are activated fibroblasts characterised by a spindle or stellate morphology with intracytoplasmic stress fibres, a contractile phenotype, expression of various mesenchymal immunocytochemical markers such as α-SMA and collagen production (**Schurch et al., 1998**). Their major roles are reconstituting a collagen-rich ECM and promoting wound closure by contraction (**Tomasek et al., 2002**). At the end

of normal wound healing the contractile and synthesizing activity of myofibroblasts is usually terminated and cell number is dramatically reduced by apoptosis (**Desmouliere et al., 2005**). Myofibroblasts are key mediators of ECM deposition, structural remodelling, and destruction of alveolocapillary units during and after lung injury (**Phan, 2002**), and as such, the knowledge of their cellular source is critical to the understanding of the pathogenesis of IPF in particular and fibrosis of the lung in general.

Three hypotheses have been proposed with regard to the cellular origin of the myofibroblast:

First: Resident intrapulmonary fibroblasts may respond to a variety of stimuli during fibrogenic responses and differentiate into myofibroblasts (**Phan, 2002**). TGF-β1, a key regulator of fibrosis, induces transdifferentiation of fibroblasts “in vitro” through a Smad 3-dependent mechanism (**Hu et al., 2003**).

Second: Bone marrow-derived progenitors could contribute to myofibroblast induction and proliferation during PF. Hashimoto and colleagues (**Hashimoto et al., 2004**) showed that collagen-producing lung fibroblasts in BLM-induced PF can be derived from bone marrow progenitor cells. However, these bone marrow-derived fibroblasts do not express α-SMA and are resistant to fibroblast-myofibroblast conversion by TGF-β1.

Third: AECs, through the process of epithelial-mesenchymal transition (EMT) also play a significant role. EMT is a process by which fully differentiated epithelial cells undergo phenotypic transition to fully differentiated mesenchymal cells, often fibroblasts and myofibroblasts (**Zavadil and Bottinger, 2005**).

It is important to stress that these potential sources of myofibroblasts are not mutually exclusive and the relative contribution of each source to the progression of fibrosis remains to be determined. Fibroblast-to-myofibroblast differentiation, a key event in the development of fibrocontractive diseases and in wound granulation tissue contraction, is hallmarked by the formation of stress fibres and the neo-expression of α-SMA isoform into stress fibres confering to myofibroblasts a high contractile activity which is transmitted to the ECM at sites of specialized adhesions, termed “fibronexus” in tissue (**Eyden, 2001**).

TGF-β has been implicated as a “master switch” in the induction of fibrosis in many organs, including the lung (**Sime and O’Reilly, 2001**). It makes intuitive sense that TGF-β1 would also play a pivotal role in the induction of EMT, given the progressively more apparent role of EMT in the fibrotic processes, the key role of TGF-β1 in fibrosis, and the ability of TGF-β1 to promote loss of the epithelial phenotype. In fact, TGF-β is a chemoatractant for fibroblasts and myofibroblasts, which can be found in areas of developing fibrosis (**Postlethwaite et al., 1987; Toti et al., 1997; Krishna et al., 2001**). TGF-β can stimulate fibroblast differentiation to the myofibroblast phenotype and suppress myofibroblast apoptosis (**Zhang and Phan, 1999**). Some of the cytokines secreted by fibroblasts, such as the monocyte chemotactic protein-1, also promote the induction of collagen expression by TGF-β (**Gharaee-Kermani et al., 1996**). TGF-β is the most potent direct stimulator of collagen production known, and all three isoforms have been demonstrated to increase collagen-expression “in vitro” (**Ignotz and Massague, 1986; Broekelmann et al., 1991**). In addition, it induces the transcription and synthesis of various other components of the ECM by immature and mature pulmonary fibroblasts, such as fibronectin, glycosamonglicans (GAGs), and proteoglycans (**Souza-Fernandes et al., 2006; Pelosi and Rocco, 2008**).

It has been suggested that PDGF and TGF-β isoforms work in concert to stimulate the cellular events that result in fibrotic lesions, with PDGF being responsible for increased fibroblast proliferation during fibrogenesis and TGF-β for stimulating ECM production by fibroblasts (**Bonner et al., 1995**). TGF-β promotes matrix synthesis and stabilizes the newly formed ECM proteins by inhibiting their degradation. Furthermore, TGF-β regulates cell-matrix interaction by modifying the expression of cell-matrix adhesion protein complexes. These interactions play an important role in tissue remodelling following injury (**Grande, 1997**).

I.2.2. The role of the alveolar epithelium in fibrogenesis

Recently, there has been a return to the notion proposed by Adamson and colleagues (**Adamson et al., 1988**) that ongoing AEC injury and retarded wound repair may be central to the pathogenesis of PF (**Pardo and Selman, 2002; Selman and Pardo, 2003**). It has long been recognized that the epithelial cells overlying fibroblastic foci are hyper- and dysplastic, with abnormal morphology and gene expression patterns (**Kasper and Haroske, 1996; du Bois and Wells, 2001**). These cells secrete a variety of profibrotic cytokines, participating in a bidirectional communication network with

neighboring fibroblasts whereby each cell type influences the proliferation/survival of the other. The alveolar epithelium serves as a major source of TGF-β1 and many other cytokines (endothelin-1 and TNF-α) during lung injury and fibrosis (**Giaid et al., 1993; Kapanci et al., 1995; Xu et al., 2003**), independent of proinflammatory mediators (**Kwong et al., 2004**). Taken together, these data suggest that the alveolar epithelium plays a major role in the pathogenesis of lung fibrosis, with the capacity to produce and respond to TGF-β1, regulate the function and differentiation of fibroblasts, and modify cell morphology and gene expression in response to injury, all independent of the degree of inflammation (**Menezes et al., 2005**).

Whether and to what extent EMT is a feature of all pulmonary fibrotic processes remains to be clarified. Elucidation of these issues and the mechanisms underlying EMT in lung await further investigation. At this point, one can only speculate on the relative contribution of alveolar epithelial EMT to the production of intrapulmonary fibroblasts and/or myofibroblasts during pulmonary fibrotic processes “in vivo”. However, given that EMT contributes at least one-third of the fibroblast population during fibrosis in other organs, that alveolar epithelial-fibroblastic cross-talk and interactions are involved in fibrosis in the lung, that AECs undergo EMT “in vitro” in response to TGF-β1, and that TGF-β1 is expressed at sites of epithelial injury and adjacent fibrosis “in vivo”, it is likely that conversion of resident AECs to fibroblasts and activated fibroblasts (myofibroblasts) contributes significantly to lung fibrogenesis “in vivo” (Fig. 5). It is possible that, depending on the degree of injury, type 1 pneumocytes may be more likely to undergo apoptosis whereas type 2 peumocytes cells preferentially undergo EMT. Type 2 pneumocytes cells (AT2) are believed to serve as the progenitors for repair of the alveolar epithelium after injury, being capable of both self-renewal and giving rise to type 1 pneumocytes cells (AT1) through a process of *transdifferentiation* (**Adamson and Bowden, 1974**). Similar to observations “in vivo”, AT2 cells in primary culture lose their phenotypic hallmarks and gradually acquire the morphologic features of AT1 cells (**Cheek et al., 1989**). The cells increasingly express all available AT1 cell phenotypic markers, suggesting that AT2 cells “in vitro” transdifferentiate toward an AT1 cell phenotype (type 1 pneumocytes -like cells) (**Borok et al., 1998a; Borok et al., 1998b**). Such remarkable phenotypic plasticity, suggests that, under certain conditions in which transition to a type 1 pneumocytes cell phenotype is inhibited (i.e. injury) AT2 cells may also have the capacity to undergo transition to fibroblasts and myofibroblasts through the process of EMT.

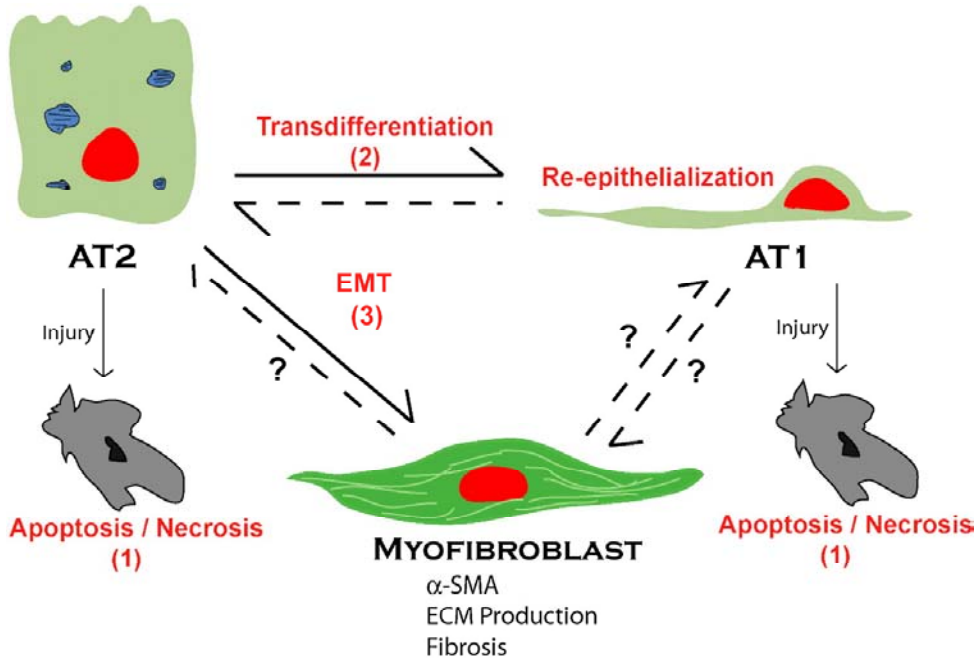

Figure 5. Alveolar epithelial transdiferentiation pathways (**Willis et al., 2006**).

I.2.3. Epithelial cells and fibroblasts: structural repair and remodelling in the airways

PDGF stimulates many of the processes involved in tissue repair, including fibroblast chemotaxis and proliferation, smooth muscle cell proliferation, and collagen synthesis (**Antoniades et al., 1990; Martinet et al., 1996**). More recently, the presence of nerve growth factor (NGF), a polypeptide believed to play a role in inflammatory response and tissue repair, has been demonstrated in airway epithelial cells, lung fibroblasts and fibrotic lung tissues (**Micera et al., 2001; Kassel et al., 2001**). NGF appears to be able to induce fibroblast migration, to modulate their phenotype into myofibroblasts and to increase their contraction, without influencing cell activation and proliferation or collagen production (**Micera et al., 2001**). Recent evidence indicates that the pulmonary fibroblast is much more than a target structural cell and can contribute directly to pulmonary inflammation and ultimately to airway wall remodelling as described in Table 1 (**Knight, 2001**). To repair the damaged interstitial tissues, fibroblasts also proliferate, migrate, synthesize and release increased amounts of collagen (mainly Types III and V), polysaccharides (such as hyaluronic acid) and fibronectin (**Brewster et al., 1990; Bethesda, 2002**). Besides being modulated by a variety of cytokines and mediators released by airway inflammatory and parenchymal cells, fibroblasts may also interact directly with inflammatory cells, as demonstrated by

the frequent observation of membrane apposition of eosinophils and myofibroblasts in the bronchial mucosa of asthmatic patients (**Brewster et al., 1990; Bethesda, 2002**).

This close contact, that likely involves adhesion molecule expression on the interacting cell surface, may allow for the stimulation of inflammatory cells by both direct cell-cell interaction and high cytokine concentrations (**Doucet et al., 1998**). Fibroblasts express a variety of integrins (**Knight, 2001**) and surface molecules that include adhesion molecule-1 (ICAM-1 or CD54), and transmembrane glycoproteins, such as hyaluronic cellular adhesion molecule (H-CAM or CD44) (**Kasper et al., 1995; Doucet et al., 1998**). As a receptor for the ECM glycan hyaluronate as well as for collagen and fibronectin, the CD44 transmembrane glycoprotein appears to be involved in the regulation of cell locomotion and in modulation of cell-cell and cell-matrix interactions that occur during fibrinogenesis (**Kasper et al., 1995**). Besides providing mechanical support to the tissues, the ECM is being increasingly recognized as a source of signals for cellular localization, migration, differentiation and activation (**Damsky and Werb, 1992**).

In IPF it is becoming apparent that the primary site of ongoing injury and repair are the regions of fibroblastic proliferation, so-called fibroblastic foci (**Katzenstein and Myers, 1998**). Therefore, an initial epithelial cell injury and activation induces fibroblast migration/ proliferation and fibroblast phenotypic change (myofibroblasts). Subsequently, myofibroblasts may provoke basement membrane disruption and AEC apoptosis, perpetuating the damage and avoiding appropriate re-epithelialization that results in an excessive ECM deposition.

The earliest and probably the only morphological change associated with progression to fibrosis is the presence of fibroblastic foci, which is characterised by a distinct cluster of fibroblasts/myofibroblasts within the alveolar wall, with little if any associated inflammation. The fibroblast proliferation occurs in an attempt to repair the damaged alveolus, and is followed by ECM accumulation. Fibroblastic foci may occur in the interstitial (subepithelial) space or in the alveolar spaces, which are later covered by reactive epithelium (**Kuhn and McDonald, 1991; Katzenstein et al., 1998**). In the later stages of fibrosis, epithelial basement membranes are frequently wavy and disrupted, and fibroblasts migrate through gaps in the epithelial basement membranes and continue proliferating and producing ECM in the alveolar spaces.

Table 1. Functions of fibroblasts involved in wound repair (**Knight, 2001**).

Functions:
a) protection from the external environment
b) deposition and remodelling of the ECM
c) collagen I, III, IV synthesis and release
d) MMP2 and MMP9 synthesis and release
e) PGE2 release
f) interaction with recruitment of inflammatory cells
g) modulation of repair processes

I.2. 3.1. The role of TGFβ in lung disease

The fibrotic response described is largely variable (**Ask et al., 2006**). Some factors are related to severe inflammation (TNF-α, IL-1β), and some cause reversible fibrosis (TNF-α, TGF-β 3, CTGF, IL-10, oncostatin M) or more progressive fibrosis (IL-1β, TGF-β1). The presence of TGF-β in the healthy lung suggests its participation in the normal regulation of physiologic processes to maintain lung homeostasis. These functions may include local immunomodulation, regulation of cell proliferation and differentiation, as well as the control of normal tissue repair. A common characteristic of many forms of lung disease is an inflammatory process with a phase of tissue injury followed by a phase of repair (**Magnan et al., 1996; Elssner et al., 2000; Bartram and Speer, 2004**). TGF-β limits some of the inflammatory reactions and plays a key role in mediating tissue remodelling and repair (**Sporn and Roberts, 1992; Ahuja et al., 1993**). If the reparative processes are exaggerated and not adequately localized, lung pathology with fibrosis will ensue. This is typically associated with increased levels of TGF-β and its receptors, and overexpression of TGF-β has been shown to result in severe PF (**Sime et al., 1998**). In addition, several other cytokines, such as TNF-α (**Ortiz et al., 1998**), keratinocyte growth factor (**Yi et al., 1998**), angiotensin II (ANGII) (**Marshall et al., 2000; Molina-Molina et al., 2008**), and IL-10 (**Arai et al., 2000**) may exhibit profibrotic effects via the TGF-β pathway. In several studies, TGF-β has been shown to be a marker of the activity of tissue repair and remodelling. In patients with sarcoidosis, Salez et al (**1998**) found the levels of TGF-β1 to be increased only in patients with an active form of the disease associated with alterations in lung functions and leading to fibrosis. Patients with PF had higher TGF-β levels if a progressive form of the disease was present (**Kuroki et al., 1995**).

Sources of TGF-β appear to be activated during lung pathogenesis associated with fibrosis. The importance of these sources may vary at different stages of the reparative process and in different forms of lung diseases. Increased levels of TGF-β have been demonstrated in epithelial cells and macrophages of the terminal airways and alveoli (**Khalil et al., 1991; Limper et al., 1991**). During the early stages, platelets and epithelial cells may be a reservoir for TGF-β (**Border and Ruoslahti, 1992; Coker et al., 1997**), while alveolar macrophages have been found to be important sources of increased production and secretion of TGF-β in several forms of chronic lung disease during the phase with maximal TGF-β levels (**Magnan et al., 1996; Asakura et al., 1996**). Similar results have been reported in an animal with BLM-induced PF, in which TGF-β was found initially in the bronchial epithelium and the subepithelial matrix, while at the time of maximal TGF-β expression it was present predominantly in macrophages in the alveolar interstitium (**Santana et al., 1995; Zhang et al., 1995**). The up-regulation of TGF-β always preceded the peak increase in ECM production (**Sime et al., 1998; Rube et al., 2000**).

I.2.3.1.1. The role of other cytokines using the TGFβ pathway

The predominant eicosanoid product of pulmonary epithelial cells, PGE_2 (**Chauncey et al., 1988; Holgate et al., 1992**), is a potent inhibitor of mesenchymal cell chemotaxis (**Kohyama, 2001**), fibroblast proliferation, fibroblast to myofibroblast differentiation mitogenesis (**Bitterman et al., 1986; Belvisi et al., 1998**), and collagen synthesis (**Goldstein and Polgar, 1982**). Furthermore, it has a variety of other downregulatory effects on such processes as leukocyte recruitment and generation of cytokines, growth factors, reactive oxygen intermediates, endothelin, and leukotrienes (**Heusinger-Ribeiro et al., 2001**). PGE_2 is therefore an excellent candidate for mediating the capacity of epithelial cells to suppress inflammation as well as fibroblast activation. Bronchoalveolar lavage (BAL) fluid from patients with IPF contain 50% less PGE_2 than normal individuals (**Borok et al., 1991; Molina-Molina et al., 2006**). Furthermore, alveolar macrophages and fibroblasts have a reduced capacity to produce PGE_2 “in vitro” (**Ozaki et al., 1990; Willborn et al., 1995**). The failure to synthesize PGE_2 has been shown to be associated with a decreased capacity to upregulate cyclo-oxygenase 2 (COX-2) (**Keerthisingam et al., 2001; Xaubet et al., 2004**). The multifunctional cytokine TGF- β1 is a well characterised profibrotic mediator that induces transformation of fibroblasts to myofibroblasts both “in vitro” and “in vivo”.

PGE_2 has the potential to limit TGF-β1-induced myofibroblast differentiation via adhesion-dependent, but Smad-independent, pathways (**Thomas et al., 2007**).

ANGII is produced by proteolytic cleavage of its precursor ANGI by angiotensin converting enzyme (ACE) being considered a crucial mediator in the pathogenesis of PF. ANGII induces proliferation of human lung fibroblasts and production of lung procollagen via activation of angiotensin type 1 receptor (AT1) and mediated by TGF-β (**Papp et al., 2002; Marshall et al., 2004; Molina-Molina et al., 2008**). Experimental evidence suggests that ANGII regulates the fibrotic response to tissue injury. In IPF, TNF-α plays a role as a cytokine that bridges inflammation, repair responses and fibrosis and may be involved in ECM remodelling. It is also implicated in orchestrating inflammatory cell accumulation, granuloma formation and fibrogenesis in granulomatous diseases including sarcoidosis (**Ye et al., 2006**).

In PF, ET-1 was initially characterised as a potent smooth-muscle spasmogen, but accumulating evidence is pointing out the ET-1 role as a proinflammatory cytokine. ET-1 is known to prime neutrophils, stimulate neutrophils to release elastase (**Halim et al., 1995**), activate mast cells (**Uchida et al., 1993**), stimulate monocytes to produce variety of cytokines such as IL-1β, IL-6, and IL-8, TNF-α, TGF-β, and granulocyte-macrophage colony-stimulating factor. Furthermore, there is evidence that ET-1 can function as a profibrotic cytokine by stimulating fibroblast chemotaxis and proliferation (**Peacock et al., 1992; Cambrey et al., 1994; Shahar et al., 1995**) and procollagen production (**Kahaleh, 1991; Dawes et al., 1996**). ET-1 can be detected in the circulation of normal subjects (**Andok, 1985**), although epithelial cells do not normally express ET-1, and is elevated in the plasma of patients with pulmonary hypertension, scleroderma, and IPF. In patients with PF associated with systemic sclerosis, bronchoalveolar lavage fluid contains 5-fold greater ET-1 levels than those of controls (**Cambrey et al., 1994**) and is elevated in patients with asthma (**Mattoli et al., 1991**).

Findings in a BLM-induced lung injury murine model are consistent with those found in lung tissue from patients with PF (**Giaid et al., 1993; Uguccioni et al., 1995**). In a time course study, a rapid 3-fold increase in lung ET-1 content was found peaking at day 7. An ET-1 increase precedes the onset of fibrosis, co-localizing with developing fibrotic lesions (**Mutsaers et al., 1998a**). Antagonists of endothelin receptor function have been used to prevent the development of PF with conflicting results. ET receptor antagonists have been shown to inhibit the effects of ET-1 on lung fibroblast proliferation (**Cambrey et al., 1994**) and collagen synthesis “in vitro” (**Dawes et al.,**

1996). In addition, other studies have shown that ET receptor antagonists are effective in attenuating ECM production “in vivo” (**Rockey and Chung, 1996; Park et al., 1997**). However, Mutsaers and colleagues provide evidence that continuous administration of nonselective ET_A and ET_B, as well as selective ET_A receptor antagonists, did not prevent collagen accumulation in the bleomycin (BLM) model (**Mutsaers et al., 1998b**). In summary, circumstantial evidence for a role of ET-1 in lung fibrosis has accumulated, but whether this is a causative or bystander role remains unknown.

I.3. EXTRACELLULAR MATRIX

I.3.1. Changes of the extracellular matrix induced by the inflammatory-remodelling process

Connective tissue and its matrix components provide for mechanical support, movement, tissue fluid transport, cell migration, wound healing, and control of metabolic processes in other tissues (**Culav et al., 1999**). The mechanical properties of the connective tissue (the ability to resist tension, compression, extensibility, and torsion) are determined primarily by the amount, type, and arrangements of an abundant ECM (Fig. 6). The most important fibrous components of the ECM are collagen and elastin, both insoluble macromolecular proteins. The striking feature of the most prominent collagens is their ability to resist tensile loads. Generally, they show minimal elongation (less than 10%) under tension. In contrast, elastic fibres may increase their length by 150%, returning to their previous configuration (**Harkness, 1980**). The second major component of the ECM is the PGs (a diverse group of soluble macromolecules) that have both structural and metabolic roles. Along with the collagen, they are located in the interstitial spaces between the cells and form part of basement membranes, and attach to cell surfaces where they function as receptors (**Hardingham and Fosang, 1992; Heinegard and Oldberg**, **1993**). Their mechanical functions include hydratation of the matrix, stabilization of collagen networks, and the ability to resist compressive forces. Hyaluronan, which is technically not a PG, is particularly important because it readily entrains large amounts of water and is abundant in hydrated soft loose tissues where repeated movement is required (**Souza-Fernandes et al., 2006**). The third group is the glycoproteins, ubiquitous in the connective tissue and like the PGs, exert both structural and metabolic roles. Their

mechanical roles include providing linkage between matrix components and between cells and matrix components.

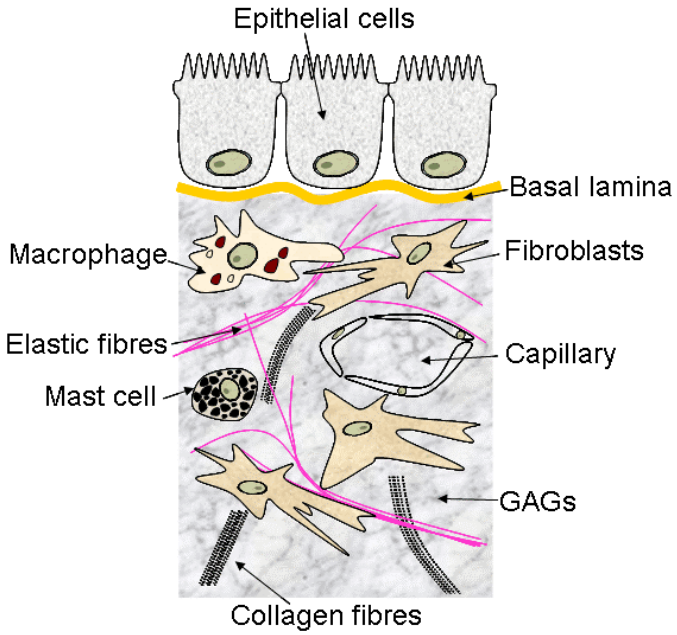

Figure 6. Scheme of the ECM.

Under normal physiological conditions, the maintenance of ECM is controlled through a balance between synthesis and degradation. This balance is maintained largely by stimulatory cytokines and growth factors in addition to the degradative MMPs and TIMPs. The synthesis and secretion of MMPs and TIMPs is similarly modulated by an intricate network of signaling factor cytokines, growth factors, and hormones (**Alexander and Werb, 1991**). The alteration of the balance between synthesis and degradation influences normal tissue architecture, impairs organ function, and changes the mechanical properties of the tissues. Net increases in synthesis over degradation leads to accumulation of ECM in fibrotic conditions, such as interstitial pulmonary fibrosis. During the initial stages of healing, rupture sites are bridged by newly synthesized type III collagen, but, as remodelling proceeds, increasing amounts of type I collagen predominate and provide greater strength (**Liu et al., 1995; Santos et al., 2006**). Tension exerted on wounds is also thought to stimulate collagen synthesis and enhance their repair process by causing the collagen fibrils to align in parallel to the direction of force (**Flint, 1990**). The connective tissue is surrounded by specialized ECM called the basal lamina, which underlies epithelial cells. Immune cells are often present too, but these are for defense, not for generation of ECM: connective tissue is primarily generated by fibroblasts.

I.3.1.1. Collagen

Collagen is found in the alveolar structures, and among the pulmonary connective tissue constituents, the molecular structure of collagen is the best characterised. The collagen molecule is a rodlike unit formed by 3 polypeptide chains (α-chains) arranged in the form of a triple helix (**Gadek et al., 1984**). These triple helical molecules polymerize to form collagen fibrils, the structures that ultimately account for the tensile strength of collagenous connective tissue. An unusually repetitive primary structure of the collagen fibrils, the structures of the collagen α-chain plays a critical role in conferring a unique helical structure to the collagen molecule. Along the collagen α-chain, glycine, proline and hydroxyproline residues appear as triplet of gly-pro-X (where X is commonly hydroxyproline), a structure that is repeated frequently along the length of the polypeptide chain (**Rennard et al., 1980**). In addition, the α-chains also contain lysine and hydroxylysine, residues that are involved in formation of covalent crosslinks that permit the assembly of collagen molecules into fibrils (**Rennard et al., 1980**). The principal differences among the collagen types are the amino acid sequence within the polypeptide chains and the types of polypeptides chains comprising the triple helical molecule. In the human alveolar structures, the ratio of Type I and Type III collagen is approximately 3:1 (**Gadek et al., 1984**).

Picture of collagen fibres in a 2-week BLM-induced lung injury. The bright dots represent collagen fibres:

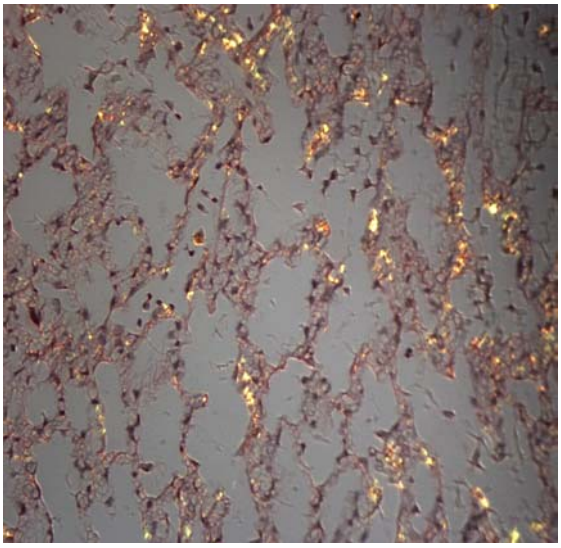

Type I collagen, composed of 2 α_1-(I)- chains and one α_2-(I)- chain, is the most abundant collagen present in the alveolar structures (**Hance and Crystal, 1975;**

Rennard et al., 1980). Type I collagen is distributed diffusely within the alveolar interstitium but is not present in the endothelial or epithelial basement membranes. Type I likely plays a dominant role, determining alveolar shape and distensibility (**Hance and Crystal, 1975; Rennard et al., 1980**). In addition, Type I collagen contributes to cellular organization of the interstitium by serving as a site of attachment for fibroblasts through another matrix glycoprotein, fibronectin (**Seyer, 1978**).

Type III collagen comprises three identical α_1 (III) polypeptide chains. Like Type I, it is an interstitial collagen and partially corresponds to “reticulin” demonstrable by light microscopy. The role of Type III is less clear, but it also serves as an anchor for fibronectin-mediated cell attachment. The mechanical properties of Type III are not known, but there is evidence that it may modulate Type I fibre formation (**Rennard et al., 1980**). Type IV collagen, also present in the alveolar structures but the exact location remains unknown, likely modulates basement membrane structure and mechanical properties (**Seyer, 1978**). The loss of gas exchange units and the alterations in lung mechanics due to the non-distensible property of the collagen fibres is likely to be responsible for the pulmonary failure observed in diffuse lung fibrosis subjects (**Rozin et al., 2005**).

I.3.1.2. Elastic fibres

Elastic fibres are composed of at least two components, elastin and microfibrils. Elastin is composed of large, extremely insoluble polymers of crosslinked, identical protein subunits called tropoelastin (**Hance and Crystal, 1975; Rennard et al., 1980**). Like collagen, elastin also contains hydroxyproline residues; however, these are infrequent and represent only 1% of tropoelastin’s amino acids (compared to 10% for collagen) (**Rennard et al., 1980; Gadek et al., 1984**). Unlike other connective tissue components present in the alveolar structures, elastin contains no carbohydrate side chains. The tropoelastin units of elastin are linked together by covalent bonds through the lysine residues. While two of these crosslink units, desmosine and isodesmosine, are unique to elastin, a third, the lysinonorleucine crosslink, is also present in collagen (**Rennard et al., 1980**). In the mature lung, elastic fibres are found in close proximity to collagen fibres and proteoglycans (**Horwitz and Crystal, 1975**). Elastic fibres have rubberlike properties, an attribute that undoubtedly plays a major role in modulating elastic recoil during the respiratory cycle.

In this context, destruction of elastic fibres is central to the pathogenesis of lung disorders associated with loss of elastic recoil (**Janoff et al., 1979; Gadek et al., 1980**). Elastic fibres provide recoil tension to restore the parenchyma to its previous configuration after the stimulus for inspiration has ceased (**Rozin et al., 2005**). In normal alveolar septa, a subepithelial layer of elastic system fibres, composed mainly of fully mature elastic fibres, confers considerable alveolar elasticity in normal situations (**Mercer and Crapo, 1990**). Increased elastin destruction takes place in certain pathological conditions due to the release of powerful elastolytic proteases by inflammatory cells (**Fukuda and Ferrans, 1988; Fukuda et al., 1990**). Reactivation of elastin synthesis is observed in response to the increased destruction, but in a highly disordered manner with deleterious consequences to the mechanical properties of the lung, contributing to the loss of normal alveolar architecture, to a collapse tendency and to an impaired mechanism of inflammatory resolution (**Rocco et al., 2001; Rocco et al., 2003; Pelosi and Rocco, 2008**).

Picture of elastic fibres in a 2-week BLM-induced lung injury. Dark lines represent the elastic fibres:

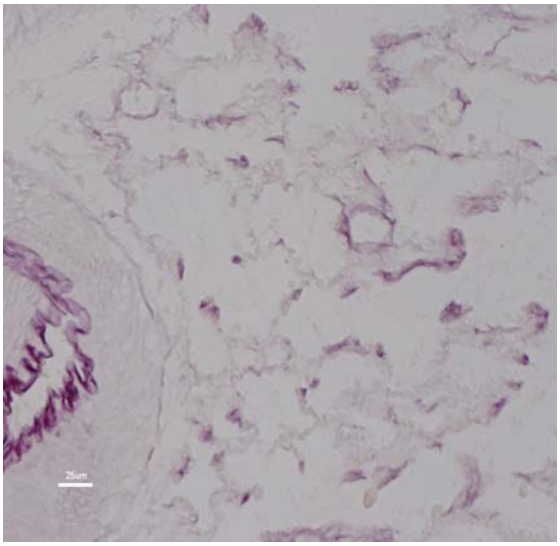

The occurrence of elastosis has been extensively demonstrated in animal models of PF, however the deposition of elastic system fibres has been largely ignored in the pulmonary remodelling of human interstitial lung disease. Rozin et al 2005, measured the content fibres of the collagenous and elastic systems of the alveolar septum in histological slides of open lung biopsies, found that the elastosis process parallels the collagen deposition in the different histological patterns except for the UIP cases, in which collagen deposition was significantly higher. This finding suggests that a profibrogenic mechanism is present in these subjects.

I.3.1.3. Matrix metalloproteinases

Pulmonary inflammation is characterised by an enhanced activation of inflammatory cells, either recruited in the pulmonary tissue, such as polymorphonuclear neutrophils, or resident in the alveolar space, such as alveolar macrophages. Neutrophils have been implicated in causing tissue damage in PF through the release of a number of mediators, including MMPs. Local concentrations of ROS/RNS can determine whether MMPs are activated or inactivated (**Kinnula et al., 2005**). A primary role for macrophages is also proposed because of their capacity to produce several metalloproteinases. Overall, oxidative stress in PF is one important activator of the MMPs (**Kinnula et al., 2005**).

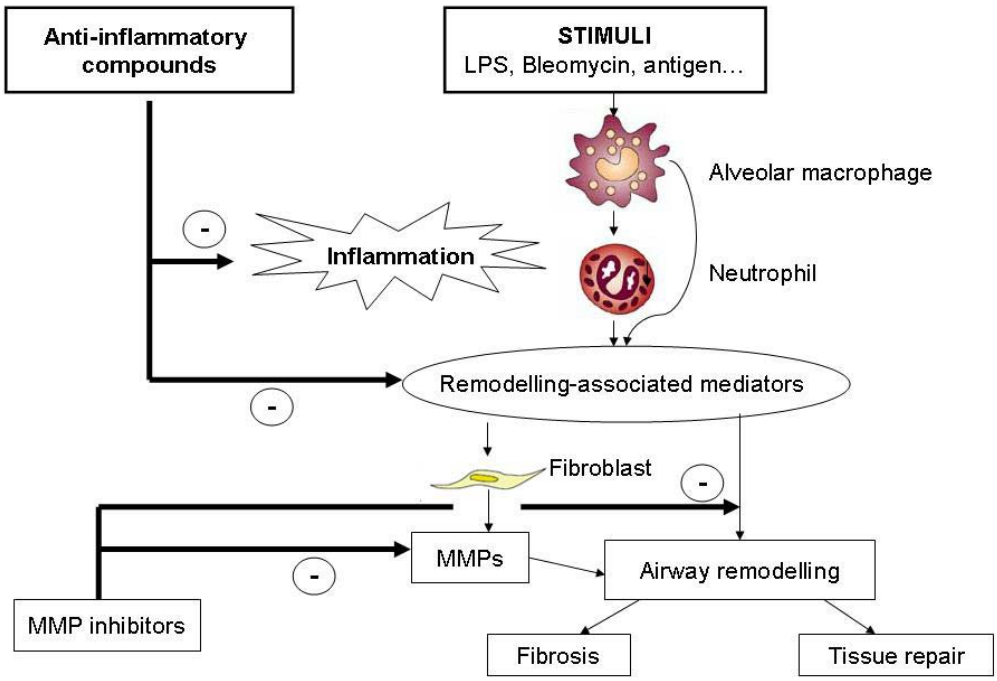

Figure 7. The effect of MMPs upon wound healing (**Corbel et al., 2002**).

In early phases of fibrotic conditions, the accumulation of inflammatory cells is a hallmark of the pathophysiological events. MMP-9 would be linked to inflammatory process-induced tissue remodelling, whereas MMP-2 (Fig. 7) may be associated with an impaired tissue remodelling leading to pathological collagen deposition and PF (**Silva et al., 2009**). MMPs activity is controlled by transcriptional regulation, proenzyme activation, and inhibition by specific tissue inhibitors of metalloproteinases (TIMPs). Actually, an imbalance between MMPs and their natural antagonists, the TIMPs, can result in pathophysiological destructive processes such as tumor invasion, wound healing and inflammatory and fibrogenic diseases (**Murphy and Docherty,**

1992). A significant component of the host defense strategy is the production of potent proteolytic enzymes, including MMPs, to facilitate clearance of foreign and noxious agents but which, in excess can also destroy ECM environment, disrupt resident cells, and stimulate further inflammation (**Tetley, 1993**).

Higher expressions of TIMPs compared with collagenases, supporting the hypothesis that nondegrading fibrillar collagen microenvironment prevails (**Selman et al., 2000**). Such observations have been confirmed “in vivo” in a murine model of BLM-induced PF (**Madtes et al., 2001**). MMPs play a central role in the regulation of multiple cellular functions such as proliferation, adhesion, migration, differentiation, angiogenesis, and apoptosis. The most important MMPs playing an important role in the pathogenesis of PF are the following:

a) MMP-1 is also known as collagenase-1, fibroblast collagenase, and interstitial collagenase. It is the prototype of MMPs capable of degrading fibrillar collagens (I and III), the most abundant proteins of the ECM (**Brinckerhoff and Matrisian, 2002; Pardo and Selman, 2005**). MMP-1 is primarily localised in reactive alveolar epithelial cells and bronchiolar epithelial cells lining honeycomb cystic spaces and is virtually absent from the interstitial compartment where collagen is being accumulated (**Fukuda et al., 1998; Selman et al., 2000**).

b) MMP-2 (gelatinase A) is known to be produced by tissue structural cells including fibroblasts and endothelial cells, and is known to degrade type IV collagen and other basement-membrane components. MMP-2 is found in alveolar and basal bronchiolar epithelial cells and in fibroblastic foci (**Fukuda et al., 1998**), which seems to be an important event in PF pathogenesis that enhances the fibroblast invasion into the alveolar spaces. The involvement of MMP-2 in ECM deposition was also suggested in a model of BLM-induced PF in rabbits (**Yaguchi et al., 1998**).

c) MMP-7 has a strong affinity for heparin and is able to degrade and process several ECMs as well as a number of bioactive substrates. MMP-7 null mice are normal in appearance and it is of note that they develop attenuated lung fibrosis in respose to BLM (**Zuo et al., 2002; Li et al., 2002**). Different studies have suggested that MMP-7 plays a physiologic role in reepithelialization, apoptosis, inflammation, and innate immunity, among others (**McIntyre and Matrisian, 2003**).

d) MMP-9 (gelatinase B) is produced by inflammatory cells such as macrophages, neutrophils, and eosinophils (**Murphy and Docherty, 1992; Hoshino et al., 1998**) and has been localised in epithelial cells, neutrophils, and macrophages with some staining in subepithelial fibroblasts. In BLM-induced PF, an increase of gelatinase B activity and disruption of the alveolar epithelial basement membrane has been reported (**Yaguchi et al., 1998**). Despite the putative role of MMP-9 in lung fibrosis, the MMP-9 null mice develop fibrosis similar to that of wild-type littermates after BLM instillation.

I.3.2. Oxidative stress (myeloperoxidase)

Pulmonary fibrosis is characterised by the presence of alveolitis, and a characteristic feature of alveolitis is the presence of neutrophils (**Hunninghake et al., 1991**). Bronchoalveolar lavage (BAL) fluid of PF patients display elevated levels of MPO, eosinophil cationic protein, 8-isoprostane, and nitrite/nitrate levels, all of which are markers of increased oxidative stress, suggesting that both neutrophilic and eosinophilic granulocytes are involved in the pathogenesis of human PF (**Kinnula and Myllarniemi, 2008**). This is especially noteworthy in experimental models of lung injury elicited by BLM. MPO, a heme protein abundantly expressed in neutrophils, is generally associated with killing of bacteria and oxidative tissue injury. Recruitment and activation of polymorphonuclear neutrophil granulocytes is among the principal defense mechanisms of innate immunity and their programmed cell death and removal are critical for efficient resolution of acute inflammation. However, neutrophil-derived proteinases and ROS are also capable of inflicting tissue damage (**Klebanoff, 2005**). These mediators induce cellular dysfunction, disturbes cell-cell contacts and shedding of cells from the basal membrane. Sensible nerve endings are uncovered promoting airway hyperreactivity. Tissue repair promoted by fibroblasts may lead to structural changes with exaggerated production of collagen fibres resulting in basal membrane thickening (remodelling). If inflammation persists, regenerated cells do not differentiate into ciliated, but into squamous epithelium (metaplasia) and goblet cells (goblet cell hyperplasia).

MPO catalyzes the formation of hypochlorous acid, a potent oxidant that has been implicated in killing bacteria (**Nathan, 2002**) and tissue destruction through induction of necrosis and apoptosis (**Wagner et al., 2000; Klebanoff, 2005**). MPO, through formation of secondary oxidants and nitration of protein tyrosine residues, could

modulate intercellular signaling in the vasculature (**Nichols and Hassen, 2005**) and affect the activation state of neutrophils (**Lau et al., 2005**). Neutrophil trafficking into inflamed tissues is intimately linked to prolonged survival. Mature neutrophils have the shortest half-life (around 7 hours) among leukocytes and die rapidly via apoptosis (**Lee et al., 1993**). This constitutively expressed cell death program renders neutrophils unresponsive to proinflammatory stimuli and promotes their removal from inflamed areas by scavenger macrophages with minimal damage to the surrounding tissue, thereby facilitating the resolution of inflammation (**Gilroy et al., 2004**). Neutrophil survival is contingent on rescue from apoptosis by signals, such as lipopolysaccharide or proinflammatory cytokines, from the inflammatory microenvironment (**Simon, 2003**). Markedly suppressed neutrophil apoptosis has been detected in patients with inflammatory diseases that are also associated with elevated intravascular MPO levels (**Brennan et al., 2003**). However, the link between MPO and the fate of neutrophils is unclear. Understanding the role of MPO in regulating neutrophil survival and apoptosis will provide important information regarding development of novel targeted therapies for dampening inflammation underlying a variety of diseases (**El Kebir et al., 2008**).

In addition, alveolar macrophages isolated from patients with PF and experimental fibrotic models generate ROS and arachidonic acid metabolites. The ROS have been implicated in mediating fibroblast proliferation (**Razzaque and Taguchi, 2003**). High levels of MPO and low levels of glutathione, an important antioxidant, have been detected in the alveolar epithelial ligning fluid of patients with PF (**Cantin et al., 1987a; Cantin et al., 1987b**) suggesting the role of oxidant-mediated injury in PF. It is believed that in PF, the destruction of lung parenchyma results from the chronic presence of neutrophils in the alveolar structures (**Hunninghake et al., 1991**). It is therefore likely that neutrophils mediate this parenchymal injury by secreting various enzymes, including collagenase, which are capable of deranging the connective tissue matrix of the lung.

Current animal models of PF, such as the BLM model, have clear involvement of ROS in their pathogenesis (**Day, 2008**). The intrapulmonary sequestration of neutrophils in the lungs of BLM-treated rodents is known to contribute to pathogenic process of acute lung injury by way of generating ROS and releasing proteolytic and and MPO enzymes (**Iyer et al., 1998**). In fact, the inflammatory response to intratracheal instillation of BLM starts with an acute neutrophilic infiltrate, followed by a transition to a lymphocyte predominant chronic inflammation (**Izbicki et al., 2002**). As already mentioned, the released MPO catalyses a reaction of H_2O_2 with chloride ions to form hypochlorous

acid. Hypochlorous acid is extremely reactive and cytotoxic and immediately oxidises various vital constituents of cells and causes depletion of cellular NAD^+ and adenosine triphosphate, leading to cell death. In fact, the drugs that decrease the BLM-induced increases of MPO activity in the lung also attenuate BLM-induced toxicity (**O'Neill and Giri, 1992**).

I.3.3 Pulmonary fibrosis

I.3.3.1 Definitions and classification

The Idiopathic interstitial pneumonias (IIPs) are a heterogeneous group of nonneoplastic disorders resulting from damage to the lung parenchyma by varying patterns of inflammation and fibrosis. The interstitium is the microscopic space between the basement membranes of the alveolar epithelium and capillary endothelium, and forms part of the blood-gas barrier (**Dempsey, 2006**) and it is the primary site of injury in the IIPs. IIPs are characterised by expansion of the interstitial compartment by inflammatory cells, with associated fibrosis in many cases (**Dempsey, 2006; Visscher and Myers, 2006**). However, these disorders frequently affect not only the interstitium, but also the airspaces, peripheral airways, and vessels along with their respective epithelial and endothelial linings **(Cushley et al., 1999)**.

Idiopathic indicates unknown cause and *interstitial pneumonia* refers to involvement of the lung parenchyma by varying combinations of fibrosis and inflammation, in contrast to airspace disease typically seen in bacterial pneumonia. In 1969, Liebow and Carrington published a landmark histopathologic classification schema for the IIPs consisting of 5 patterns (**Liebow and Carrington, 1969; Kim et al., 2006**). Three decades later, Katzenstein and Myers incorporated several distinguishing features: the temporal heterogeneity of inflammation and fibrosis, the extent of inflammation, the extent of fibroblastic proliferation, the extent of accumulation of intraalveolar macrophages, and the presence of honeycombing of hyaline membranes (**Katzenstein and Myers, 1998; Kim et al., 2006**). In the American Thoracic Society/European Respiratory Society consensus classification (**ATS, 2002**), idiopathic interstitial pneumonias are classified into seven clinicopathologic entities (Table 2). The classification is largely based on histopathology, but depends on the close interaction of clinician, radiologist, and pathologist (**Kim et al., 2006**).

Idiopathic pulmonary fibrosis (IPF) is the most common form, accounting for approximately 60% of cases and is associated with a classic pathologic pattern called usual interstitial pneumonia (UIP) (**Dempsey, 2006**). It is important to be aware that in UIP, *pneumonia* is used to describe inflammation (rather than infection), while *usual* indicates that the histological pattern is that most commonly observed. However, the IIPs that best characterise our animal model of BLM-induced lung injury are NSIP, DIP, AIP and LIP, rather than IPF.

Table 2. Histologic and clinical classification of Idiopathic Interstitial Pneumonias (**Kim et al., 2006**).

		ATS/ERS (2002)	
Liebow & Carrington (1969)	Katzenstein & Myers (1998)	Histologic patterns	Clinical-Radiologic-Pathologic Diagnosis
UIP	UIP	UIP	Idiopathic pulmonary fibrosis/ cryptogenic fibrosing alveolitis
	NSIP	NSIP	Nonspecific interstitial pneumonia (provisional)
BIP		OP	Cryptogenic organizing pneumonia
	AIP	DAD	Acute interstitial pneumonia
	RB-ILD	RB	Respiratory bronchiolitis interstitial lung disease
DIP	DIP	DIP	Desquamative interstitial pneumonia
LIP		LIP	Lymphoid interstitial pneumonia

Definition of abbreviations: AIP= acute interstitial pneumonia; BIP= Bronchiolitis obliterans interstitial pneumonia and diffuse alveolar damage; DAD= diffuse alveolar damage; DIP= desquamative interstitial pneumonia; GIP= giant cell interstitial pneumonia; LIP= lymphocytic interstitial pneumonia; NSIP= nonspecific interstitial pneumonia; OP= organizing pneumonia; RB= respiratory bronchiolitis; RB-ILD= respiratory bronchiolitis-interstitial lung disease; UIP= usual interstitial pneumonia.

I.3.3.2 Pathogenesis

IIPs result from persistent inflammation with attendant activation of inflammatory cells, i.e. alveolar macrophages, neutrophils, eosinophils, T-cells, B-cells, basophils and mast cells, which release various oxidants, proteases, cytokines and growth factors

that further modulate the inflammatory response. Also epithelial, endothelial and mesenchymal cells act as chemoattractants and further release polypeptides contributing to the inflammatory milieu (**Wolff and Crystal, 1997**). MMPs contribute to the breakdown and remodelling that occurs during lung injury **(Fukuda et al., 1998; Selman et al., 2000**), and may also modulate inflammatory response by releasing growth factors and cytokines known to influence growth and differentiation of target cells within the lung into damaged lung tissues (**Winkler and Fowlkes, 2002**). Growth factors modulate the emergence and persistence of myofibroblasts, synthesis of ECM proteins, production of MMPs and their inhibitors, expression of adhesion molecules, chemotaxis, angiogenesis, and probably apoptosis of parenchymal cells (**Allen and Spiteri, 2002**).

A basic morphological defect is injury in the intraluminal epithelium and its basal membrane leading to migration of fibroblasts and myofibroblasts from the interstitial compartment into air spaces. This leads to formation of intraluminal fibrosis, which mediates fusion of adjacent alveolar structures and further remodelling of interstitium (**Basset et al., 1986**). In advanced PF there is finally disorder of the tissue, distorted matrix deposition, mesenchymal cell proliferation and alteration to normal lung structure, with compromised gas exchange function (**Wolff and Crystal, 1997**).

I.4. LUNG BIOMECHANICS

I.4.1. Physiology of the lung

The lung inflates due to negative pressure (respective to the atmosphere) applied at its surface by the respiratory muscles. Deflation normally occurs passively as a result of the static recoil of the lung and chest wall, but effort by the internal intercostals and abdominal muscles can supply an active contribution during exercise. Most of the mechanical energy expended during inflation is elastic and is thus recovered during deflation. The remaining energy is dissipated through viscous effects in both the airways and the tissues. These processes comprise the mechanics of the respiratory system.

I.4.2. Lung structure

Surrounding the lung is the visceral pleura, which smoothly slides against the parietal pleura lining the ribcage, diaphragm and mediastinum. Upon inspiration, air is conducted from the mouth and nose through the airways to the sites of gas exchange, the alveoli. The airways form an asymmetric tree-like structure branching through a series of bifurcations to successively smaller bronchi, lobar, segmental and subsegmental bronchi, small bronchi, bronchioles, respiratory bronchioles, and finally to the alveolar ducts and alveoli.

In humans, the mean number of generations of branching airways from the trachea to alveoli is 23, but a given path can have many more or less branches. Some alveoli are located along the respiratory bronchioles, but most alveoli line the alveolar ducts. The walls of the airways larger than generations 12-16 contain cartilage which contributes to maintaining airway caliber. In the smaller airways, caliber is maintained through connection with the surrounding parenchyma. The alveoli are the sites of gas exchange and comprise a total surface area from 43 to 102 m^2 depending on body size (**Weibel and Gil, 1977**).

Gas is exchanged by passive diffusion through the alveolar walls to an extensive network of pulmonary capillaries that form part of the pulmonary circulation. Separating the blood within the capillaries from the air in the lung are the endothelial layer of the capillaries, the pulmonary interstitium filled with the interstitial fluid, and the alveolar epithelium. The alveoli and septa comprise the large part of the lung parenchyma which tethers both airways and vasculature. The septa are thicker bands of fibrous tissue which branch through the parenchyma subdividing different lung structures from the acini (the collection of alveoli fed by a single terminal bronchiole) to the largest segments dividing the lung lobes. Within the alveolar walls, free edges and septa run a complex interconnected network of collagen and elastin fibres both embedded in the ground substance (**Hance and Crystal, 1975**).

I.4.3. Concepts of mechanical parametres

I.4.3.1. Resistance

Resistance is the amount of pressure required to cause a unit change of gas flow. Pulmonary resistance, the sum of airway resistance and lung tissue resistance, can be measured during spontaneous breathing from simultaneous measurements of transpulmonary pressure, airflow, and volume. However, in this thesis we will only address the lung tissue resistance (Rti) or tissue damping (G). Tissue is closely related to tissue resistance and reflects the energy dissipation in the lung tissues. Tissue damping is calculated by fitting the constant phase model (which is described in 4.4 section and in the study design) to input impedance (Z) or Young complex modulus (Ψ). Unlike tissue resistance, tissue damping is independent of frequency, so that it can be reported without including the frequency at which it was measured. G can be calculated from Rti for any given frequency.

$$G = Rti \cdot \omega$$

where Rti is lung tissue resistance and ω is the angular frequency.

I.4.3.2. Elastance and compliance

The lung is an elastic structure with an anatomical organization that promotes its deflation, much like an inflated balloon. Surface forces at alveolar level (alveolar lining or surfactant), prevent the complete deflation of alveoli. The word elasticity is defined as the tendency of the body to return to its original shape after it has been stretched or compressed. While the elastic properties of the lung are important to bring about expiration, they also oppose lung inflation. As a result, lung inflation depends upon contraction of the inspiratory muscles. How easily a lung inflates will relate to the compliance of the lung. Elastance is defined as the amount of pressure needed to modify pulmonary volume. In this thesis we will describe elastance as tissue elastance (Eti) or H. The parameter H is closely related to Eti and reflects the energy conservation in the lung tissues:

$$Eti = H\omega^{1-\alpha}$$

Compliance is the reciprocal of elastance. In the intact lung, the increase in the pulmonary volume during the inspiratory phase leads to lung inflation resulting in a distension of the elastic structures. The relationship between the inspired volume and the variation in the transpulmonary pressure represents the compliance of the lung (open-chest).

$$C_L = \frac{\Delta Vol}{\Delta Ptp} \qquad \text{(L/cm } H_2O\text{)}$$

where C_L is the compliance of the lung, ΔVol is the change of volume, and $\Delta Palv$ is the change of transpulmonary pressure (alveolar minus pleural pressure). In lung strips, tissue compliance (Cti) is determined by the strain obtained for a unit change in stress. Low compliance indicates a stiff lung and means extra work is required to bring in a normal volume of air. This occurs as the lungs in this case become fibrotic, lose their distensibility and become stiffer.

I.4.3.3. Hysteresivity

Hysteresivity (η), introduced by Fredberg and Stamenovic (**Fredberg and Stamenovic, 1989; Sakai et al., 2001**), is a material property of the tissue and is defined as the energy dissipated relative to the elastic energy stored in the tissue in a cycle. As such, η should only depend on the material composition of the tissue. The value of η for lung, which is usually obtained in isolated-lung (IL) or open-chest (OC) conditions, is between 0.12 and 0.25 (**Hantos et al., 1987; Hantos et al., 1992; Lutchen et al., 1993**). In contrast, the values of η for tissue strip range from 0.05 to 0.1 (**Fredberg and Stamenovic, 1989; Navajas et al., 1995; Rocco et al., 2001**). This discrepancy between lung and tissue strip η values may be attributed to 1) the lack of surface tension in the tissue strip; 2) differences in mechanical behaviour due to the three-dimensional uniform stretching of the lung versus uniaxial stretching of the tissue strip; and 3) heterogeneity of the lung and the respiratory system contributing to η extracted from whole lung measurements but not to η of the tissue strip.

Furthermore, potential factors contributing to tissue hysteresis include: changes in the behaviour of the air-liquid interface (**Bachofen et al., 1970**), modification of the collagen-elastin-proteoglycan network after contractile element activation (**Yuan et al.,**

2000; Romero et al., 2001), changes in the hysteretic properties of contractile elements located either in the parenchyma or in subtended airways (**Kapanci et al., 1978; Romero et al., 1998**), or differences in the recruitment-derecruitment of alveolar spaces duryin cycling (**Smaldone et al., 1983**).

I.4.4. Measurements of lung tissue mechanics

Traditional biomechanics has focused on characterising the macroscopic structural and mechanical properties of living tissues and organs by establishing mathematical relations, called the constitutive equations, that describe how mechanical stresses (force per unit area) change in response to a change in the size and/or shape of a body usually given in terms of strain (relative change in dimension). The constitutive equations are often nonlinear and can describe the static relationship between stress and strain. When the constitutive equations also include time-dependent or dynamic relations between stresses and strains, the tissue is referred to as viscoelastic. All living tissues display viscoelastic behaviour (**Fung, 1993**), reflecting the finite time required for the constituent fibres, cells and fluids to adjust their local configurations in response to a change in macroscopic tissue strain. The precise link between the complex rheology of biological soft tissue and its microstructure is still poorly understood, although various theories have been proposed such as the notion that stress relaxation may occur through cascades of micro-ruptures within the tissue (**Bates, 2007**) or slow undulation of fibres (**Suki et al., 1994**). In any case, the constitutive equations are commonly determined from measured static or dynamic stress–strain relationships. These relations depend on the mechanical behaviour of the individual constituents and their structural distribution in the tissue (**Fung, 1993**).

All connective tissues are composed of cells and ECM that includes water and a variety of biological macromolecules. The macromolecules that are most important in determining the mechanical properties of these tissues are collagen, elastin and proteoglycans. Among the macromolecules, collagen is the most abundant and perhaps most critical for structural integrity. One might expect therefore that the amount of collagen in a tissue is the primary determinant of its mechanical properties. However, different connective tissues with similar collagen content can exhibit different mechanical behaviour matching the specific needs of the organ (**Fung, 1993**). During the last decade, the advent of novel imaging techniques (**Cox et al., 2003**) and quantitative computational modelling (**Redaelli et al., 2003**) have allowed the study of

micromechanics of specific components of tissues and hence improved our understanding of the relationships between tissue composition, microstructure, and macrophysiology. In particular, it has become evident that macrophysiology reflects both the mechanical properties of the individual components of the tissues, as well as the complexity of its structure (**Suki et al., 2005**).

The assessment of lung mechanical function in animal models of pulmonary disease is widely used for investigation of various pathologies. The mechanical properties of pulmonary parenchyma are major determinants of lung physiological function (**Leite-Junior et al., 2003**). Knowledge of the contribution of the lung tissues to the mechanics of breathing can be obtained in 3 ways: via direct measurements “in vitro”, by partitioning tissue and airway behaviour “in vivo” using alveolar capsule technique (**Fredberg et al., 1984; Ludwig et al., 1991; Romero et al., 1998**), or via modeling approaches. Direct measurements of the tissue are done on excised samples of lung parenchyma, usually maintained in a tissue bath, by uniaxial, biaxial or triaxial stretching. Each method has advantages and disadvantages, and can be viewed as complementary to the others. Lung parenchymal strips are considered a good approximation of the peripheral lung tissue, and are commonly used in studies of the mechanical and pharmacological properties of lung periphery (**Romero et al., 2001**). Examining the behaviour of the lung parenchyma “in vitro” offers some potential advantages, as some of the mechanisms contributing to hysteresis “in vivo” should not be present in the “in vitro” preparation: surfactant and localised atelectasis.

The first measurements of lung tissue “in vitro” were made by Radford in 1957 (**Radford, 1957**), who found that tissue strips from dog lungs exhibited very nonlinear elastic properties. Suwa et al. (**1966**) measured the length-tension relationships for a single extension of human lung parenchymal strips, and found that force was an exponential function of the strain. The length-tension relationship of human alveolar wall segments was found to be similar by Fukaya et al. (**1968**), who showed that the length-tension curves exhibited tissue hysteresis. They also observed that lung tissue exhibited stress-relaxation after a step change in force. Sugihara et al. (**1971, 1972**) measured human alveolar wall segments and showed very similar results, and demonstrated that neither age, nor sex nor diseases altered the amounts of hysteresis or stress-relaxation.

Measurements of larger samples (1 cm^3) of parenchyma subjected to triaxial loading were obtained by Hoppin et al. (**1975**), who searched for tissue anisotropy by looking

for differences in the stress-strain curves and hysteresis along different axes. They concluded that either the degree of anisotropy was small and not systematically distributed throughout the lung, or that the observed anisotropy was due to differences in experimental handling of each sample. Tai and Lee (**1981**) also examined isotropy and homogeneity in triaxial tests of dog parenchyma. They found less than 10% anisotropy in young dogs and less in older dogs. Also, no regional variation was discovered in lung samples taken from different parts of the lung. They therefore concluded that biomechanical properties of lung tissue can be reasonably estimated from measurements done in uniaxial loading or deformation.

The mechanical properties of the lung parenchyma are determined partly by a tension skeleton made up of connective tissue fibres that spread throughout the lung in an organised fashion (network) and partly by surfaces acting forces (**Sly et al., 2003**). The tension skeleton consists of 1) axial fibres that fan out centrifugally from the hilum along the branching airway tree, 2) peripheral fibres that originate in the pleura and penetrate centripetally into the lung, and 3) alveolar septal fibres that join the two. The pulmonary interstitium contains myofibroblasts that contain actin and myosin microfilaments of the smooth muscle type, collagen and elastin fibres, and some free extracellular fluid related to lymph.

From the mechanical point of view, the collagen and elastin fibres are intimately associated and cannot really be considered to be separate. Fredberg and Stamenovic (**1989**) proposed the structural damping paradigm, according to which dissipative properties of lung tissue (G or frequency-dependent tissue resistance) and the elastic properties were coupled and could be expressed as η. Under this paradigm, η should only depend on the material composition of the tissue. Indeed, η has been shown to be relatively constant across species under a variety of experimental circumstances, although η has been shown to increase in response to constrictor agonists both “in vivo” and “in vitro” **(Hantos et al., 1995; Petak et al., 1997; Nagase and Ludwig, 1998**) and to differ in magnitude between intact lungs and tissue strips (**Sakai et al., 2001**).

As above mentioned, Fredberg and Stamenovic (**1989**) noted that the ratio between the dissipative and elastic parts of lung tissue impedance were well conserved across species, and was nearly independent of frequency and oscillation amplitude. Accordingly, they introduced the structural damping hypothesis, which relates the

dissipation and elastic storage of energy through a single constant which they called tissue hysteresivity, η, where

$$\eta = \omega \frac{R}{E} = \frac{G}{H} \qquad (1)$$

This hypothesis implies that energy dissipation and storage in lung tissue are intimately coupled. To describe the dynamic behaviour of the tissue strip, Hantos et al. (**1987**) introduced the constant phase model

$$Z(\omega) = \frac{G_{ti} - jH_{ti}}{\omega^{\alpha_1}} \qquad (2)$$

where Z (ω) is the mechanical impedance of the lung tissues, G_{ti} and H_{ti} are coefficients of damping and elastance in tissue strips (ti), *j* is the positive square root of –1, and

$$\alpha_t = (2/\pi)\arctan(H_{ti}/G_{ti}) \qquad (3)$$

Both elastic and dissipative parts of Z (ω) follow the same frequency dependence, and the phase is independent of frequency. This model was used in other studies as a tissue compartment for the lungs and chest walls of cats (**Hantos et al., 1992**) and for dog lungs (**Hantos et al., 1992; Petak et al., 1993; Lutchen et al., 1994**). In the time domain, the step response of the constant phase tissue model is

$$P(t)/\Delta V = ct^{-d} \qquad (4)$$

which is essentially to the description of stress-relaxation in elastic balloons given by Hildebrandt (**1969**). Suki et al. (**1994**) developed a mathematical framework for the basis of the constant phase model. They showed that one could develop in this model by replacing ordinary time derivatives with fractional derivatives, and introduced a new constitutive element called the springpot based on the fractional calculus as defined by Koeller (**1984**). The stress response of the springpot is determined by the fractional derivative of the strain which incorporates dependence on the past strain with a fading memory, rather than the instantaneous derivative of integer calculus. A physical basis for this model was provided from models of polymer viscoelasticity, which take into

account the complexity and statistical nature of the motion of long polymer chains (**Suki et al., 1994**).

The structure of the constant-phase model is extremely simple and obviously neglects many potentially important details of a real lung. In particular, it assumes uniform alveolar ventilation, which occurs when the regional mechanical properties of the lung are identical throughout the organ. In other words, the rigorous application of the constant-phase model to Z_L data becomes problematic once the behaviour of the lungs departs significantly from that upon which the model is based, namely homogeneity and linearity. Heterogeneity occurs when either the rheological properties of different regions of parenchyma (i.e local G and H) or the resistances of their subtending airways start to diverge from each other, and seems to be characteristic specific mechanical properties means greater heterogeneity of function. Even so, the constant-phase model still frequently fits Z_L spectra with remarkable precision during pathological conditions such as bronchoconstriction, acute lung injury and emphysema (**Bates and Allen, 2006**).

The ratio G/H known as hysteresivity (η), also increases with the development of heterogeneity. However, this leaves open the question as to why decreases in η never seem to be observed experimentally in situations where heterogeneity would be expected to increase. Indeed, on the basis of these findings, some studies have used an increase in η to infer the presence of mechanical heterogeneity in the lung, due either to variations in local airway resistance or local tissue rheology. Nevertheless, this behaviour of η with heterogeneity remains an empirical finding, so its generality remains in question. One hypothesis is that η can once again decrease when heterogeneity becomes extreme because there is a limit to how narrow an airway can become before it suddenly closes completely, perhaps due to liquid bridge formation across the lumen, a phenomenon that is known to occur in the lung.

I.4.5. Mechanical forces in pulmonary fibrosis

The connective tissue of the lung is a dynamic structure, both in normal functioning and diseased lungs. The tissue is formed as a result of a molecular hierarchical organisation living in a dynamic balance between continuous breakdown and remodelling, both modulated by mechanical forces. When this delicate dynamic balance is altered by external or internal chemical changes, the system dynamically

remodels itself either by an excess of producing or breaking up these large complex macromolecular structures. As a result, the tissue modifies its chemical and structural composition depending on how altered the biomechanical properties are. However, we will not fully understand tissue mechanics and lung function only by biochemical purification and biophysical study of the molecules. Thus, connective tissues must be studied as an integrated system within their natural biochemical and mechanical environments (**Suki et al., 2005**).

Additionally, to ascertain how PF propagate spatially in the tissue and how it progresses with time, it is essential to map the regional correlation between cell signalling, matrix composition, and the local biomechanical properties of the tissue. Hitherto, it is reckoned that PF is triggered by changes in the biochemical microenvironment. However, as soon as the composition of the ECM is altered, either because of the direct injury or cellular remodelling, there are corresponding changes in the biomechanical properties of the matrix and consequently of the alveolar wall. This alteration in matrix properties enhances a change in the local deformation of the alveolar wall. To maintain the mechanical balance, the network of the alveoli has to reorganise itself. Consequently, local prestress on the alveolar walls changes, causing a feedback effect on cell signaling that leads to further assembly of matrix molecules.

During fibrosis, there is significant collagen deposition in the lung that is accompanied by stiffening of the lung tissue (**Dolhnikoff et al., 1999; Ebihara et al., 2000; Faffe et al., 2001**). Interestingly, while both the elastic and collagen fiber contents increase, changes in the overall viscoelastic properties of the lung tissue appear to correlate with the contents of collagen (**Dolhnikoff et al., 1999**) or proteoglycans **(Ebihara et al., 2000**), suggesting that it is reorganisation of the fibres that is most responsible for the altered mechanical properties of the tissue. However, little is known about the organisation and stiffness of individual collagen fibrils and fibres in fibrosis, making this an important area for future research. In cardiovascular tissues, the fibrotic increase in stiffness is attributed to the deposition of extra collagen and also possibly to increased collagen cross-linking associated with the formation of advanced glycosylation end-products (**Suki and Bates, 2008**). If the maturation of cross-linking is faster than the turnover of collagen itself then fibrotic lesions develop and lead to an increased local stiffness, a process similar to aging (**Avery and Bailey, 2005**). It is unclear, however, how the locally formed fibrotic lesions influence organ level function. Indeed, the few published studies in the lung are somewhat contradictory in their accounts of the

correlation between mechanical properties and collagen content (**Goldstein et al., 1979; Ebihara et al., 2000**).

I.5. ANIMAL MODELS OF LUNG INJURY

I.5.1. Objectives

The idea behind the use of animal models is to ascertain an accurate representation of human disease “in vivo”. The targets are to elucidate the pathophysiology/pathogenetic basis and to identify the cellular interactions and molecular pathways involved in lung tissue remodelling. In the study of PF, there is an increasing need to use the most appropriate animal model that mimics every aspect of human PF. As no single method has been able to fulfil this criterion, the final choice it is basically driven by the scant knowledge of the PF features the target of the study and money-wise considerations.

I.5.2. Advantages and disadvantages of animal models

What differentiate each animal model are two aspects: 1) the ease by which PF is developed and 2) the approach of mimicking an established clinical feature. Thus, its relevance will fall on the maximal approximation of the aspects mentioned before. Furthermore, animal models have the potential to understand the genetic factors, biochemical molecules and environmental interactions that altogether lead to the development of PF. In fact, much of the knowledge acquired in the biological processes involved in the pathogenesis of PF is due to data extracted from animal models (**Chua et al., 2005b; Chaudary et al., 2006**). However, caution is needed when interpreting data derived from such models and extrapolating them to the human disease, even if they show to be able to replicate the major structural and biochemical abnormalities described in the human PF (**Cooper, 2000**). Especially, when cessation or removal of the fibrogenic agent, reverse or diminish the previously induced fibrotic changes, an event not seen in human lung fibrosis. In other words, the use of drugs to recreate fibrosis in certain animal models, act “in lieu” and cannot equate to a disease state (**Chua et al., 2005b**). Another major limitation of animal models is the attempt to reproduce aberrant lung matrix remodelling, that takes years in humans, over shorter periods of time. In the BLM model, lung remodelling is accelerated (the induced lung damage does not mature stepwise into progressive interstitial alveolar fibrosis) and

when chronic, develops focal emphysema-like changes (the pathologic features revealed at the time of the analysis does not equate to the human PF). To conclude, the BLM model is a more useful model to study general PF than to study a concrete disease such as IPF.

I.5.3. Animal models for the development of pulmonary fibrosis

A number of exogenously administered agents can induce PF in a variety of animal species (Table 3). It is important to bear in mind that most (if not all) experimental animal models of fibrosis represent an inflammatory-driven lung fibrosis and do not develop the typical progressive and destructive pattern that characterises IPF (**Selman and Pardo, 2006**). Regardless of the inciting agent, one crucial requirement of any model is the capacity to produce long-lasting lesions akin to those seen in fibrotic human lungs. It is not casual that the advancements of molecular techniques coincided with major advances in transgenic technologies. *Knockout* or null mice are those in which a target gene is removed or mutated and thus, prone to develop PF when elicited by BLM. Bleomycin-induced lung injury model has been recently utilized in either transgenic or *knockout* rodents, to better understand the molecular mechanisms that lead to PF, as well as for novel drug assessments in therapy.

Table 3. Approaches for inducing PF in animal models (**Chua et al., 2005b**).

Exogenous Agent	Nature of Tissue Damage	Animal species used
Bleomycin	Oxidant-mediated DNA scission, leading to fibrinogenic cytokine release	Mice, rats, hamsters, rabbits, dogs, primates, pheasants
Inorganic particles(silica, asbestos)	Type IV hypersensitivity reactions with or without granuloma formation	Mice, rats, hamsters, sheep, rabbits
Irradiation	Free radical-mediated DNA damage	Mice, rats, rabbits, dogs, hamsters, sheep, primates
Gene transfer (TGF-β, IL-1β, GM-CSF)	Downstream activation of specific cytokine pathway/s	Mice, rats
Fluorescein isothiocyanate	Incompletely understood.	Mice

	Presumed T-cell independent	
Vanadium pentoxide	Incompletely understood. An inorganic metal oxide	Mice, rats
Haptenic antigens (i.e. trinitrobenzen sulphonic acid compounds)	Recall cell-mediated immune response	Mice, hamsters

I.5.3.1. Bleomycin molecule

Bleomycin is an antibiotic originally isolated in the early 1960s from *Streptomyces verticillis* (**Umezawa et al., 1966**). Bleomycins are a family of glycopeptide antibiotics with antitumor activity. This drug has been used as cytostatic treatment of many malignant tumors, such as germ cell tumors, lymphomas, head and neck, and Kaposi's sarcomas. Minor important adverse effects are myelossupression, nauseas, vomiting, allergic reactions, mucositis, alopecia, erythema, hyperkeratosis, hypopigmentation, skin ulceration, and acute arthritis (**Azambuja et al., 2005**). The side effects of the bleomycins are dose-dependent and involve lung inflammation that often proceeds to lung fibrosis (**Chen and Stubbe, 2005**). Thus, at high doses (>235mg), BLM can induce PF, a condition that is triggered by lipid peroxidation resulting in pulmonary insufficiency and leading to fatal hypoxemia (**Ramotar and Wang, 2003**).

Bleomycin is comprised of three functional domains, the N-terminal metal-binding domain, the C-terminal DNA-binding domain, and the carbohydrate moiety (Fig. 8). The N-terminal domain also binds to molecular oxygen, in addition to the minor groove of DNA, and is largely responsible for the antitumor activity of BLM. The BLM molecule has also, two main structural components; a bithiazole component which partially intercalates into the DNA helix, parting the strands, as well as pyrimidine and imidazole structures, which bind iron and oxygen forming an activated complex capable of releasing damaging oxidants in close proximity to the polynucleotide chains of DNA. This may lead to chain scission or structural modifications leading to release of free bases or their propenal derivatives. Its mechanism of action is breaking the DNA double helix by the production of free radicals, which is oxygen and iron dependent. Bleomycin may be inactivated by BLM hidrolase presents in normal and tumoral cells. The complex BLM-Fe has been the most studied because BLM joins the DNA and Fe at the same time, and release of free radicals happens in the presence of molecular oxygen.

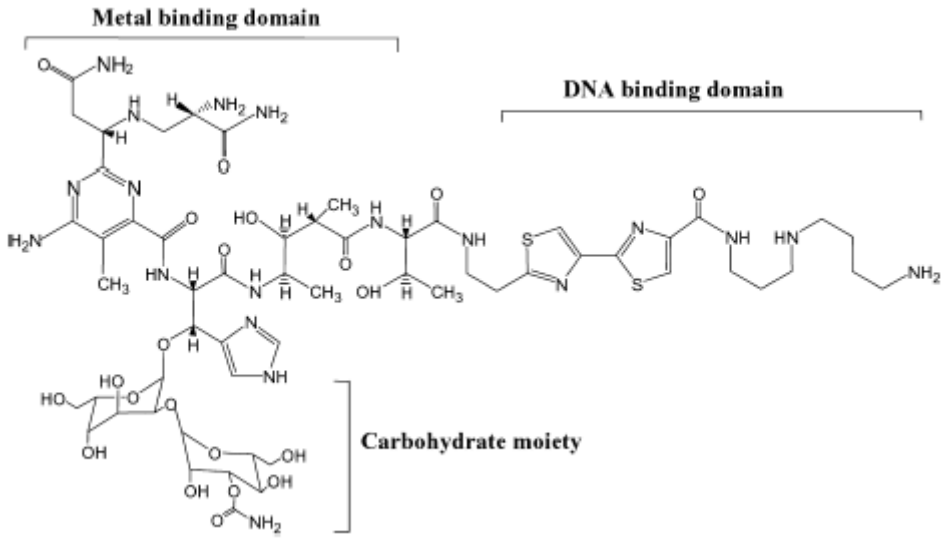

Figure 8. Structure of the antineoplastic BLM depicting the three domains.

I.5.3.2. Bleomycin-induced lung injury model

The potential of BLM to induce experimental PF was first described in dogs by Fleischmann in 1971 (**Fleischmann et al., 1971**). It was not until 8 years later, that Snider and colleagues reported and popularized the single-dose intratracheal route of administration in smaller animals (**Snider et al., 1978**). Since then, the BLM model has been widely used in the study of general PF as it shows a good approach regarding histological PF patterns such as patchy parenchymal inflammation of variable intensity (**Kaminski et al., 2000**), epithelial cell injury with reactive hyperplasia, basement membrane damage, fibroblast proliferation and ECM deposition (**Snider et al., 1978; Bowden, 1984**). Differences in the route administration (intratracheally, intravenous (i.v) and intraperitoneal (i.p)) have been reported. Intratracheal instillation induces broncholocentric distribution of fibrosis while the i.v and i.p route induce subpleural scarring (**Chua et al., 2005b**). Additionally, Harrison and Lazo (**1987**) developed a subcutaneous pathway to induce lung injury by means of implantation of osmotic minipumps containing BLM (100 mg/kg) in C57Bl/6 mice and the drug was delivered as a continuous s.c. infusion over 1 week. This subcutaneous way, was performed in an attempt to eradicate variable distribution of lesions, high mortality or a requirement for multiple procedures associated in drug-induced PF via a single intratracheal injection, a single i.v. injection or multiple s.c. injections.

The BLM model has been well established to study early stages of the disease. In the early stages, interstitial oedema, chronic inflammatory process, immune system reaction leading to the development of PF: fibroblast proliferation and ECM accumulation resulting in an aberrant architecture of the lung (**Hay et al., 1991; Harari and Caminati, 2005**) is seen in the BLM-induced lung injury in animals (Fig. 9). Single-dose induces subchronic lesions, and the structural abnormalities observed in animals resemble those seen in humans. However, to study pulmonary diseases in chronic stages, entails repeated drug dosing but from the histological point of view, what is observed in the animal it is not seen in the late chronic phase of PF in humans (**Borzone et al., 2001**). The importance of early inflammatory components in the pathogenesis of PF has been extensively debated (**Gauldie et al., 2002; Strieter et al., 2002; Lagente et al., 2005**). Thus, arguments in favor or against the role of acute and chronic inflammation have been reported on the basis of the data of numerous studies. It has been proposed that “fibrogenic microenvironment” including some tissue remodelling mediators interacting with the ECM could suffice to launch the fibrogenic process. It seems that the early inflammatory response is critical for the development of BLM-induced fibrosis.

Moreover, BLM-induced lung injury in susceptible strains of mice, provoked changes (lung epithelial cell death, followed by acute neutrophilic influx, subsequent chronic inflammation, and parenchymal fibrosis) within 4 weeks (**Dunsmore and Shapiro, 2004**). In some ways, these changes mimicked adult respiratory distress syndrome better than PF. However, the model does replicate some key pathologic features of human IPF, including fibroproliferation within the lung parenchyma, and hence pathologic mechanisms discerned in the mouse are worthy of consideration in humans. Furthermore, the clinical diagnosis of IPF is made late in the disease course when lung function is already half of that which existed prior to disease. Hence, causative factors and early natural history of IPF are largely unknown, making it a difficult disease to model.

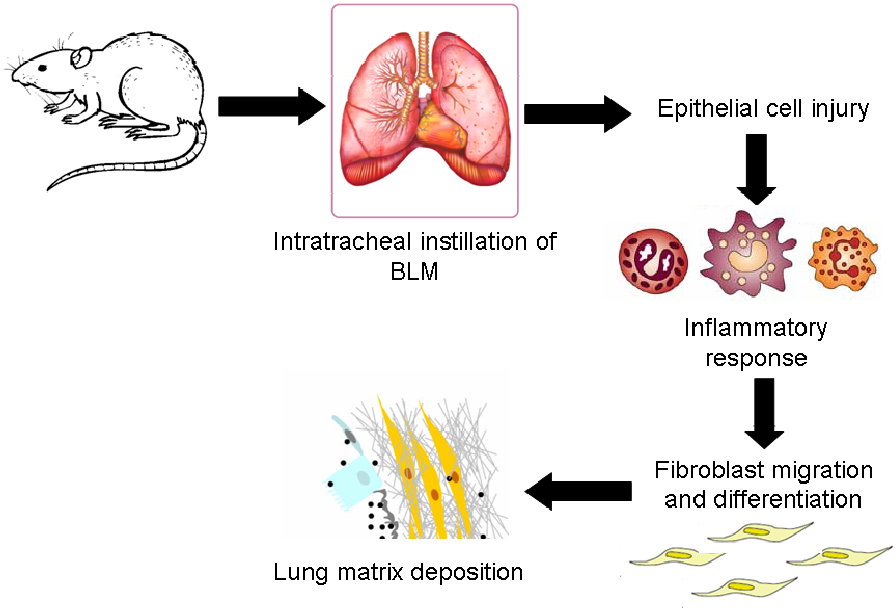

Figure 9. Scheme of BLM-induced lung injury model.

I.5.3.3. Mechanisms of bleomycin-induced lung damage

Bleomycin is able to cause cell damage independent from its effect on DNA by inducing lipid peroxidation. This may be particularly important in the lung and in part account for its ability to cause alveolar cell damage and subsequent pulmonary inflammation. The lung injury seen following BLM comprises an interstitial oedema with an influx of inflammatory and immune cells. This may lead to the development of PF, characterised by enhanced production and deposition of collagen and other matrix components (**Hay et al., 1991**).

In this line, Jones and Reeve (**1978**) injected BLM i.p. in mice and studied pulmonary changes for 4 weeks. Bleomycin damaged the pulmonary vessels and produced type I pneumocyte necrosis, resulting in non-uniform PF. The sequence of events leading to PF may be arbitrarily divided into three phases: firstly, a focal perivascular lesion consisting of interstitial oedema with plasma cell and lymphocyte infiltration; followed by the middle proliferative phase characterised by type I pneumocyte necrosis, intra-alveolar fibrin deposition, an increase in the numbers of type II pneumocytes and fibroblasts and an overall decrease in the alveolar diameter. The third phase consisted of organization, with intra-alveolar and interstitial collagen formation and the synthesis of elastin. These phases, although occurring sequentially, did not bear a constant time

relationship to the dosage schedule, for new early focal lesions continued to appear throughout the period of the experiment. These ultrastructural changes are not specific for BLM, but represent a general reaction of the lung to injury. The exact mechanism whereby BLM produces the lung damage has yet to be ascertained.

As mentioned before, this model is characterised by an early neutrophilic response, increased collagen deposition and fibroblast proliferation (**Chua et al., 2005b; Cuzzocrea et al., 2007**). Bleomycin alters the balance between oxidants and antioxidant defense systems in the lung. In this particular organ the selective absence of BLM hydrolase activity gives a high susceptibility to BLM-induced oxidative stress (**Filderman et al., 1988**). Contemporarily, hydroxyl radicals, superoxide anion radical, hydrogen peroxide, and peroxynitrite are increased by BLM administration (**Pron et al., 1994**). Reactive oxygen species (ROS) overproduction ultimately results in tissue injury, with activation of several intracellular signaling pathways leading to the production of pro- inflammatory cytokines (**Hubbard et al., 2002**). DNA is a target for ROS activity as well. Radical oxygen species by determining DNA damage in turn activates poly-(ADP-ribose) polymerase (PARP). This largely expressed nuclear protein contributes to the maintenance of genomic stability and to the repair of oxidative DNA damage (**Benjamin and Gill, 1980**). Although PARP activity promotes cell survival, PARP activation depletes NAD+, decreases ATP levels, thus leading to cell death after extensive DNA strand breaks (**Cosi and Marien, 1999**). Therefore, ROS produced in response to oxidative stress are able to contribute by multiple pathways to the pathogenesis of BLM induced lung injury.

The lung injury that develops in the initial 48h following intratracheal BLM is characterised histologically by perivascular oedema, capillary congestion and alveolar wall thickening. There is an inflammatory cell infiltrate in the alveolar wall thickening. There is an inflammatory cell infiltrate in the alveolar walls and spaces, together with intra-alveolar hemorrhage (**Thrall et al., 1979; Hay et al., 1987**). Some areas of alveoli are denuded of epithelium with necrosis of capillary endothelium. Despite the severity of lung injury, the process is patchy, with some normal areas of lung interspersed. Chandler et al. (**1983**) quantitated the cellular changes in hamsters 4 days following administration of BLM. They found about 10-fold increase in the number of macrophages and monocytes per unit area, an 8-fold increase in the number of neutrophils, and also the appearance of eosinophils. At this early stage is no evidence of fibrosis as assesses histologically or biochemically (**Thrall et al., 1979**). A common but not invariant outcome of the acute phase of BLM-induced lung injury is PF with

excessive accumulation of fibrous tissue in the lung interstitium. BLM administration leads to deposition of various matrix proteins including collagens of various type, elastin and proteoglycans.

Collagen deposition usually follows within a week after BLM administration in experimental animals and this is preceded by increased collagen synthesis. The localization of collagen deposition may be altered by the route of administration, i.e, intratracheal administration causes focal deposits, both peribronchial and subpleural (**Harrison and Lazo, 1987**). The precise nature of the interaction between BLM and the lung which leads to collagen deposition is uncertain. BLM could act directly on cells inducing collagen production, either on fibroblasts or other cells modifying their phenotype so that expression of type I and II collagens is enhanced, or by stimulating replication. It seems more likely that collagen production is linked with the response to BLM involving increased permeability and influx of proteins and inflammatory cells. Neutrophils are likely involved, since they reach their peak within several days after challenge, and they contain serine and metal proteases capable of breaking down collagen (**Clark et al., 1980**).

Recent studies demonstrated that excessive apoptotic cell death was responsible for acute lung injury leading to PF induced by BLM (**Okudela et al., 1999**). In fact, direct evidence for a role for TGF-β in BLM-induced lung fibrosis was suggested by studies of Khalil et al. (**1989**). They showed TGF-β levels were elevated within hours of BLM administration and that peak levels precede the maxima for collagen synthesis. Although TGF-β certainly plays some role in PF due to BLM or IPF, there may also be other pathways that result in epithelial cell apoptosis or other cellular alterations or other cellular alterations that play a part in the process. TGF-β induces p53 expression that, in turn, causes Fas-receptor clustering and caspase-8 activation with subsequent cellular apoptosis (**Muller et al., 1997; Tschopp et al., 1998; Allen and Cooper, 2000**) as seen in Fig. 10.

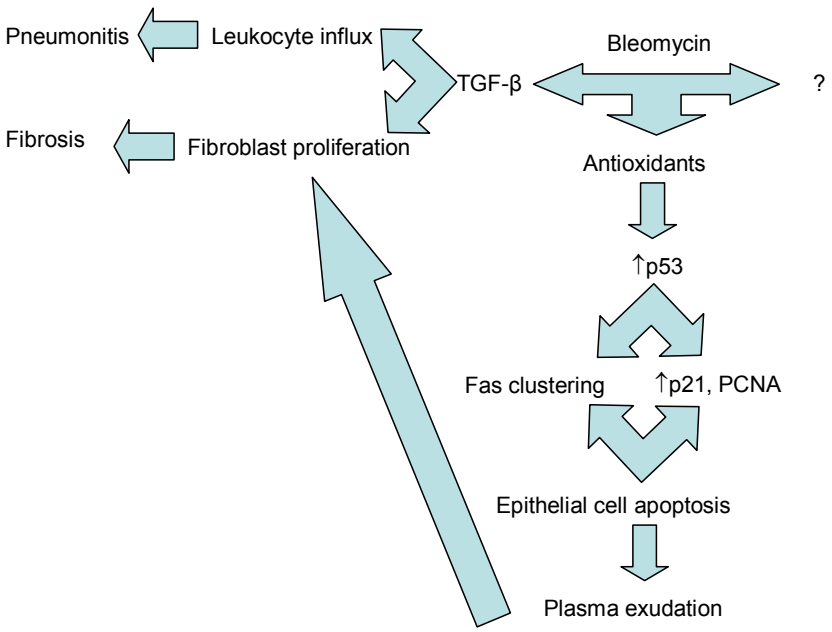

Figure 10. Potential pathways of pulmonary injury occurring during the process of pneumonitis/fibrosis. Adapted from **Allen and Cooper, 2002**.

Clustering of Fas is the result of altered receptor dynamics by p53. Apoptosis of malignant cells induced by BLM is also dependent on p53 through enhanced Fas expression. In other words, when cells are exposed to DNA-damaging agents such as BLM, they undergo cell cycle arrest to allow repair of the damaged DNA and/or apoptotic cell death to remove unrepairable DNA. In these processes, p53 may also be working through transcriptional activation of p21 $^{WAF1/PiC1}$ and PCNA (**Mishra et al., 2000**). Because p21 blocks the effect of PCNA on DNA polymerase, this could result in cell-growth arrest and apoptosis. As noted by Mishra and colleagues, p53 is expressed during normal wound healing (**Antoniades et al., 1994**). What differentiates normal lung repair from abnormal scar formation is still under debate. In fact there may be multiple pathways of p53 activation, either through activation of cytokines, particularly TGF-β, or by producing DNA abnormalities through production of reactive oxygen species.

II. HYPOTHESIS OF THE THESIS AND OBJECTIVES

II.1 HYPOTHESIS OF THE THESIS

Interstitial lung disorders (ILD) constitute a group of diseases that are both unresponsive to treatment and life threatening. These diseases are characterised by abnormal interstitial remodelling, but the biochemical mechanisms and pathophysiology are still poorly understood (**Chapman, 2004; Strieter, 2008**). Thus, many attempts have been made to develop an animal model able to reproduce the basic features of ILD in order to develop effective therapies (**Chua et al., 2005b; Molina-Molina et al., 2007**). Albeit BLM-induced murine models of lung injury have been extensively used to study the pathophysiology of lung fibrosis (**Dolhnikoff et al., 1999; Iraz et al., 2006**), most studies employing BLM models have been addressed in the first 2–3 weeks after drug insult, when the inflammatory response is still relevant (**Sogut et al., 2004; Boyaci et al., 2006; Yao et al., 2006**).

We believe that mechanical parametres can be of great help in the follow up, design of therapeutic strategies and general knowledge of the natural history of the disease. However, the mechanical changes that accompany the structural changes that occur in this model have been incompletely characterised. In addition, we have found few reports that studied this model at a biomechanical level. In this line, Dolhnikoff et al., 1999 showed that structural changes of ECM induced by BLM caused modifications in the oscillatory mechanics of the lung tissue both “in vivo” and “in vitro”; and Ebihara et al., 2000 demonstrated a positive correlation between the volume fraction of byglican and “in vitro” tissue resistance and elastance. However, little is known about the influence of the inflammatory response in the early phase or the progression of fibrosis in the later phase upon lung biomechanics in a two-week murine model and a 4-week murine model elicited by single or repeated doses of BLM.

In the present thesis we hypothesised that:

i. Biomechanical changes in lung tissue may differ depending on the inflammatory or remodelling process after BLM challenge.

ii. After BLM challenge, lung remodelling in the process of healing or reparation will lead to a different pattern of mechanical changes than the ones observed in human PF elicited by BLM.

II.2 OBJECTIVES

1. To characterise the time course of biomechanical changes of the lung after a single-dose BLM challenge in a murine model of lung injury.

2. To determine whether the early changes in the mechanical properties of lung parenchyma are related to markers of lung inflammation and/or remodelling in a BLM-induced lung injury.

3. To characterise the time course of biomechanical changes of the lung after repeated doses of BLM challenge in a murine model of lung injury.

4. To compare “in vitro” lung mechanics, inflammatory and fibrogenic parametres after a single and repeated BLM intratracheal instillation 28 days after last challenge.

Albeit we know that studies on pulmonary mechanics in normal or challenged animals generally require an open chest approach, to answer the questions above mentioned we used lung parenchymal strips as a model to study the mechanical behaviour of lung tissue. The reason why we chose this model is due to the fact that “in vitro” measurements can exclude confusions derived from surface film, alveolar flooding, and ventilation heterogeneities to the mechanical behaviour (**Yuan et al., 1997**).

III. STUDY DESIGN

This work has been mainly conducted at the Laboratory of Experimental Pneumology of the Department of Clinical Sciences, School of Medicine, UB. For the study of lung histological parametres this work has been carried out at the Laboratory of Pulmonary Investigation, Carlos Chagas Filho Biophysics Institute at the Federal University of Rio de Janeiro and the Department of Pathology at the University of São Paulo, Brazil. The biochemical analysis was performed at the Department of Experimental Pathology, IIBB-CSIC, IDIBAPS.

III.1. BLEOMYCIN-INDUCED MURINE MODEL

All experiments were carried out in accordance with the current legislation on animal experiments in the European Union (Directive 86/609/EEC). The experimental protocols were approved by the institutional committee of animal care and research of the University of Barcelona and the experimental model was carried out at the animal facility of Bellvitge.

III.1.1. Animals

For this study, male rats (*Rattus norvergivus*) of the Sprague-Dawley strain (Harlan Ibérica, Spain), weighting 225-300 g, were used. Rats arrived one week prior the beginning of the experiments to ensure a proper acclimatisation and avoid the development of potential pathologies. Animals were fed a standard rat chow and housed under SPF controlled environmental conditions (temperature 22ºC, 12-h light: 12-h dark cycle). Water and food were given *ad libitum*.

III.1.2. Anaesthesia and analgesia

Pentobarbital sodium: is a short-acting barbiturate (5-10') commonly used as an anaesthetic agent for rodents.

Buprenorphine: is a thebaine derivative with powerful analgesia approximately twenty-five to forty times as potent as morphine.

Ketamine: is often used with sedative drugs to produce balanced anaesthesia and analgesia.

Diazepam: is a mild tranquilizer in the class of drugs known as benzodiazepines. Diazepam is used as a short term sedative in combination with ketamine to diminish the adverse effects caused by the anesthetic.

Isoflurane: is a halogenated ether used for inhalational anesthesia. Isoflurane is always administered in conjunction with air and/or pure oxygen. Isoflurane reduces pain sensitivity (analgesia) and relaxes muscles.

III.1.3. Experimental model

Pulmonary inflammation and fibrosis was elicited intratracheally by single sublethal dose of BLM (0.25 U/100 g body weight) dissolved in a volume of 0.25 ml of saline solution (0.9% NaCl). Control animals were subjected to the same protocol but received the same volume of intratracheal saline instead of BLM. Tracheal instillation was carried out under 4% isoflurane (Forane ®) anaesthesia by means of a special device and was considered day 0. A control of their weight was performed every other day. Depending on the study rats were sacrificed at different time points:

- ✓ Study 1: at day 3, 7 and 15.
- ✓ Study 2: at day 28 (SD group). The other group (RD group) was subjected to repeat doses and sacrificed 28 days after the last instillation (day 0, week 2 and week 4). The group that received a single dose of BLM was called SD group, and the one exposed to repeated doses of BLM was called RD group.

In the first study before sacrifice, animals were sedated with buprenorphine 0.05 mg·Kg body weight^{-1} s.c., anaesthetised with pentobarbital sodium (40-50 mg·Kg body weight^{-1} i.p., and heparine (1000 IU) dissolved with saline solution was intravenously injected 5 minutes before exsanguinations by sectioning abdominal aorta and vena cava. Lungs were removed *en bloc*, weighted and placed in a modified Krebs-Henseleith (K-H) solution.

In the second study before sacrifice, animals were sedated with diazepam 5 mg·Kg body weight^{-1} i.p., anesthetised with ketamine (75 mg·Kg body weight^{-1} i.p., and heparine (1000 IU) dissolved with saline solution was intravenously injected 5 minutes before exsanguinations by sectioning abdominal aorta and vena cava. Lungs were removed *en bloc*, weighted and placed in a modified Krebs-Henseleith (K-H) solution.

For biomechanical studies a supleural strip of 15 mm x 3 mm x 3 mm were cut from the right lung and placed in a modified Krebs-Henseleith (K-H) solution bubbled with a mixture of 95% O_2 -5% CO_2 and kept iced 4ºC prior the start of the experiment. For biochemical studies, lung parenchyma was cut into pieces and frozen at -80ºC. For histological studies pieces were fixed with 4% paraformaldehyde for 24h.

Image that represents the way we elicited the lung injury by intratracheal instillation of the drug BLM or saline at day 0:

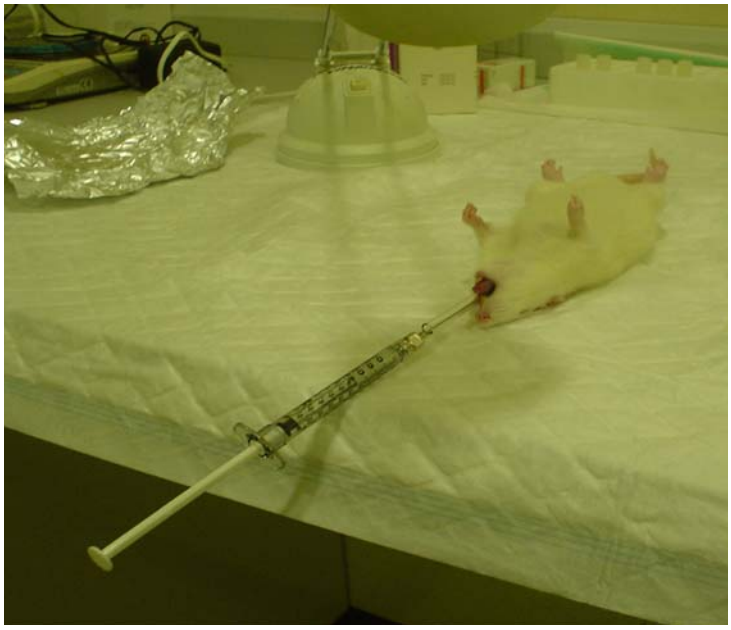

Lung oedema 3 days after injury:

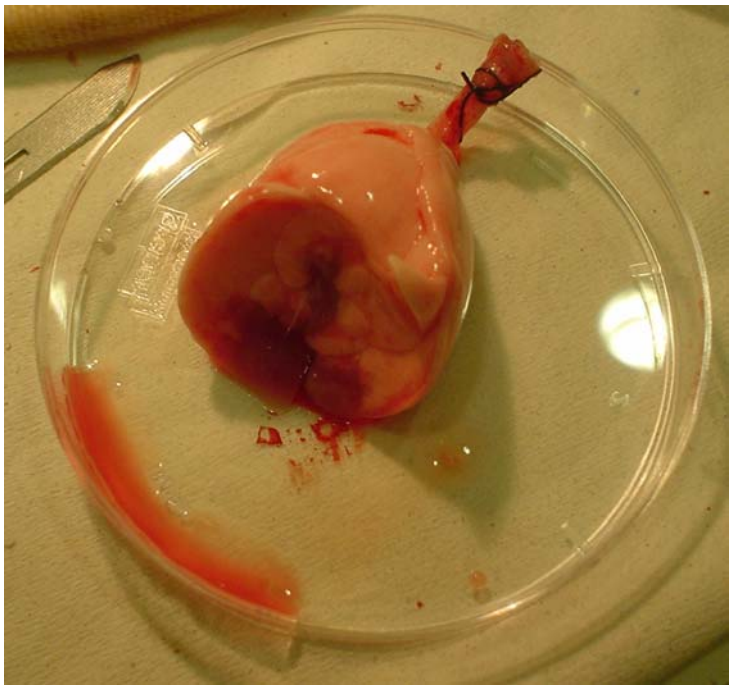

III.1.4. Biomechanical analysis

III.1.4.1. Apparatus

Subpleural strips (15mm×3mm×3mm) were cut from right lung and suspended vertically in a K–H organ bath maintained at 37ºC, continuously bubbled with a mixture of 95% O_2–5% CO_2. Lung strips were weighed (*W*), and their unloaded resting lengths (L_0) were determined with a calliper. Lung strip volume was measured by simple densitometry: vol= F/δ, where *F* is the total change in force before and after strip immersion in K–H solution and δ is the mass density of K–H solution (**Lopez-Aguilar and Romero, 1998; Romero et al., 2001**). Parenchyma strips were suspended vertically in a K–H organ bath (10 ml internal volume) maintained at 37ºC and continuously bubbled with 95% O2–5% CO2 as previously described (**Romero et al., 2001**). Briefly, one end of the strip was attached to a force transducer (FT03, Grass-Telefactor, RI, USA), and the other was fastened to a lever arm actuated by means of a modified woofer driven by the signal generated by a computer and analogue-to-digital converted (AT-MIO-16-E-10, National Instruments, Austin, TX, USA). A sidearm of this rod was linked to a second force transducer (LETICA TRI-110, Scientific Instruments, Barcelona, Spain) by means of a silver spring of known Young's modulus, thus allowing displacement to be measured.

Images of the biomechanical setting (two organ baths):

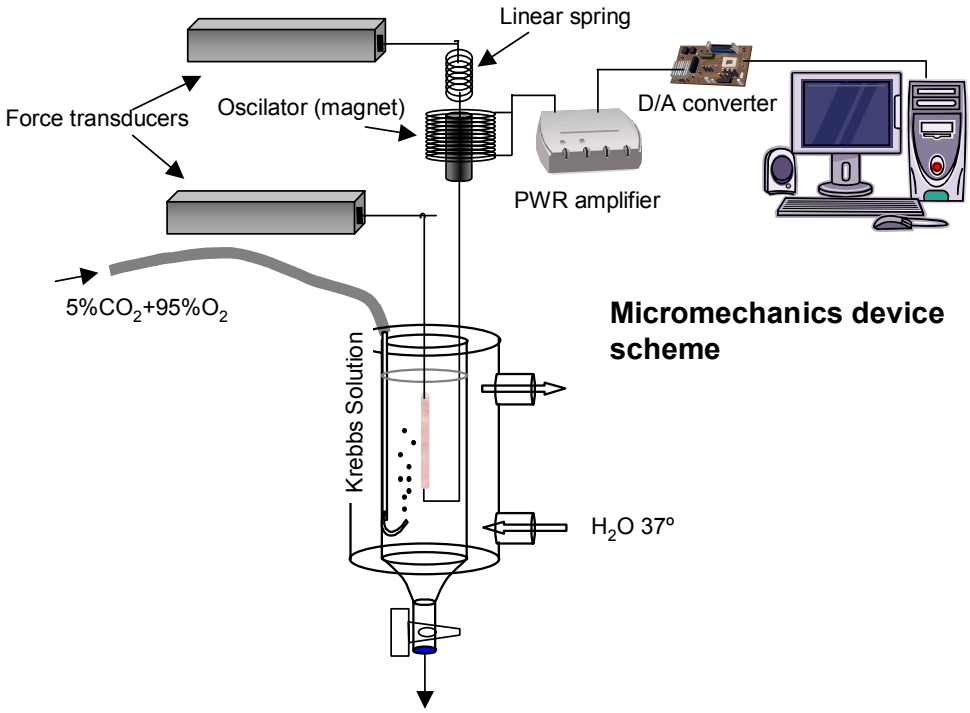

III.1.4.2. Preconditioning

Cross-sectional, unstressed area (A_0) of the strip was determined from strip volume and unstressed length, according to A_0 = vol/L_0. Basal force (FB) for a stress of 10 h Pa was calculated as FB (g) = 10(h Pa)·A_0 (cm^2) and adjusted by vertical displacement of the force transducer as described before (**Romero et al., 2001**). The displacement signal was then set to zero. Once basal force and displacement signals were adjusted, the length between bindings (L_B) was measured by means of a precision calliper. Instantaneous length during oscillation around L_B was determined by adding the value of L_B to the measured value of displacement at any time. Instantaneous average cross-section area (Ai) was determined as $Ai = Vs/Li$ (cm^2).

Instantaneous stress (σi) was calculated by dividing force (g) by Ai (cm^2). Strain was calculated as $\Delta\varepsilon = (L - L_B)/L_B$. Thereafter, the amplitude was adjusted to 5% L_0 and the oscillation maintained for another 30 min, or until a stable length-force loop was reached. After preconditioning, the strips were oscillated at a frequency (f) = 1 Hz. Bath solution was renewed regularly (every 20 min) with 37ºC K–H solution. The whole process lasted no longer than 90 min.

After preconditioning, samples were set at an operating stress of 10 hPa. Then, three 20-second recordings of multifrequency forced oscillations were performed.

Pseudorandom driving signal was composed of five sinusoids of the same power amplitude and frequencies (f) 0.2, 0.5, 1.1, 1.9, and 3.1Hz. Both force and displacement signals were pre-amplified, filtered at 30Hz, and sampled at a frequency of 150Hz.

Scheme of the pseudorandom driving signal of frequencies 0.2, 0.5, 1.1, 1.9 and 3.1 Hz:

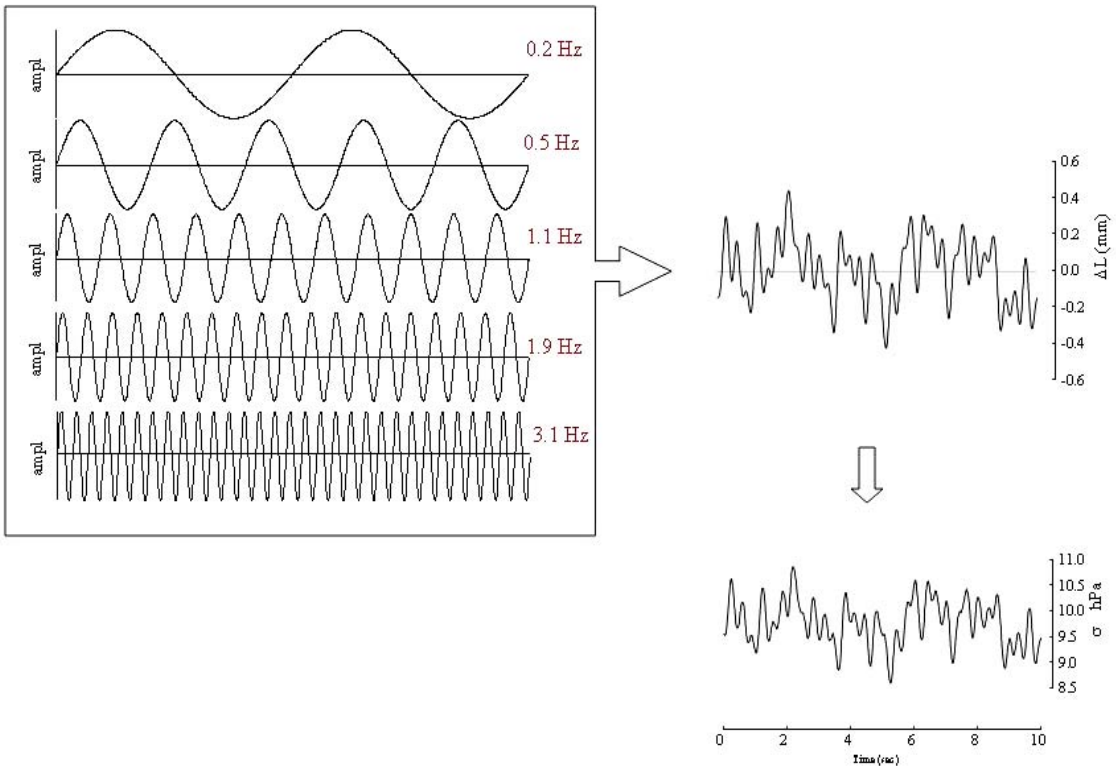

III.1.4.3. Data analysis

Analysis and parameter estimation were performed by means of specific software elaborated with LabVIEW 5.1 and 7.0 (National Instruments Co., Austin, TX, USA).

We used the constant phase model in both studies, although this model was fitted according to Romero et al. (**2001**) in study 1 and according to Hantos et al. (**1992**) in study 2.

Study 1: Strain to stress relationships are characterised by the complex Young or elastic modulus Ψ(ω) as follows:

$$\psi_{\omega} = E_{\omega} + j{\cdot}\omega{\cdot}Rti_{\omega} = E_0{\cdot}\omega^{\beta} + j{\cdot}\left[R_v{\cdot}\omega + R_0{\cdot}\omega^{\beta}\right]$$

where E_{ω} corresponds to elastance and is the real component of the complex Young and $j \cdot \omega \cdot Rti_{\omega}$ is the imaginary component and corresponds to the resistance (resistive component).

$\alpha + \beta = 1$ (Constant phase model)

$$E = E_0{\cdot}\omega^{\beta} = E_0{\cdot}\omega^{(1-\alpha)} = \frac{(E_0{\cdot}\omega)}{\omega^{\alpha}}$$ (Real part)

$$R = R_v{\cdot}\omega + R_0{\cdot}\omega^{\beta} = R_v{\cdot}\omega + R_0{\cdot}\omega^{-\alpha}$$ (Imaginary part)

The equation to calculate hysteresivity at ω=1 (η_0) is the following:

$$\eta_0 = \frac{R_0}{E_0}$$

Study 2: Lung tissue impedance (*Z*ti), a magnitude that relates stress to the rate of change in strain was determined according to the constant-phase model first described by Hantos et al. (**1992**). To account for the Newtonian or frequency-independent resistance (*R*v) of tissue we used the following expression:

$$Z = R_v + \left[\frac{(G - jH)}{\omega^{\alpha}}\right]$$

where R_v is flow-independent or newtonian resistance of lung tissue, G is tissue damping, H is tissue elastance, j is the imaginary unit, and $\alpha = (2/\pi){\cdot}\tan^{-1}(H/G)$. Fitting of the model was performed as follows: after calculation of the real and imaginary components of impedance:

$$Z_{real} = R_v + G{\cdot}\omega^{-\alpha}$$

$$Z_{im} = H{\cdot}\omega^{-\alpha}$$

the value of R_v was obtained by recursive linear regression to obtain the value that accomplish the constant phase paradigm ($\alpha_{real} = \alpha_{im}$). According to Ito et al. (**2004**), we have used the normalised angular frequency ($\omega_n = \omega/\omega 0$), where ω_0 = 1 rad/s. This allows expressing *G* and *H* in "elastance" units (hPa). Hysteresivity at ω=1 (η_0) has been calculated as:

$$\eta_0 = \frac{G}{H}$$

Both models are related as follows:

$$Z_{real} \cdot \omega = \Psi_{im}$$

$$\frac{\Psi_{real}}{\omega} = Z_{im}$$

$$Z_{real} = \frac{\psi_{im}}{\omega} = \frac{R_v \cdot \omega + R_0 \cdot \omega^{\beta}}{\omega} = R_v + R_0 \cdot \omega^{-\alpha} = \frac{R_v + G}{\omega^{\alpha}} \qquad G = R_0 \cdot \omega_0 = R_0 \cdot 1 = R_0$$

$$\Psi_{real} = Z_{im} \cdot \omega = H \cdot \omega^{-\alpha} \cdot \omega = H \cdot \omega^{(1-\alpha)} = \frac{H \cdot \omega}{\omega^{\alpha}} = \frac{E_0 \cdot \omega}{\omega^{\alpha}} \qquad E_0 = H$$

III.1.5. Statistical analysis

The normality of the data (Kolmogorov-Smirnov test with Lilliefors' correction) and the homogeneity of variances (Levene median test) were tested. If both conditions were satisfied, One-way ANOVA test followed by Bonferroni's post hoc test was used. Otherwise, One-way ANOVA on ranks followed by Mann-Whitney post hoc test was selected instead.

Spearman correlation test was used to correlate functional and biochemical or morphometrical data. All analyses were made using the SPSS 12.0 statistical software package. In all instances the significance level was set at 5% (α=0.05).

III.2. PARAMETRES STUDIED IN LUNG PARENCHYMA

III.2.1. Myeloperoxidase

Myeloperoxidase is a peroxidase enzyme most abundantly present in neutrophil granulocytes that is often employed as a marker of neutrophilic infiltration. Myeloperoxidase produces hypochlorus acid (HOCl) from hydrogen peroxidase (H_2O_2) and chloride anion (Cl^-) during the neutrophils respiratory burst. It requires heme as a cofactor. Furthermore, it oxidises tyrosone radical using hydrogen peroxide as oxidising agent. Hypochlorus acid and tyrosil radical are cytotoxic, so they are used by the neuthrophil to kill bacteria and other pathogens.

The method is based on the reaction of tetramethylbenzidine catalysed by MPO. Tetramethylbenzidine is a non-carcinogenic analogous of the o-dianisidine used originally. It is important to obtain a good enzyme extraction, for this purpose we homogenise with buffer without detergent and break the granulocytes. Lung tissue samples were macerated with 0.5% hexadecyltrimethylammonium bromide in 50 mM phosphate buffer pH 6.0. Homogenates were then disrupted for 30 s using a Labsonic U sonicator at 20% power and subsequently snap frozen in dry ice and thawed on three consecutive occasions before a final 30 s sonication. Samples were incubated at 60ºC for 2 h to deactivate MPO inhibitors present in different tissues, and then spun at 15000 g for 15 min. The supernatant was collected for myeloperoxidase assay. Enzyme activity was assessed photometrically at 620 nm. The assay mixture consisted in 20 µl supernate, 10 µl 3,3',5,5'-tetramethylbenzidine (final concentration 1.6 mM) dissolved in DMSO and 140 µl H_2O_2 diluted in 80 mM phosphate buffer pH 5.4. An enzyme unit is defined as the amount of enzyme that produces an increase of 1 absorbance unit per minute.

III.2.2. Hydroxyproline

Hydroxyproline is produced by hydroxylation of the amino acid proline by the enzyme prolyl hydroxylase following protein synthesis. This amino acid appears only when there is collagen formation in the connective tissue. Collagen is the most predominant protein in the connective tissue, representing a third of the total proteins in the body. Hydroxyproline is a major component of the protein collagen. For this reason,

hydroxyproline measurement is used to study the metabolism and regulation of collagen. Hydroxyproline levels constitute a marker of PF and are an indicator of the amount of newly synthesised collagen.

This method is based on tissue hydrolisation to determine the presence of hydroxyproline. Briefly, samples from the right lung weighting 300-350 mg were dried for 48 h at 60ºC, and then± 30 g of the pulverised sample was homogenised and hydrolised in 6N HCL for 24 h at 120ºC. The hydrolysate was then neutralised with 6N NaOH. Aliquots (2 ml) were analysed for hydroxyproline content after addition of 1ml Chloramine-T, which is employed to oxidise hydroxyproline, 1 ml of perchloric acid, and 1 ml of dimethylaminobenzaldehyde (Ehrlich reagent). Then a chromophore is formed, which can be measured espectophotometrically at a wavelength of 561 nm. The amount of hydroxyproline was determined by comparing with a standard curve. Results were expressed as µg of hydroxyproline per lung.

III.3. HISTOLOGY

III.3.1. Morphometry

The left lung was fixed by intratracheal instillation of buffered formalin at a constant pressure of 10 h Pa, dehydrated in a graded series of ethanol dilutions, embedded in paraffin, cut into 3 µm thick serial sections, and stained with haematoxylin–eosin.

In each slice, 10 different microscopic fields were randomly selected to quantify for tissue fraction, alveolar wall thickness and cell count. Non-aerated areas as well as bronchi or vessels were also excluded. Quantification (x 400 magnification) was carried out with the aid of a digital analysis system, using specific software (IMAQ, National Instruments, Austin TX). Tissue area (μm^2) was computed after spatial calibration, by pixel counting of the binary converted monochrome (grey) images by visual threshold. Tissue fraction was then obtained by dividing by the total area of the field. The volume of tissue (μm^3) was determined as tissue area x 3 (section thickness). Total number of cells (nuclei) by field were counted, divided by the volume of tissue and expressed as cells/μm^3.

III.3.2. Collagen fibres

Subpleural strips were fixed with 4% paraformaldehyde in PBS pH 7.0 for 24 h, dehydrated in a graded series of ethanol, embedded in paraffin, and cut into 4-µm thick serial sections. They were stained with Masson's trichrome to quantify collagen deposition. A total of five photomicrographs of each preparation were used to quantify collagen fibre content at x400. Total tissue surface was measured after binary conversion. After identification of an area of interest (blue stained collagen), colour threshold analysis was applied and binary converted. Area covered by collagen was expressed as percentage of total tissue surface. The program used was IMAQ Vision Builder 5.0 (National Instruments, Austin, TX, USA).

III.3.3. Elastic fibres

III.3.3.1. Protocol of dehydration of lung tissue strips

Immediately after mechanical measurements, lung tissue strip was quick-frozen by immersion in liquid nitrogen, fixed with Carnoy's solution for 24 h at -70ºC. Carnoy solution consisted in 60% ethanol, 30% chloroform and 10% acetic acid. Afterwards, strips were dehydrated in 3 successive series for 1h at -20ºC:

	Ethanol %	Chloroform %	Acetic acid %
MC1	70	22.5	7.5
MC2	80	15	7.5
MC3	90	7.5	2.5

Finally, a solution of 100% ethanol for 1 h at -20ºC and then kept in the fridge (4ºC) for 24 h.

III.3.3.2. Sample staining

Elastic staining was performed by Weigert's resorcin-fuchsin method, modified with a previous oxidation. This method stains the three types of elastic system fibres (oxytalan, elaunin and fully developed elastic fibres), but does not allow separate identification. The complex formed from the basic fuchsin, an iron resorcin lake, binds

to the elastic fibres, resulting in the blue-black staining. With this method it is possible to quantify all the elastic tissue in the sample without losing the oxytalan component.

The sections were subsequently treated with 1% potassium permanganate for 10 min, washed in distilled water for 1 min, immersed in 3% oxalic acid for 1 min and washed again in distilled water for 1min. After one wash with 95% ethanol for 1 min, the sections were stained with Weigert's resorcin-fuchsin for 5 h, immersed in 95% ethanol for 1 min, counter-stained with Harris' haematoxylin for 3 min, washed in tap water for 10 min, dehydrated in ethanol, clarified in xylol and mounted in Canada balsam.

III.3.3.3. Quantification of elastic fibres

In each strip, 20 different microscopic fields were randomly selected to quantify elastic fibres. Quantification (x 200 magnification) was carried out with the aid of a digital analysis system, using specific software (Bioscan- Optimas 5:1, Bioscan, Edmond, WA, USA). The images were generated by a microscope (Axioplan, Zeiss, Oberkochen, Germany) connected to a camera (Trinitron CCD, Sony, Tokyo, Japan) and fed into a computer through a frame grabber (Oculus TCX, Coreco, St. Laurent, Quebec, Canada) for off-line processing. The thresholds for fibres of the elastic systems were established after enhancing the contrast up to a point at which the fibres were easily identified. The area occupied by fibres was determined by digital densitometric recognition. Bronchi and blood vessels were carefully avoided during the measurements. In order to avoid any bias due to septum oedema or alveolar collapse, we have divided the surface occupied by the elastic fibres measured in each alveolar septum by the length of the corresponding septum. The results were expressed as the surface covered by elastic fibres per unit of septum length ($\mu m^2/\mu m$).

IV. RESULTS

IV.1 Objectives 1 and 2

OBJECTIVE 1: "To characterise the time course of biomechanical changes of the lung after a single-dose BLM challenge in a murine model of subacute lung injury".

OBJECTIVE 2: "To determine whether the early changes in the mechanical properties of lung parenchyma are related to markers of lung inflammation and/or remodelling in a BLM-induced lung injury".

Specific objectives

- To characterise the mechanical behaviour at the established time points (day 3, 7 and 15) after BLM challenge.
- To measure inflammatory and remodelling parametres at the above mentioned time points.
- To analyse the impact of each of the inflammatory and remodelling parametres at each time point.
- To establish correlations to ascertain which of the two phases (inflammation and remodelling) have an impact or are related to the changes of the lung tissue mechanical parametres.

M. Pinart, A. Serrano- Mollar, E.M. Negri, R. Cabrera, P.R.M. Rocco, P.V. Romero. Inflammatory related changes in lung tissue mechanics after bleomycin-induced lung injury, in *Respiratory Physiology & Neurobiology*. 2008; 160(2):196-203.

Lung injury after BLM challenge consists of two phases: a first phase where inflammation is more prominent and a second phase where there is an enhanced production and deposition of collagen resulting in distortion of pulmonary architecture which in turn influences the biomechanical changes. In this line, we wanted to know if these two phases occurred in a two-week BLM model. If so, the next question was to ascertain which of the two phases were more prominent and had a higher impact on lung tissue mechanical changes. To answer all these questions we characterised the time course of lung tissue strips mechanical changes after BLM challenge and analysed the impact of pulmonary inflammation and remodelling indices at different time points upon the tissue biomechanical changes.

In this study rats were intratracheally instilled with a single dose of BLM and were sacrificed at days 3, 7 and 15. Forced oscillatory mechanics (elastance, resistance and hysteresivity) as well as indices of inflammation (myeloperoxidase content, total cell count, alveolar wall thickness, lung index and lung water content) and remodelling (elastic fibre content and hydroxyproline) were studies in lung tissue strips. Our results showed that lung tissue resistance increased only at day 15, while hysteresivity was significantly higher at all time points. Elastic fibres, hydroxyproline and myeloperoxidase contents augmented at days 7 and 15. Both tissue resistance and hysteresivity were correlated to myeloperoxidase, lung water content and lung index. Hydroxyproline was not correlated with mechanical parametres, but elastic fibres were strongly correlated with hysteresivity and alveolar wall thickness.

Inflammation seems to alter pulmonary functions by eliciting biomechanical changes in the first 15 days. Furthermore, elastogenesis seems to affect the coupling between elastic and dissipative processes within the tissue. Therefore, inflammation and elastogenesis are the main determinants for hysteretic changes observed in the first 15 days after BLM challenge in rats. However, the fact that there is no correlation between hydroxyproline and the biomechanical parametres does not mean that fibrogenesis is absent in this model, but the amount of collagen fibres is not sufficient to have a significant impact upon tissue mechanics.

Available online at www.sciencedirect.com
ScienceDirect
Respiratory Physiology & Neurobiology 160 (2008) 196–203
RESPIRATORY PHYSIOLOGY & NEUROBIOLOGY
www.elsevier.com/locate/resphysiol

Inflammatory related changes in lung tissue mechanics after bleomycin-induced lung injury

M. Pinart [a], A. Serrano-Mollar [b], E.M. Negri [c], R. Cabrera [a], P.R.M. Rocco [d], P.V. Romero [a,*]

[a] *Laboratory of Experimental Pneumology, IDIBELL, L'Hospitalet, Barcelona, Spain*
[b] *Department of Experimental Pathology, IIBB-CSIC, IDIBAPS, Barcelona, Spain*
[c] *Department of Pathology, University of Sao Paulo, Sao Paulo, Brazil*
[d] *Laboratory of Pulmonary Investigation, Carlos Chagas Filho Biophysics Institute, Federal University of Rio de Janeiro, Rio de Janeiro, Brazil*

Accepted 21 September 2007

Abstract

The impact of lung remodelling in respiratory mechanics has been widely studied in bleomycin-induced lung injury. However, little is known regarding the relationship between the amount of lung inflammation and pulmonary tissue mechanics. For this purpose, rats were intratracheally instilled with bleomycin ($n = 29$) or saline ($n = 8$) and sacrificed at 3, 7, or 15 days. Forced oscillatory mechanics as well as indices of remodelling (elastic fibre content and hydroxyproline) and inflammation (myeloperoxidase content, total cell count, alveolar wall thickness, and lung water content) were studied in lung tissue strips. Tissue resistance increased significantly at day 15, while hysteresivity was significantly higher in bleomycin group compared to control at all time points. Elastic fibres, hydroxyproline and myeloperoxidase contents augmented after bleomycin at days 7 and 15. Tissue resistance and hysteresivity were significantly correlated with myeloperoxidase, elastic fibre and lung water content. In conclusion, inflammatory structural changes and elastogenesis are the main determinants for hysteretic changes in this 2-week bleomycin-induced lung injury model.

Keywords: Hysteresivity; Myeloperoxidase; Hydroxyproline; Elastin; Bleomycin

1. Introduction

Lung injury observed after bleomycin challenge is heterogeneous and rapid at onset, with an initial alveolitis phase characterized by interstitial edema and influx of inflammatory cells such as neutrophils, macrophages, and lymphocytes (Thrall et al., 1982), leading to fibroblast proliferation. In a second phase, enhanced production and deposition of collagen and other matrix components in the interstitium result in distortion of pulmonary architecture (Hay et al., 1991; Dolhnikoff et al., 1999), which in turn influences the biomechanical properties of lung parenchyma. These phases, although occurring sequentially, do not bear a constant time relationship to the dosage schedule (Jones and Reeve, 1978).

Bleomycin-induced murine models of lung injury have been extensively used to further assess the relationship between lung structural and biomechanical changes focusing on lung fibrosis related changes (Dolhnikoff et al., 1999; Iraz et al., 2006). However, most studies employing bleomycin models have been addressed in the first 2–3 weeks after drug insult, when the inflammatory response is still relevant (Sogut et al., 2004; Boyaci et al., 2006; Yao et al., 2006). The inflammatory response leads to a cascade of events resulting in an impairment of extracellular matrix (ECM) constitution and lung tissue mechanical properties.

Lung parenchymal strips have been used as a model to study the mechanical behavior of lung tissue (Yuan et al., 1997; Salerno et al., 2004). The advantage of making *in vitro* measurements is that contributions to the mechanical behavior related to surface film, alveolar flooding, and ventilation

* Corresponding author at: Unitat de Pneumologia Experimental, Unitat Docent de Bellvitge, IDIBELL, Universitat de Barcelona, C/ Feixa Llarga s/n, 08907 L'Hospitalet de Llobregat, Spain. Tel.: +34 93 403 5807; fax: +34 93 260 7689.
E-mail address: pvromero@csub.scs.es (P.V. Romero).

1569-9048/$ – see front matter © 2007 Elsevier B.V. All rights reserved.
doi:10.1016/j.resp.2007.09.012

heterogeneities can be excluded (Yuan et al., 1997). Bleomycin-induced changes in mechanical properties of lung tissue are relatively well documented. Dolhnikoff et al., 1999 showed that structural modifications of ECM induced by bleomycin caused modifications in the oscillatory mechanics of the lung tissue both *in vivo* and *in vitro*. Ebihara et al., 2000 in a study using the same elicited lung injury model demonstrated a positive correlation between the volume fraction of byglican and parenchymal strip resistance and elastance. It is unclear whether extracellular matrix components are involved in the early lung injury and the pulmonary inflammatory response that lead to fibrosis (Zhao et al., 1998).

This study was undertaken to determine whether the early changes in the mechanical properties of lung parenchyma are related to markers of lung inflammation and/or remodelling in a bleomycin-induced lung injury. For this purpose, we have characterized the time course of lung tissue strips mechanical changes (elastance, resistance and hysteresivity) after bleomycin challenge and analyzed the impact of pulmonary inflammation (myeloperoxidase, lung index of inflammation, and lung water contents) and remodelling (hydroxyproline, and elastic fibres) indices at different time points upon the tissue biomechanical changes.

2. Methods

2.1. Animal preparation

Thirty-seven specific pathogen-free (SPF), male Sprague–Dawley rats, weighing 279 ± 15 g (mean ± S.D.) were obtained from Harlan Ibérica S.L (Sant Feliu de Codines, Spain). Rats were fed a standard rat chow and housed under SPF controlled environmental conditions (temperature 22 °C, 12-h light:12-h dark cycle). Animals were given water and food *ad libitum*. The experiments were carried out in accordance with the current legislation on animal experiments in the European Union (Directive 86/609/EEC) and Spanish guidelines for the use of experimental animals and approved by the institutional committee of animal care and research. Thirty rats received a single intratracheal dose of bleomycin (2.5 U/kg in 0.5 ml) at day 0, and were studied at days 3 (BLM3, $n = 9$), 7 (BLM7, $n = 10$) or 15 (BLM15, $n = 10$). In the control group (CTRL, $n = 8$) animals received 0.5 ml sterile saline (0.9% NaCl) intratracheally and were studied at days 3, 7 or 15. Because mechanical parameters and histological data of CTRL group at days 3, 7 and 15 were similar we used a single control group. Indeed, in previous experiments (unpublished data), lung tissue mechanical and histological parameters were not statistically significant with alfa error = 0.05% between days 3, 7 and 15 in control animals. At the time of the study, animals were sedated (buprenorphine 0.05 mg kg body weight^{-1} *s.c.*), anesthetized [pentobarbital sodium (40–50 mg kg body weight^{-1} *i.p.*)], and heparine (1000 IU) was intravenously injected 5 min before exanguination by sectioning abdominal aorta and vena cava. The lungs were removed *en bloc*, and placed in a modified Krebs–Henseleith (K–H) solution [mM: 118.4 NaCl, 4.7 KCl, 1.2 K_3PO_4, 25 $NaHCO_3$, 2.5 $CaCl_2{\cdot}H_2O$, 0.6 $MgSO_4{\cdot}H_2O$, and 11.1 glucose] at pH 7.40 and 6 °C (Lopez-Aguilar and Romero, 1998; Rocco et al., 2003; Faffe et al., 2006).

2.2. Apparatus

Subpleural strips (15 mm × 3 mm × 3 mm) were cut from right lung and suspended vertically in a K–H organ bath maintained at 37 °C, continuously bubbled with a mixture of 95% O_2–5% CO_2. Lung strips were weighed (W), and their unloaded resting lengths (L_0) were determined with a calliper. Lung strip volume was measured by simple densitometry: vol = $\Delta F/\delta$, where ΔF is the total change in force before and after strip immersion in K–H solution and δ is the mass density of K–H solution (Lopez-Aguilar and Romero, 1998; Romero et al., 2001).

Parenchyma strips were suspended vertically in a K–H organ bath (10 ml internal volume) maintained at 37 °C and continuously bubbled with 95% O_2–5% CO_2 as previously described (Romero et al., 2001). Briefly, one end of the strip was attached to a force transducer (FT03, Grass-Telefactor, RI, USA), and the other was fastened to a lever arm actuated by means of a modified woofer driven by the signal generated by a computer and analogue-to-digital converted (AT-MIO-16-E-10, National Instruments, Austin, TX, USA). A sidearm of this rod was linked to a second force transducer (LETICA TRI-110, Scientific Instruments, Barcelona, Spain) by means of a silver spring of known Young's modulus, thus allowing displacement to be measured.

2.3. Preconditioning

Cross-sectional, unstressed area (A_0) of the strip was determined from strip volume and unstressed length, according to $A_0 = \text{vol}/L_0$. Basal force (F_B) for a stress of 10 h Pa was calculated as F_B (g) = 10(h Pa)·A_0 (cm^2) and adjusted by vertical displacement of the force transducer as described before (Romero et al., 2001). The displacement signal was then set to zero. Once basal force and displacement signals were adjusted, the length between bindings (L_B) was measured by means of a precision calliper. Instantaneous length during oscillation around L_B was determined by adding the value of L_B to the measured value of displacement at any time. Instantaneous average cross-section area (A_i) was determined as $A_i = V_s/L_i$ (cm^2). Instantaneous stress (σ_i) was calculated by dividing force (g) by A_i (cm^2). Strain was calculated as $\Delta\varepsilon = (L - L_B)/L_B$.

Thereafter, the amplitude was adjusted to 5% L_0 and the oscillation maintained for another 30 min, or until a stable length-force loop was reached. After preconditioning, the strips were oscillated at a frequency (f) = 1 Hz. Bath solution was renewed regularly (every 20 min) with 37 °C K–H solution. The whole process lasted no longer than 90 min.

2.4. Biomechanical study

After preconditioning, samples were set at an operating stress of 10 h Pa. Then, three 10-s recordings of multifrequency forced oscillations were performed. Pseudorandom driven signal was

composed of five sinusoids of same amplitude and frequencies (f) 0.2, 0.5, 1.1, 1.9, and 3.1 Hz. Both force and displacement signals were preamplified, filtered at 30 Hz, and sampled at a frequency of 150 Hz.

2.5. Data analysis

Analysis and parameter estimation were performed by means of specific software elaborated with LabVIEW 5.1 (National Instruments Co., Austin, TX, USA) as previously described (Romero et al., 2001). Briefly, the frequency response was computed from the time-domain strain (stimulus) and the time-domain stress (response) as:

$$\psi_\omega = \frac{\mathrm{FFT}(\sigma)}{\mathrm{FFT}(\varepsilon)}$$

where Ψ_ω is the elastic or Young complex modulus; FFT the fast Fourier transform; σ the stress; ε the strain; and ω is the angular frequency ($2\pi f$). This result was transformed into single-sided magnitude $|\Psi|$ and phase (Φ). For values of magnitude and phase corresponding to relevant frequencies (ω), tissue elastance (E), resistance (Rti), and hysteresivity (η) were calculated according to:

$$E_\omega = |\psi| \cdot \cos(\Phi)$$

$$\eta_\omega = \tan(\Phi)$$

$$\mathrm{Rti}_\omega = E_\omega \cdot \frac{\eta_\omega}{\omega}$$

The following model was fitted according to Romero et al. (2001)

$$\Psi_\omega = E_\omega + j \cdot \omega \cdot \mathrm{Rti}_\omega = E_0 \cdot \omega^\beta + j \cdot [R_\mathrm{v} \cdot \omega + R_0 \cdot \omega^\beta] \quad (1)$$

where Ψ_ω is the complex Young modulus, E_0 and R_0 are the values of elastance and resistance at $\omega = 1$, R_v is the newtonian tissue component, and β defines an intrinsic property of lung tissue related to hysteresivity (Suki et al., 1994). Note that for $R_\mathrm{v} = 0$ the above equation corresponds to the constant phase model proposed by Hantos et al. (1992). Values of R_v were coerced to be ≥ 0. The equation to calculate hysteresivity at $\omega = 1$ (η_0) is the following:

$$\eta_0 = \frac{R_0}{E_0}$$

2.6. Biochemical and morphometric analysis

Immediately after mechanical measurements, lung tissue strip was quick-frozen by immersion in liquid nitrogen, fixed with Carnoy's solution according to Silva et al. (1998). Four-μm-thick slices were obtained by means of a microtome and stained with specific staining method to characterize the amount of elastic fibres (Weigert's resorcin fuchsin method modified with oxidation) (Fullmer et al., 1974) in the alveolar septa (Negri et al., 2000; Rocco et al., 2003). In each strip, 20 different microscopic fields were randomly selected to quantify elastic fibres. Quantification (×200 magnification) was carried out with the aid of a digital analysis system, using specific software (Bioscan-Optimas 5:1, Bioscan, Edmond, WA, USA). The images were generated by a microscope (Axioplan, Zeiss, Oberkochen, Germany) connected to a camera (Trinitron CCD, Sony, Tokyo, Japan) and fed into a computer through a frame grabber (Oculus TCX, Coreco, St. Laurent, Quebec, Canada) for off-line processing. The thresholds for fibres of the elastic systems were established after enhancing the contrast up to a point at which the fibres were easily identified. The area occupied by fibres was determined by digital densitometric recognition. Bronchi and blood vessels were carefully avoided during the measurements. In order to avoid any bias due to septum oedema or alveolar collapse, we have divided the surface occupied by the elastic fibres measured in each alveolar septum by the length of the corresponding septum. The results were expressed as the surface covered by elastic fibres per unit of septum length ($\mu m^2/\mu m$).

Lung hydroxyproline (HP), an aminoacid of collagen, and thus a marker of fibrogenesis, was determined spectrophotometrically (Woessner, 1961). Samples from the right lung were homogenized and hydrolyzed in 6N HCl for 24 h at 60 °C. The hydrolysate was then neutralized with 6N NaOH. Afterwards, 1 ml of chloramine T, 1 ml of perchloric acid, and 1 ml of dimethylaminobenzaldehyde (Ehrlich's reagent) were added in 2 ml aliquots. Samples were read for absorbance at 561 nm. Results are expressed as μg of hydroxyproline per lung (HP_L).

Lung myeloperoxydase (MPO) activity was measured photometrically employing 3,3′, 5,5′-tetramethylbenzidine as a substrate as previously reported (Trush et al., 1997) with some modifications (Folch et al., 1998).

The left lung was fixed by intratracheal instillation of buffered formalin at a constant pressure of 10 h Pa, dehydrated in a graded series of ethanol dilutions, embedded in paraffin, cut into 3 μm-thick serial sections, and stained with haematoxylin–eosin. In each slice, 10 different microscopic fields were randomly selected to quantify for tissue fraction, alveolar wall thickness and cell count. Non-aerated areas as well as bronchi or vessels were also excluded. Quantification (×400 magnification) was carried out with the aid of a digital analysis system, using specific software (IMAQ, National Instruments, Austin TX). Tissue area (μm^2) was computed after spatial calibration, by pixel counting of the binary converted monochrome (grey) images by visual threshold. Tissue fraction was then obtained by dividing by the total area of the field. The volume of tissue (μm^3) was determined as tissue area × 3 (section thickness). Total number of cells (nuclei) by field were counted, divided by the volume of tissue and expressed as cells/μm^3.

Lung wet weight (LW) was measured after excision of non-pulmonary tissues. Then, pieces of peripheral right lung were cut, weighed (wet weight), and frozen by immersion in liquid nitrogen and stored at −80 °C until the time of analysis. After defrost, the same pieces of tissue utilized for hydroxyproline quantification were dried at 60 °C for 48 h, and weighed to obtain the dry weight of the piece. Dry-to-wet weight lung ratio (D/W) was obtained by the quotient of both measurements (Serrano-Mollar et al., 2002), by assuming the pieces are representative of the whole lung.

Lung water content (W_L) in grams/lung was obtained from LW and the dry-to-weight ratio (D/W) according to Flemmer et al. (2000):

$$W_L\,(\text{ml}) = \text{LW}\,(\text{g}) \cdot \left(\frac{1-D}{W}\right)$$

Lung index (LI), a marker of inflammation, was determined by the equation (Moore et al., 1981):

$$\text{LI} = \frac{(\text{LW/BW})_{\text{blm}}}{(\text{LW/BW})_{\text{avgctrl}}}$$

where BW is body weight, and subscripts blm and avgctrl indicate bleomycin challenged and average control values, respectively. This index relates to the degree of lung injury (Duchaine et al., 1996).

2.7. Statistical analysis

The normality of the data (Kolmogorov–Smirnov test with Lilliefors' correction) and the homogeneity of variances (Levene median test) were tested. If both conditions were satisfied, one-way ANOVA test followed by Bonferroni's post hoc test was used; Kruskal–Wallis, and Mann–Whitney as post hoc test, were applied otherwise. Spearman correlation test was run to identify associations between functional and biochemical or morphometrical data. All analyses were made using the SPSS 12.0 statistical software package. In all instances the significance level was set at 5% ($\alpha = 0.05$).

3. Results

Lung water (W_L) and LI were higher in bleomycin treated animals compared with controls at all days (Table 1). Both HP_L and MPO_L were significantly increased in the bleomycin group at days 7 and 15. The amount of elastic fibres increased at day 15 in the bleomycin group.

Table 2 shows biomechanical tissue changes. R_0 increased significantly only in BLM15 group, while η_0 was significantly higher in bleomycin than in control rats at all time points. Conversely, E_0 and β remained invariant. Changes in R_v were not significant.

Changes in tissue resistance were significantly different only at the lowest frequency for both parameters (Fig. 1). Tissue elastance did not show significant changes at any frequency.

Table 1
Biochemical and morphometric data in control and bleomycin groups

Post hoc	CTRL	BLM3	BLM7	BLM15	Kruskal–Wallis	
					χ^2	P
Elast ($\mu m^2/\mu m$)†	0.38 ± 0.08	0.41 ± 0.15	0.56 ± 0.17	1.00 ± 0.54§	20.4	<0.001
HP_L (mg/g)†	3.29 ± 0.70	3.00 ± 0.50	4.77 ± 1.64*	5.30 ± 2.19*	9.25	0.026
MPO_L (U/g)†	235 ± 133	351 ± 114	488 ± 245§	511 ± 213§	11.3	0.01
	CTRL	BLM3	BLM7	BLM15	ANOVA	
					F	P
Lung water (g)††	1.13 ± 0.06	1.63 ± 0.21§	1.91 ± 0.25§	1.98 ± 0.25§	33.58	<0.001
Lung index (LI)††	1.03 ± 0.07	1.72 ± 0.31§	1.85 ± 0.29§	1.92 ± 0.41§	18.92	<0.001

Descriptive and ANOVA analysis of biochemical, morphometric data, and indexes of inflammation of control (CTRL) and bleomycin (BLM) animals at days 3, 7, and 15. Values are mean ± S.D. Mann–Whitney's U (†) or Bonferroni (‡) post hoc test BLM versus CTRL. Significance: *$P < 0.05$; §$P < 0.01$). Elast: amount of elastic fibres in alveolar septa; HP_L: total hydroxyproline content of the lung, MPO_L: total myeloperoxydase content of the lung.

Table 2
Biomechanical data in control and bleomycin groups

	CTRL	BLM3	BLM7	BLM15	ANOVA	
					F	P
E_0	116 ± 14	127 ± 21	126 ± 15	140 ± 32	1.62	0.204
R_0	6.22 ± 0.9	7.38 ± 1.0	8.22 ± 1.28	9.60 ± 2.18§	7.78	<0.001
η_0	0.053 ± 0.003	0.058 ± 0.003*	0.065 ± 0.004§	0.068 ± 0.004§	27.69	<0.001
β	0.04 ± 0.003	0.03 ± 0.005	0.04 ± 0.007	0.04 ± 0.009	2.04	0.13
	CTRL	BLM3	BLM7	BLM15	Kruskal–Wallis	
					χ^2	P
R_v	0.11 (0.02–0.18)	0.07 (0.00–0.63)	0.09 (0.00–0.45)	0.16(0.00–0.95)	6.89	0.076

Descriptive and ANOVA or Kruskal–Wallis analysis of biomechanical parameters of control (CTRL) and bleomycin (BLM) animals at days 3, 7, and 15. Values are mean ± S.D. Bonferroni post hoc test BLM versus CTRL: *$P < 0.05$; §$P < 0.01$. E_0 (h Pa): elastance at $\omega = 1\,\text{rad}^{-1}$. R_o (h Pa s^{-1}): resistance at $\omega = 1\,\text{rad}^{-1}$. η_0: hysteresivity at $\omega = 1\,\text{rad}^{-1}$. β is the logarithmic slope of elastance and resistance versus ω (constant phase model). For R_v (the frequency invariant component of tissue resistance) 5 and 95% confidence intervals have been shown.

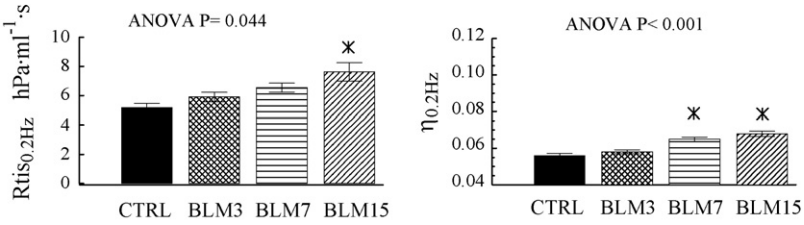

Fig. 1. Comparison of tissue resistance (left side) and hysteresivity (η, right) in control and bleomycin groups analyzed separately for the frequency of 0.2 Hz ($\omega = 1.26\,rad^{-1}$). Values are mean ± S.E.M. CTRL: control; BLM3, BLM7 and BLM15: bleomycin group at days 3, 7, and 15, respectively.

Table 3
Histological data in control and bleomycin groups

Post hoc	CTRL	BLM3	BLM7	BLM15	Kruskal–Wallis	
					χ^2	P
Total cell count (μm)†	73 ± 16	108 ± 26.9§	104 ± 23§	89 ± 28.3	11.4	0.010

	CTRL	BLM3	BLM7	BLM15	ANOVA	
					F	P
Alveolar wall thickness (μm)††	3.5 ± 1.1	3 ± 0.3	3.8 ± 0.4	4.3 ± 1.2	4.10	0.014
Tissue fraction (%)††	13 ± 5.2	22 ± 5.6§	16 ± 3.2	14 ± 3.9	7.96	<0.001

Descriptive and ANOVA analysis of histological parameters of control (CTRL) and bleomycin (BLM) animals at days 3, 7, and 15. Values are mean ± S.D. Mann–Whitney's U (†) or Bonferroni (‡) post hoc test BLM versus CTRL significance: $^{*}P < 0.05$; §$P < 0.01$.

Alveolar wall thickness diminished at day 3 but increased thereafter (Table 3). The tissue fraction increased significantly at day 3 and total cell count increased significantly at days 3 and 7.

Table 4 shows the correlation matrix (Spearman's Rho) between R_0 or η_0 and biochemical or morphological data in all animals. R_0 and η_0 were significantly correlated with MPO_L, lung water and LI. It is worth pointing out that the correlation between hysteresivity and elastic fibres content, displayed in Fig. 2 shows a nonlinear pattern. A positive correlation between alveolar wall thickness and the amount of elastic fibres ($\rho = 0.62$, $P < 0.001$) and between LI and elastic fibre contents ($\rho = 0.47$, $P = 0.002$) or W_L ($\rho = 0.92$, $P < 0.001$) were also found. W_L was correlated with MPO_L ($\rho = 0.68$, $P < 0.001$), and elastic fibre contents ($\rho = 0.53$, $P < 0.001$). As seen in Fig. 3, LI was correlated with MPO_L ($\rho = 0.65$, $P < 0.001$). Fig. 4 shows the correlation between LI and R_0.

Table 4
Correlations between tissue mechanical data and biochemical and morphological parameters

	MPO_L	Elast	Lung water	Lung index (LI)	Alveolar wall thickness
R_0	0.491†	0.34*	0.62††	0.61††	0.06 (n.s.)
η_0	0.41*	0.71††	0.68††	0.51†	0.36*

Correlations between tissue mechanical data and biochemical and morphological parameters obtained by Spearman's correlation test. Spearman's Rho and significance level ($^{*}P < 0.05$, $^{\dagger}P < 0.01$, and $^{\dagger\dagger}P < 0.001$) are shown. n.s.: non-significant. R_0: resistance at $\omega = 1\,rad^{-1}$. η_0: hysteresivity at $\omega = 1\,rad^{-1}$. MPO_L: total myeloperoxydase content of the lung. Elast: amount of elastic fibres in the alveolar septa.

4. Discussion

This study provides new evidence concerning the pathophysiology of bleomycin-induced lung injury and the relationship between inflammatory changes and lung tissue mechanics. Lung tissue dissipative parameters showed significant changes after bleomycin injury. Both R_0 and η_0 were correlated with MPO_L, lung water and LI (Table 4). HP_L showed no significant correlation with mechanical parameters, but elastin was strongly correlated with hysteresivity and alveolar wall thickness (Table 4, Fig. 2). According to these results, inflammation seems to alter pulmonary functions by eliciting biomechanical changes in the first 15 days after bleomycin challenge in rats. Furthermore, elastogenesis seems to affect the coupling between elastic and dissipative processes within the tissue.

Little is known about the mechanisms that govern viscoelastic properties of intraparenchymal connective tissues. Some authors favour the view that dissipation in connective tissues may originate at the microstructural level. The dissipation may be originated by contact phenomena between stress-bearing connective tissue fibres, such as contact (coulomb) friction (Fredberg and Stamenovic, 1989). Additionally, energy dissipation could occur at the molecular level by shearing of the proteoglycan ground substance between fibres, or it could occur at surfaces of direct fibre–fibre sliding contact (Suki et al., 1994). Correlations between lung mechanical properties and changes related to inflammation (W_L, LI, MPO_L) may be connected to changes in the composition of the ground substance related to the inflammatory process. In this line, previous studies have found an increase in proteoglycans in the histologic samples obtained at 7 and 14 days after administration of bleomycin, when inflammation was prominent, and diminished at day 28, when much

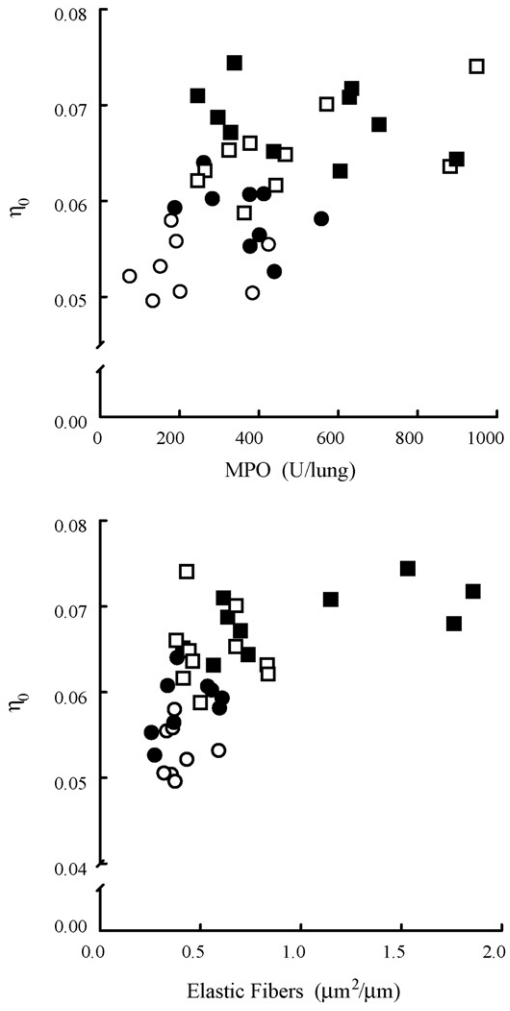

Fig. 2. Scatter plot showing the correlation between hysteresivity at $\omega = 1$ rad^{-1} frequency and myeloperoxydase lung content (top) or elastic fibres content in the lung (bottom) in control animals (open circles) and bleomycin treated rats at days 3 (close circles), 7 (open squares), and 15 (close squares).

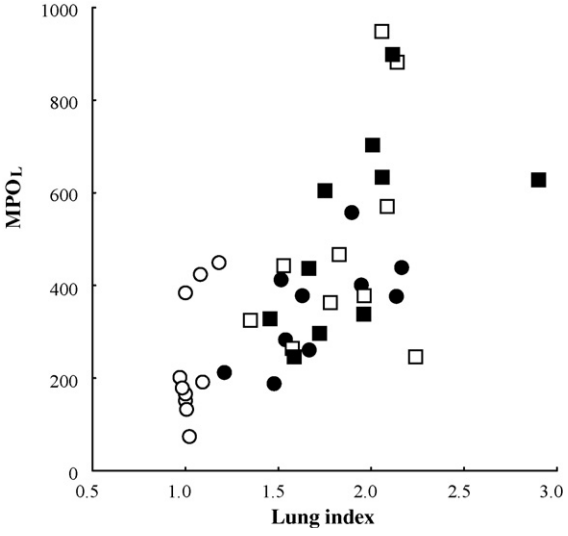

Fig. 3. Scatter plot showing the correlation myeloperoxidase (MPO) and lung index in control animals (open circles) and bleomycin treated rats at days 3 (close circles), 7 (open squares), and 15 (close squares).

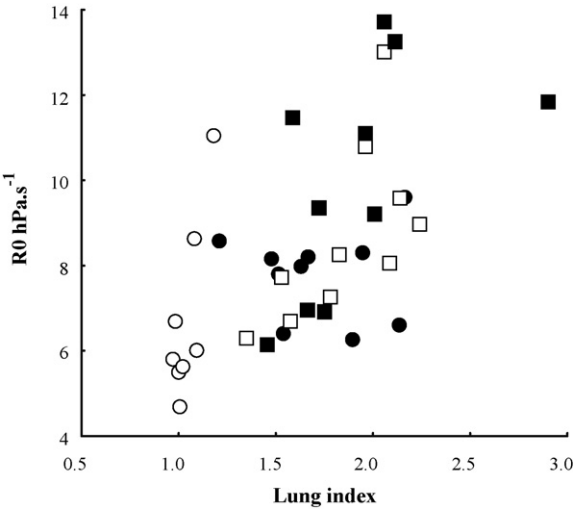

Fig. 4. Scatter plot showing the correlation between lung index and R_0 (resistance at $\omega = 1$ rad^{-1}) in control animals (open circles) and bleomycin treated rats at days 3 (close circles), 7 (open squares), and 15 (close squares).

of the inflammatory response had resolved, and heterogeneous distribution of fibrosis was observed (Westergren-Thorsson et al., 1993; Venkatesan et al., 2000). According to Venkatesan et al. (2000) the increased deposition of versican during the early inflammatory phase may be the clue to the increase in ECM water content, enhancing the migration of cells to the sites of inflammation. Other authors have suggested that water-embedded lung tissue might not only alter total respiratory compliance, but also viscoelastic properties of lung tissue such as stress-adaptation pressures (Flemmer et al., 2000). Cavalcante et al. (2005) suggested that proteoglycans influence the extent to which collagen fibres fold and stretch and, consequently, have an effect on the mechanical behavior of the stress-bearing element. Therefore, it is reasonable to think that the relationship between LI or lung water and lung tissue viscoelastic properties may be related to proteoglycan mechanical dysfunction in the ECM (Dolhnikoff et al., 1999). The increase of η_0 prior to the increase in MPO and elastic fibres in the alveolar septa supports this hypothesis.

ECM fibres (elastin and collagen) account for most of the viscoelastic mechanical properties of lung tissue strips (Rocco et al., 2001). While collagen turnover has been the scope of the majority of publications, few studies have focused on the role of elastin turnover on lung mechanics (Hoff et al., 1999; Rocco et al., 2001). Once ECM composition is altered, either because of the direct injury or cellular remodelling, there are corresponding changes in the biomechanical properties of the matrix and consequently of the alveolar wall (Suki et al., 2005).

Considering that collagen and elastin form two entangled and probably cross-linked networks, we wondered to what extent the increase in elastic fibres contributes to the changes in lung tissue mechanics. Following previous studies (Rocco et al., 2001; Faffe et al., 2001) we hypothesized that neoelastogenesis decreases the mechanical efficiency of lung parenchyma by increasing internal friction. Most of our knowledge about the structure–function relationships in the ECM matrix comes from studies on enzymatic digestions. The constancy of hys-

teresivity after elastase digestion suggests that disruption of the elastin–collagen network does not alter the coupling between elastic and dissipative processes in lung tissue (Moretto et al., 1994; Lopez-Aguilar and Romero, 1998). However, we can expect that the impact of ECM changes on lung tissue biomechanics during remodelling substantially differ from enzymatic digestion. Viscoelastic properties of ECM depend largely on the interaction with "ground substance" especially proteoglycans (Cavalcante et al., 2005). These interactions explain why elastin, the most "linearly" biosolid materials known when isolated (Fung, 1993), has a viscoelastic behavior *in situ*. In a paraquat-induced acute lung injury model, the mechanical properties of lung tissue were related to the amount of non-mature (oxytalan) elastic fibres, while elastance was related to collagen fibres (Rocco et al., 2001). Similarly, both tissue resistance and hysteresivity were related to the amount of elastic fibres in a murine model of silicosis (Faffe et al., 2001). In our model setting, both elastic fibres and HP_L increased significantly from day 7. Internal frictions in viscoelastic materials tend to increase dissipation at low frequencies (Fung, 1993). We have found that dissipative properties of lung tissue at low frequency increase at day 15 ($Rti_{0.2\,Hz}$ and $\eta_{0.2\,Hz}$), or even at day 7 ($\eta_{0.2\,Hz}$). Furthermore, the increase in R_0 and η_0 are maximal at day 15. It seems reasonable to think that the increase in the amount of fibres at day 15 would increase the internal frictions in the tissue interacting with changes in the ground substance.

In our study, hysteresivity was related to MPO_L, a marker of neutrophilic infiltration and oxidative stress during the inflammatory process. Hitherto, no studies have assessed the inflammatory process derived from the bleomycin challenge, nor changes in lung tissue biomechanical parameters under the scope of induced inflammation. Studies on allergen-sensitized animals have shown an increase in pulmonary hysteresivity either *in vivo* (Collins et al., 2003) or in lung tissue strips (Nagase and Ludwig, 1998). This is the first study, to our knowledge, to show a correlation between an intrinsic property of lung tissue, hysteresivity, and a marker of inflammation (MPO_L). We interpreted this correlation as an indicator of the dependence of tissue biomechanics on the underlying structural changes induced by inflammation.

On the other hand, Horgan et al. (1993) have examined whether the generation of tumour necrosis factor (TNF-alpha) after lipopolysaccharide (LPS) challenge contributes to increases in lung vascular permeability and water content. They concluded that activation of the sequestered PMN increases pulmonary vascular permeability and tissue water content. Certainly, whether the correlation between MPO_L and biomechanical parameters indicates a direct effect of oxidative stress on ECM remains in the field of speculation.

The fact that there is no correlation between hydroxyproline and the biomechanical parameters does not mean that fibrogenesis is absent in a 2-week model of pulmonary fibrosis, but the amount of collagen fibres is not sufficient to have a significant impact upon tissue mechanics.

We concluded that inflammation and elastogenesis are the main determinants for hysteretic changes observed in the first 15 days after bleomycin challenge in rats. Moreover, in this 2-week model, the inflammatory process triggered by the bleomycin challenge leads to changes in biomechanical parameters such as resistance and hysteresivity. According to our results, the interpretation of studies employing the bleomycin-induced model of pulmonary fibrosis, especially when testing new therapeutic approaches, should take the high impact of the inflammatory process into account.

Acknowledgements

(a) We would like to express our gratitude to Mrs. Anna Bachs for her skilful technical assistance.
(b) This study was supported by Red Respira (ISCiii RTIC 03/011) Spain, Centres of Excellence Program (PRONEX-FAPERJ), Brazilian Council for Scientific and Technological Development (CNPq), Carlos Chagas Filho, Rio de Janeiro State Research Supporting Foundation (FAPERJ), Mariona Pinart is granted by a Research Scholarship of IDIBELL.

References

Boyaci, H., Maral, H., Turan, G., Basyigit, I., Dilliolugil, M.O., Yildiz, F., Tugay, M., Pala, A., Ercin, C., 2006. Effects of erdosteine on bleomycin-induced lung fibrosis in rats. Mol. Cell. Biochem. 281, 129–137.

Cavalcante, F.S., Ito, S., Brewer, K., Sakai, H., Alencar, A.M., Almeida, M.P., Andrade Jr., J.S., Majumdar, A., Ingenito, E.P., Suki, B., 2005. Mechanical interactions between collagen and proteoglycans: implications for the stability of lung tissue. J. Appl. Physiol. 98, 672–679.

Collins, R.A., Sly, P.D., Turner, D.J., Herbert, C., Kumar, R.K., 2003. Site of inflammation influences site of hyperresponsiveness in experimental asthma. Respir. Physiol. Neurobiol. 139, 51–61.

Dolhnikoff, M., Mauad, T., Ludwig, M.S., 1999. Extracellular matrix and oscillatory mechanics of rat lung parenchyma in bleomycin-induced fibrosis. Am. J. Respir. Crit. Care Med. 160, 1750–1757.

Duchaine, C., Israel-Assayag, E., Fournier, M., Cormier, Y., 1996. Proinflammatory effect of Pediococcus pentosaceus, a bacterium used as hay preservative. Eur. Respir. J. 9, 2508–2512.

Ebihara, T., Venkatesan, N., Tanaka, R., Ludwig, M.S., 2000. Changes in extracellular matrix and tissue viscoelasticity in bleomycin-induced lung fibrosis. Temporal aspects. Am. J. Respir. Crit. Care Med. 162, 1569–1576.

Faffe, D.S., D'Alessandro, E.S., Xisto, D.G., Antunes, M.A., Romero, P.V., Negri, E.M., Rodrigues, N.R., Capelozzi, V.L., Zin, W.A., Rocco, P.R., 2006. Mouse strain dependence of lung tissue mechanics: role of specific extracellular matrix composition. Respir. Physiol. Neurobiol. 152, 186–196.

Faffe, D.S., Silva, G.H., Kurtz, P.M., Negri, E.M., Capelozzi, V.L., Rocco, P.R., Zin, W.A., 2001. Lung tissue mechanics and extracellular matrix composition in a murine model of silicosis. J. Appl. Physiol. 90, 1400–1406.

Flemmer, A., Simbruner, G., Muenzer, S., Proquitte, H., Haberl, C., Nicolai, T., Leiderer, R., 2000. Effect of lung water content, manipulated by intratraqueal furosemide, surfactant, or a mixture of both, on compliance and viscoelastic tissue forces in lung-lavaged newborn piglets. Crit. Care Med. 28, 1911–1917.

Folch, E., Closa, D., Prats, N., Gelpi, E., Rosello-Catafau, J., 1998. Leukotriene generation and neutrophil infiltration after experimental acute pancreatitis. Inflammation 22, 83–93.

Fredberg, J.J., Stamenovic, D., 1989. On the imperfect elasticity of lung tissue. J. Appl. Physiol. 67, 2408–2414.

Fullmer, H.M., Sheetz, J.H., Narkates, A.J., 1974. Oxytalan connective tissue fibers: a review. J. Oral. Pathol. 3, 291–316.

Fung, Y.C., 1993. Biomechanics: Mechanical Properties of Living Tissues. Springer-Verlag, New York.

Hantos, Z.A., Daroczy, B., Suki, B., Nagy, S., Fredberg, J.J., 1992. Input impedance and peripheran inhomogeneity of dog lungs. J. Appl. Physiol. 72, 168–178.

Hay, J., Shahzeidi, S., Laurent, G., 1991. Mechanisms of bleomycin-induced lung damage. Arch. Toxicol. 65, 81–94.

Hoff, C.R., Perkins, D.R., Davidson, J.M., 1999. Elastin gene expression is upregulated during pulmonary fibrosis. Connect. Tissue Res. 40, 145–153.

Horgan, M.J., Palace, G.P., Everitt, J.E., Malik, A.B., 1993. TNF-alpha release in endotoxemia contributes to neutrophil-dependent pulmonary edema. Am. J. Physiol. 264, H1161–H1165.

Iraz, M., Erdogan, H., Kotuk, M., Yagmurca, M., Kilic, T., Ermis, H., Fadillioglu, E., Yildirim, Z., 2006. Ginkgo biloba inhibits bleomycin-induced lung fibrosis in rats. Pharmacol. Res. 53, 310–316.

Jones, A.W., Reeve, N.L., 1978. Ultrastructural study of bleomycin-induced pulmonary changes in mice. J. Pathol. 124, 227–233.

Lopez-Aguilar, J., Romero, P.V., 1998. Effect of elastase pretreatment on rat lung strip induced constriction. Respir. Physiol. 113, 239–246.

Moore, V.L., Mondloch, V.M., Pedersen, G.M., Schrier, D.J., Allen, E.M., 1981. Strain variation in BCG-induced chronic pulmonary inflammation in mice: control by a cyclophosphamide-sensitive thymus-derived suppressor cell. J. Immunol. 127, 339–342.

Moretto, A., Dallaire, E., Romero, P., Ludwig, M.S., 1994. Effect of elastase on oscillation mechanics of lung parenchymal strips. J. Appl. Physiol. 77, 1623–1629.

Nagase, T., Ludwig, M.S., 1998. Antigen-induced responses in lung parenchymal strips during sinusoidal oscillation. Can. J. Physiol. Pharmacol. 76, 176–181.

Negri, E.M., Montes, G.S., Saldiva, P.H., Capelozzi, V.L., 2000. Architectural remodelling in acute and chronic interstitial lung disease: fibrosis or fibroelastosis? Histopathology 37, 393–401.

Rocco, P.R., Souza, A.B., Faffe, D.S., Passaro, C.P., Santos, F.B., Negri, E.M., Lima, J.G., Contador, R.S., Capelozzi, V.L., Zin, W.A., 2003. Effect of corticosteroid on lung parenchyma remodeling at an early phase of acute lung injury. Am. J. Respir. Crit. Care Med. 168, 677–684.

Rocco, P.R.M., Negri, E.M., Kurtz, P.M., Vasconcellos, F.P., Silva, G.H., Capelozzi, V.L., Romero, P.V., Zin, W.A., 2001. Lung tissue mechanics and extracellular matrix remodeling in acute lung injury. Am. J. Respir. Crit. Care Med. 164, 1067–1071.

Romero, P.V., Zin, W.A., Lopez-Aguilar, J., 2001. Frequency characteristics of lung tissue during passive stretch and induced pneumoconstriction. J. Appl. Physiol. 91, 882–890.

Salerno, F.G., Fust, A., Ludwig, M.S., 2004. Stretch-induced changes in constricted lung parenchymal strips: role of extracellular matrix. Eur. Respir. J. 23, 193–198.

Serrano-Mollar, A., Closa, D., Cortijo, J., Morcillo, E.J., Prats, N., Gironella, M., Panes, J., Rosello-Catafau, J., Bulbena, O., 2002. P-selectin upregulation in bleomycin induced lung injury in rats: effect of *N*-acetyl-L-cysteine. Thorax 57, 629–634.

Silva, M.F., Zin, W.A., Saldiva, P.H., 1998. Airspace configuration at different transpulmonary pressures in normal and paraquat-induced lung injury in rats. Am. J. Respir. Crit. Care Med. 158, 1230–1234.

Sogut, S., Ozyurt, H., Armutcu, F., Kart, L., Iraz, M., Akyol, O., Ozen, S., Kaplan, S., Temel, I., Yildirim, Z., 2004. Erdosteine prevents bleomycin-induced pulmonary fibrosis in rats. Eur. J. Pharmacol. 494, 213–220.

Suki, B., Ito, S., Stamenovic, D., Lutchen, K.R., Ingenito, E.P., 2005. Biomechanics of the lung parenchyma: critical roles of collagen and mechanical forces. J. Appl. Physiol. 98, 1892–1899.

Suki, B., Varabais, A.L., Lutchen, K.R., 1994. Lung tissue viscoelasticity: a mathematical framework and its molecular basis. J. Appl. Physiol. 76, 2749–2759.

Thrall, R.S., Barton, R.W., D'Amato, D.A., Sulavik, S.B., 1982. Differential cellular analysis of bronchoalveolar lavage fluid obtained at various stages during the development of bleomycin-induced pulmonary fibrosis in the rat. Am. Rev. Respir. Dis. 126, 488–492.

Trush, M.A., Egner, P.A., Kensler, T.W., 1997. Myeloperoxidase as a biomarker of skin irritation and inflammation. Food Chem. Toxicol. 32, 143–147.

Venkatesan, N., Ebihara, T., Roughley, P.J., Ludwig, M.S., 2000. Alterations in large and small proteoglycans in bleomycin-induced pulmonary fibrosis in rats. Am. J. Respir. Crit. Care Med. 161, 2066–2073.

Westergren-Thorsson, G., Hernnas, J., Sarnstrand, B., Oldberg, A., Heinegard, D., Malmstrom, A., 1993. Altered expression of small proteoglycans, collagen, and transforming growth factor-beta 1 in developing bleomycin-induced pulmonary fibrosis in rats. J. Clin. Invest. 92, 632–637.

Woessner, J.F., 1961. The determination of hydroxiproline in tissue and protein samples containing small proportions of this amino acid. Arch. Biochem. Biophys. 93, 440–447.

Yao, H.W., Zhu, J.P., Zhao, M.H., Lu, Y., 2006. Losartan attenuates bleomycin-induced pulmonary fibrosis in rats. Respiration 73, 236–242.

Yuan, H., Ingenito, E., Suki, B., 1997. Dynamic properties of lung parenchyma: mechanical contributions of fiber network and interstitial cells. J. Appl. Physiol. 83, 1420–1431.

Zhao, Y., Young, S.L., McIntosh, J.C., 1998. Induction of tenascin in rat lungs undergoing bleomycin-induced pulmonary fibrosis. Am. J. Physiol. 274, L1049–L1057.

IV.1 Objectives 3 and 4

OBJECTIVE 3: "To characterise the time course of biomechanical changes of the lung after repeated doses of BLM challenge in a murine model of a chronic subacute lung injury".

OBJECTIVE 4: "To compare "in vitro" lung mechanics, inflammatory and fibrogenic parametres after a single and repeated BLM intratracheal instillation 28 days after last challenge".

Specific objectives

- To characterise the mechanical behaviour at the established time point (day 28) after a single-dose BLM challenge.
- To characterise the mechanical behaviour 28 days after the last dose in a rat model of 3 repeated doses (day 0, week 2 and week 4).
- To measure inflammatory and remodelling parametres at day 28 in the single-dose model and at day 28 after the last dose in the repeat dose model.
- To analyse the impact of each of the inflammatory and remodelling parametres on each model.
- To compare "in vitro" lung mechanics, inflammatory and fibrogenic parametres after a single and repeated BLM intratracheal instillation 28 days after challenge.
- To ascertain whether the repeat dose model mimics the pathophysiology of ILD and the single dose model leads to fibrotic phase or to a reparative process.

M. Pinart, A. Serrano-Mollar, R. Llatjos, P.R.M. Rocco, P.V. Romero. Single and repeated intratracheal instillations of bleomycin lead to different biomechanical changes in lung tissue in *Respiratory Physiology & Neurobiology*. 2009; 166(1):41-46.

In the first study we demonstrated that the time course of a two-week model is not long enough to observe the fibrotic phase. However, many studies have shown that a single dose of BLM lead to a reparative process after 4 weeks because the injury provoked by BLM is dose-dependent. Under the premise that alveolitis is induced by a single dose of BLM resulting in a reparative process whilst repeated doses lead to a progressive fibrosis, we compared “in vitro” lung mechanics, inflammatory and fibrogenic parametres after a single and repeated BLM intratracheal instillation 28 days after challenge.

For this purpose, rats were intratracheally instilled with a single dose of belomycin or three times one week apart, and sacrificed 28 days after challenge. Forced oscillatory mechanics (elastic modulus, tissue damping and hysteresivity) as well as inflammatory (myeloperoxidase and lung index) and remodelling (amount of collagen fibres) indices were studies in lung tissue strips.

Both elastic modulus, tissue damping, and myeloperoxidase increased only in repeat doses-challenged rats. Although fibroblast focus was found in the repeat dose model, collagen fibre content increased in both challenged groups. However, the amount of collagen fibre in single-dose group was not enough to induce lung tissue mechanical changes.

Single and repeat doses of BLM led to different inflammatory and fibrogenic behaviour resulting in distinct lung biomechanical changes 28 days after challenge. The model of three repeated doses of BLM simulated the key events in some human interstitial diseases (non specific interstitial pneumonia, desquamative interstitial pneumonitis, hypersensitivity pneumonitis, etc) characterised by inflammation, aberrant epithelial repair, deregulated fibrosis activity and progressive tissue scarring. Although longer trials are required, the present experimental model of repeated sublethal doses of BLM and the evaluation of lung damage by studying lung tissue strip biomechanics may be a promising method for testing antifibrotic drugs and for providing new insights into ILD pathophysiology.

Respiratory Physiology & Neurobiology 166 (2009) 41–46

Contents lists available at ScienceDirect

Respiratory Physiology & Neurobiology

journal homepage: www.elsevier.com/locate/resphysiol

Single and repeated bleomycin intratracheal instillations lead to different biomechanical changes in lung tissue

M. Pinart[a], A. Serrano-Mollar[b], R. Llatjós[c], P.R.M. Rocco[d], P.V. Romero[a,*]

[a] Laboratory of Experimental Pneumology, IDIBELL, L'Hospitalet, Barcelona, Spain
[b] Department of Experimental Pathology, IIBB-CSIC, IDIBAPS, Barcelona, Spain
[c] Department of Pathology, Hospital de Bellvitge, Barcelona, Spain
[d] Laboratory of Pulmonary Investigation, Carlos Chagas Filho Biophysics Institute, Federal University of Rio de Janeiro, Rio de Janeiro, Brazil

ARTICLE INFO

Article history:
Accepted 13 January 2009

Keywords:
Bleomycin
Acute alveolitis
Myeloperoxydase
Interstitial lung diseases
Lung mechanics

ABSTRACT

Single dose of bleomycin induces acute alveolitis followed by a reparative process whilst a repeated dose results in progressive fibrosis, which may lead to distinct lung tissue biomechanical changes. To test this hypothesis, rats were intratracheally instilled with saline ($N = 11$) or bleomycin (2.5 U/kg) once (SD, $N = 8$) or three times (RD, $N = 9$) one week apart, and sacrificed 28 days after challenge. Forced oscillatory mechanics as well as the amount of collagen fibre and myeloperoxidase content (MPO_L) were studied in lung tissue strips. Both elastic modulus (H), tissue damping (G), and MPO_L increased only in RD-challenged rats. Although fibroblast focus was found in RD, collagen fibre content increased in both challenged groups. However, the amount of collagen fibre in SD group was not enough to induce lung tissue mechanical changes. In conclusion, repeated doses of bleomycin induce inflammatory and fibrogenic behaviour with biomechanical changes mimicking interstitial lung disease in humans.

1. Introduction

Interstitial lung disorders (ILD), constitute a group of diseases that are both unresponsive to treatment and life threatening. These diseases are characterised by abnormal interstitial remodelling, but the biochemical mechanisms and pathophysiology are still poorly understood (Chapman, 2004; Strieter, 2008). Researchers ask for an animal model able to reproduce the basic features of ILD in order to develop effective therapies (Chua et al., 2005; Molina-Molina et al., 2007). In fact, many agents have been shown to inhibit bleomycin-induced lung fibrosis, however, none of these compounds presented antifibrotic effects in human disease. These negative effects could be attributed to the choice of the animal model. In this regard, Moeller et al. (2008) stated that it is critical to distinguish between drugs interfering with the inflammatory and early fibrogenic response from those preventing progression of fibrosis. The latter requires the use of animal models of ILD reproducing more likely human disease.

Bleomycin is a drug frequently used in the induction of lung fibrosis. Immediately after intratracheal instillation of bleomycin, a patchy inflammatory reaction, characterised by diffuse alveolitis, is followed by fibroblast proliferation, and extracellular matrix (ECM) deposition (Bowden, 1984; Molina-Molina et al., 2007). Single sub-lethal dose of bleomycin in rats usually induces an inflammatory and fibrotic process (Bowden, 1984), which tends to recede with the time course of lung injury (Brown et al., 1988). We recently reported that during the first two weeks after a single bleomycin challenge, pulmonary inflammation was mainly responsible for lung tissue mechanical changes (Pinart et al., 2008). Repeated doses of bleomycin cause an inflammatory process resulting in progressive fibrosis with increase in collagen deposition and proliferative activity of fibroblasts (Brown et al., 1988). Hitherto no studies have analysed the impact of repeated bleomycin challenge on lung tissue mechanics.

Alveolitis is induced by a single sub-lethal dose of bleomycin resulting in a reparative process whilst repeated doses lead to a progressive fibrosis which may cause distinct lung tissue biomechanical changes. For this purpose, we compared *in vitro* lung mechanics, inflammatory and fibrogenic parameters after a single and repeated bleomycin intratracheal instillation 28 days after challenge. Lung tissue strips were used since they allow the exploration of the biomechanical behaviour of ECM without the interference of surface forces, airways or distribution factors, which influence *in vivo* studies (Yuan et al., 2000; Romero et al., 2001).

* Corresponding author at: Unitat de Pneumologia Experimental, Unitat Docent de Bellvitge, IDIBELL, Universitat de Barcelona, C/Feixa Llarga s/n, 08907 L'Hospitalet de Llobregat, Spain. Tel.: +34 93 403 5807; fax: +34 93 260 7689.
E-mail address: pvromero@csub.scs.es (P.V. Romero).

1569-9048/$ – see front matter © 2009 Elsevier B.V. All rights reserved.
doi:10.1016/j.resp.2009.01.002

2. Material and methods

2.1. Animals and experimental protocol

Specific pathogen-free (SPF), male Sprague–Dawley rats (225–300 g) at the beginning of the experiments, were obtained from Harlan Ibérica S.L (Sant Feliu de Codines, Spain). Rats were fed a standard rat chow and housed under SPF controlled environmental conditions (temperature 22 °C, 12 h light/dark cycle). Animals were given water and food *ad libitum*. The experiments were carried out in accordance with the current legislation on animal experiments in the European Union and approved by our institutional committee for animal care and research. After anaesthesia with 4% isofluorane, eight rats received a single sub-lethal dose of bleomycin (2.5 U/kg dissolved in 0.25 mL of 0.9% NaCl) intratracheally, and were studied at day 28 (SD or single dose group), and a second group of 9 rats received similar doses of bleomycin three times one week apart and were sacrificed 28 days after the last dose (RD or repeat dose group). Control groups (CTRL, $n = 11$) received either a single dose ($n = 8$) or repeat doses ($n = 3$) of sterile saline solution (0.9% NaCl) intratracheally (0.25 mL i.t.) (Serrano-Mollar et al., 2002; Molina-Molina et al., 2006) and were studied 28 days after the last instillation. RD rats were two weeks younger than those in SD group when added to the study, due to the longer duration of the experiment in RD group. Since there were no significant differences in lung mechanical and histological parameters of CTRL group between single and repeat doses, we pooled all control data into a single group. The day of the last intratracheal injection with BLM or saline was designated day 0. Body weight was recorded daily or every 2 days after instillation.

At the time of the study, the rats were anaesthetised with intraperitoneal injection of ketamine (75 mg kg^{-1}) and diazepam (5 mg kg^{-1}). After anaesthesia, heparin (1000 IU) was intravenously injected and, 5 min later the animals were exsanguinated by sectioning abdominal aorta and vena cava. The lungs were removed *en bloc*, and placed in a modified Krebs–Henseleith (K–H) solution [mM: 118.4 NaCl, 4.7 KCl, 1.2 K_3PO_4, 25 $NaHCO_3$, 2.5 $CaCl_2 \cdot H_2O$, 0.6 $MgSO_4 \cdot H_2O$, and 11.1 glucose] buffered at pH 7.40 and stored at 6 °C (Lopez-Aguilar and Romero, 1998).

2.2. Apparatus

Subpleural strips (15 mm × 3 mm × 3 mm) were cut from right lung and suspended vertically in a K–H organ bath maintained at 37 °C, continuously bubbled with a mixture of 95% O_2–5% CO_2 (Romero et al., 2001). Lung strips were weighed (W), and their unloaded resting lengths (L_0) were determined with a calliper. Lung strip volume was measured by simple densitometry: vol = $\Delta F/\delta$, where ΔF is the total change in force before and after strip immersion in K–H solution and δ is the mass density of K–H solution (Lopez-Aguilar and Romero, 1998; Romero et al., 2001). One end of the strip was attached to a force transducer (FT03, Grass-Telefactor, RI, USA), and the other end was fastened to a lever arm actuated by means of a modified woofer driven by the signal generated by a computer and analogue-to-digital converter (AT-MIO-16-E-10, National Instruments, Austin, TX, USA). A sidearm of this rod was linked to a second force transducer (LETICA TRI-110, Scientific Instruments, Barcelona, Spain) by means of a silver spring of known Young's modulus, thus allowing the measurement of displacement.

2.3. Preconditioning

Cross-sectional, unstressed area (A_0) of the strip was determined from strip volume and unstressed length, according to $A_0 = \text{vol}/L_0$. Basal force (F_B) for a stress of 10 hPa was calculated as F_B (g) = 10(hPa)·A_0 (cm^2) and adjusted by vertical displacement of the force transducer as described before (Romero et al., 2001). The displacement signal was then set to zero.

Once basal force and displacement signals were adjusted, the length between bindings (L_B) was measured by means of a precision calliper. Instantaneous length (L_i) during oscillation around L_B was determined by adding the value of L_B to the measured value of displacement at any time. Instantaneous average cross-section area (A_i) was determined as $A_i = Vs/L_i$ (cm^2). Instantaneous stress (σ_i) was calculated by dividing force (g) by A_i (cm^2). Instantaneous strain was calculated as $\varepsilon_i = (L_i - L_B)/L_B$.

Amplitude was adjusted to 5% L_B and the oscillation maintained for another 30 min, or until a stable length–force loop was reached. After preconditioning, the strips were oscillated at a frequency (f) = 1 Hz. Bath solution was renewed regularly (every 20 min) with 37 °C K–H solution.

2.4. Biomechanical study

After preconditioning, samples were set at an operating stress of 10 hPa. Then, three 20-s recordings of multifrequency forced oscillations were performed. Pseudorandom driving signal was composed of five sinusoids of the same power amplitude and frequencies (f) 0.2, 0.5, 1.1, 1.9, and 3.1 Hz. Both force and displacement signals were pre-amplified, filtered at 30 Hz, and sampled at a frequency of 150 Hz.

2.5. Calculation of complex impedance parameters of lung tissue

Strain to stress relationships in a nearly linear system is characterised by the complex Young or elastic modulus $\Psi(\omega)$ (Yuan et al., 2000; Romero et al., 2001):

$$\Psi(\omega) = \frac{\sigma(\omega)}{\varepsilon(\omega)} = G' \cdot (\omega) + j \cdot G'' \cdot (\omega)$$

where σ is stress and ε is strain j is the imaginary unit, G' is the storage modulus and G'' is the loss modulus or the component of the stress that is in phase with the strain rate.

Lung tissue impedance (Z_{ti}), a magnitude that relates stress to the rate of change in strain was determined according to:

$$Z_{ti}(\omega) = \frac{\sigma(\omega)}{[d\varepsilon(\omega)/dt]}$$

Both σ and $d\varepsilon/dt$ are functions of angular frequency ($\omega = 2\pi f$). $d\varepsilon(\omega)/dt$ is the derivative of displacement strain with respect to time (t). $Z(\omega)$ was fitted with the constant-phase model first described by Hantos et al. (1992):

$$Z(\omega) = \left[\frac{G - jH}{\omega^{\alpha}}\right]$$

where G is tissue damping, H is tissue elastance, j is the imaginary unit, and $\alpha = (2/\pi)\cdot\tan^{-1}(H/G)$. To account for the newtonian or frequency-independent resistance (R_v) of tissue we used the following expression:

$$Z_{ti}(\omega) = R_v + \left[\frac{G - jH}{\omega^{\alpha}}\right]$$

Model fit was performed as follows: after calculation of the real and imaginary components of tissue impedance:

$$Z_{real} = R_v + G \cdot \omega_n^{-\alpha}$$
$$Z_{im} = -j \cdot H \cdot \omega_n^{-\alpha}$$

the value of R_v was obtained by recursive linear regression to obtain the value that accomplished the constant phase paradigm ($\alpha_{real} = \alpha_{im}$). According to Ito et al. (2004), we have used the normalised angular frequency ($\omega_n = \omega/\omega_0$), where $\omega_0 = 1$ rad/s. This allows to express G and H in "elastance" units (hPa).

Table 1
Demographic data in control and bleomycin groups.

	CTRL	SD	RD	ANOVA	
	$N = 11$	$N = 8$	$N = 9$	F	(P)
LW (g)	1.90 ± 0.24	2.58 ± 0.11*	3.35 ± 0.23*,‡	120.2	<0.001
Body weight$_i$ (g)	268 ± 11.87	275 ± 9.89	255 ± 9.91*,‡	8.11	0.002
Body weight$_f$ (g)	365 ± 26.16	328 ± 11.94	292 ± 45.0*	13.58	<0.001
Lung index (LI)	0.95 ± 0.05	1.47 ± 0.08*	2.00 ± 0.32*,‡	77.8	<0.001

Descriptive and ANOVA analysis of demographic data of control (CTRL) and bleomycin challenged animals (SD: single dose; RD: repeat doses). Values are mean ± SD. LW: lung weight; Body weight$_i$: initial body weight; Body weight$_f$ (g): final body weight.

* Significantly different from CTRL ($P < 0.05$).

‡ Significant difference between SD and RD ($P < 0.05$).

Table 2
Biochemical and morphometric data in control and bleomycin groups.

	CTRL	SD	RD	ANOVA	
	$N = 11$	$N = 8$	$N = 9$	F	(P)
MPO_L (U/g)	245 ± 124	247 ± 68	1825 ± 539*,‡	75.8	<0.001
Collagen % tissue	12.2 ± 8.3	23 ± 13*	43.2 ± 16*,‡	33.7	<0.001

Total myeloperoxydase content of the lung (MPO_L) and the percentage of collagen fibre in lung tissue in control (CTRL) and bleomycin challenged animals (SD: single dose; RD: repeat doses). Values are mean ± SD.

* Significantly different from CTRL ($P < 0.05$).

‡ Significant difference between SD and RD ($P < 0.05$).

Analysis and parameter estimation were performed by means of specific software elaborated with LabVIEW 7.0 (National Instruments Co., Austin, TX, USA). Hysteresivity (η) was calculated as:

$$\eta = \frac{G}{H}$$

2.6. Biochemical studies

Lung wet weight (LW) was measured after excision of non-pulmonary tissues. Lung index (LI), a marker of lung damage, was determined by the equation (Moore et al., 1981; Duchaine et al., 1996):

$$\mathrm{LI} = \frac{(\mathrm{LW/BW})_{\mathrm{blm}}}{(\mathrm{LW/BW})_{\mathrm{avgctrl}}}$$

where BW is body weight, and subscripts blm and avgctrl indicate bleomycin challenged and average control values respectively.

Lung myeloperoxydase (MPO) activity was measured photometrically employing 3,3′-5,5′-tetramethylbenzidine as a substrate (Trush et al., 1994) but with some modifications (Folch et al., 1998).

2.7. Histological assessment

Subpleural strips were fixed with 4% paraformaldehyde in PBS for 24 h, dehydrated in a graded series of ethanol, embedded in paraffin, and cut into 4-μm thick serial sections. They were stained with hematoxilin-eosin for histological analysis, and Masson's trichrome to quantify collagen deposition. A total of five photomicrographs of each preparation were used to quantify collagen fibre content at ×400. Total tissue surface was measured after binary conversion. After identification of an area of interest (blue stained collagen), colour threshold analysis was applied and binary converted. Area covered by collagen was expressed as percentage of total tissue surface. The program used was IMAQ Vision Builder 5.0 (National Instruments, Austin, TX, USA).

2.8. Drug sources

Bleomycin sulphate (BLM) was purchased from Almirall-Prodesfarma (Barcelona, Spain). Isoflurane (Forane) was obtained from Abbot Laboratories S.A. (Madrid, Spain). Unless otherwise stated, chemicals and reagents used were purchased from standard commercial sources.

2.9. Statistical analysis

SPSS 12.0 statistical software package was used. Data are expressed as mean ± SD unless otherwise specified. One-way ANOVA test followed by Bonferroni's post hoc test was used to compare bleomycin-induced group with controls. Correlation between lung tissue mechanical parameters and MPO_L, LI, and collagen fibre content was determined by Spearman correlation test. In all instances the significance level was set at 5% ($\alpha = 0.05$).

Table 3
Biomechanical data in control and bleomycin groups at 10 hPa stress.

	CTRL	SD	RD	ANOVA	
	$N = 11$	$N = 8$	$N = 9$	F	(P)
H (hPa)	128 ± 32.74	138 ± 32.14	245 ± 19.14*,‡	42.19	<0.001
G (hPa)	5.10 ± 0.97	5.43 ± 1.93	9.36 ± 2.63*,‡	13.78	<0.001
G/H	0.041 ± 0.009	0.039 ± 0.007	0.038 ± 0.011	0.25	0.78
α	−0.977 ± 0.01	−0.976 ± 0.01	−0.983 ± 0.02	0.84	0.45

Biomechanical parameters in control (CTRL) and bleomycin challenged animals (SD: single dose; RD: repeat doses). Values are mean ± SD. H (hPa): elastic modulus. G (hPa): tissue damping. G/H: hysteresivity. α: is the logarithmic slope of Real and Imaginary components of tissue impedance *versus* ω (constant phase model).

* Significantly different from CTRL ($P < 0.05$).

‡ Significant difference between SD and RD ($P < 0.05$).

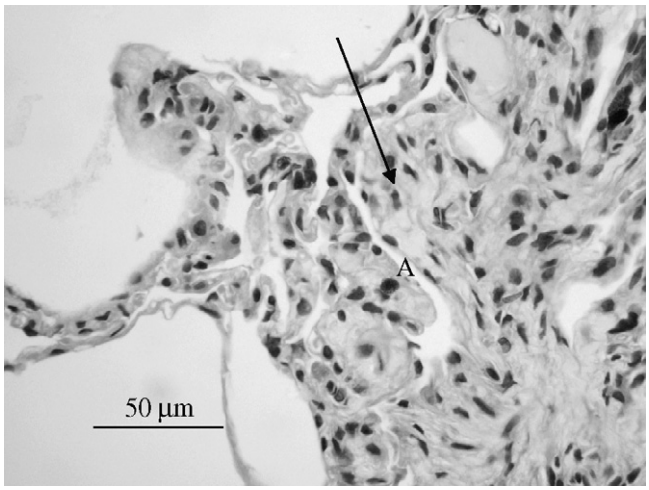

Fig. 1. Photomicrographs of lung parenchyma stained with haematoxilin eosin in a RD animal. Note the presence of a fibroblast focus (arrow) protruding into the alveolar space (A).

3. Results

Lung weight and lung index were higher in both bleomycin-challenged groups compared to CTRL. The final body weight was significantly lower in RD compared to CTRL group (Table 1).

Myeloperoxidase (MPO_L) was significantly increased only in RD group. Although fibroblast focus was found only in RD group (Fig. 1), collagen fibre content was higher in both challenged groups compared to CTRL, but lower in SD than RD (Table 2). Lymphocyte and macrophage infiltration were observed in RD-challenged group, but not in SD.

At stress of 10 hPa, both elastic modulus (H) and tissue damping (G) were higher in RD compared to CTRL and SD groups (Table 3). In Fig. 2 both real and imaginary parts of tissue impedance presented a different behaviour in RD-challenged animals, whilst no significant differences were found between CTRL and SD. Significant correlation was found between G and MPO ($\rho = 0.571$, $P = 0.021$), and LI ($\rho = 0.759$, $P = 0.001$) in bleomycin-challenged animals (Fig. 3). The amount of collagen fibre in bleomycin-challenged animals correlated with H ($\rho = 0.534$, $P = 0.023$) but not with G ($\rho = 0.244$, $P > 0.05$).

4. Discussion

The present study has shown that repeat doses of bleomycin induced inflammatory cell infiltration, an increase in myeloperoxidase, collagen fibre deposition, and fibroblast focus, augmenting both elastic modulus (H) and tissue damping (G) 28 days after challenge. In contrast, a single dose of bleomycin results in an increase in collagen fibre content with no significant changes in lung mechanics.

Previous studies in rats have shown that biochemical and histological changes suggestive of pulmonary fibrosis are maximal between 14 and 28 days after single bleomycin challenge, with peak response around day 21 (Moore and Hogaboam, 2008). After this time point, fibroblastic activity decreases and fibrosis begin to resolve (Phan et al., 1983; Gharaee-Kermani et al., 2005). Our results are in agreement with these reports: collagen fibre content was augmented at day 28 in SD, but lung tissue biomechanics was similar to controls. In 1988, Brown et al. showed that the fibrosis score was highest two weeks after a single dose of bleomycin (0.5 U/animal) reducing late in the course of lung injury, although it remained higher than controls at day 30. According to these authors, in order to induce a progressive fibrosis, both in extent and severity, a minimum of three doses of bleomycin have to be given a week apart. Using the same dose of bleomycin (0.25 U/100 g for animals weighing 200–250 g), we observed similar results. Furthermore, Brown et al. (1988) showed a maximal increase in polymorphonuclear leucocyte (PMN) and macrophage infiltration 14 days after the single dose of bleomycin receding at day 30. In our previous study, a single dose of bleomycin led to maximal MPO_L concentration at day 14 (Pinart et al., 2008), and in the current study no increase in MPO_L was observed at day 28 (Fig. 4A). In this line, Moeller et al. (2008) reported that a single dose of bleomycin resulted in a significant

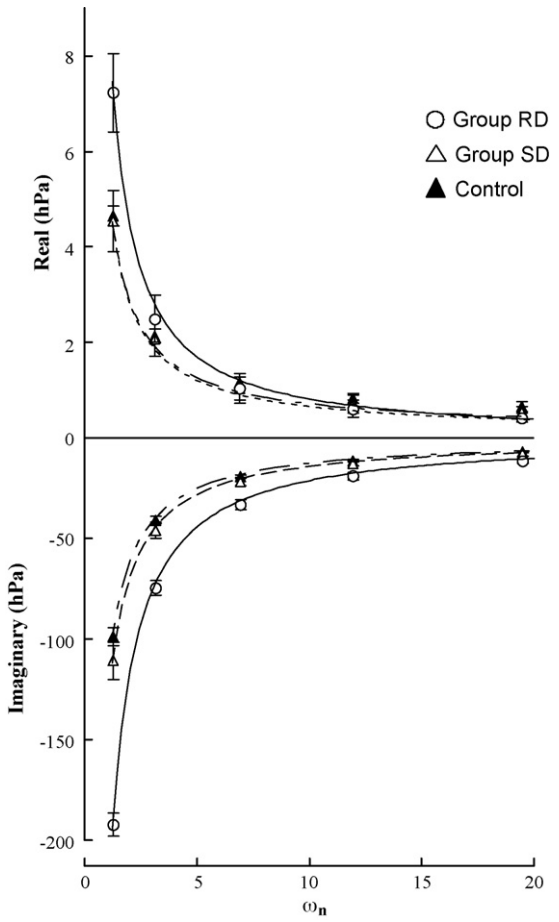

Fig. 2. Real and imaginary parts of lung tissue impedance *versus* normalised angular frequency, in CTRL (▲), SD (△), and RD (O) groups. Lines represent the fit of the model to impedance data.

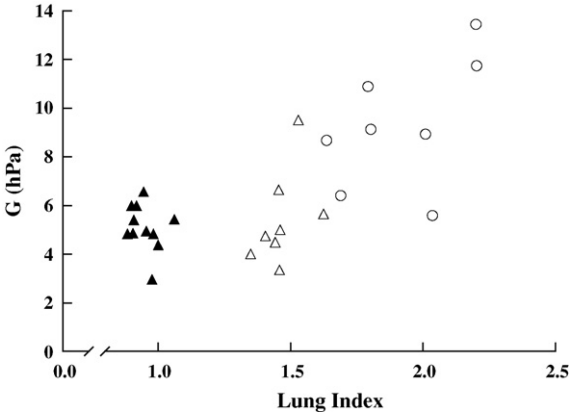

Fig. 3. Scatter plot of G (hPa) *versus* LI (▲ CTRL; △ SD; ○ RD). Spearman correlation for bleomycin-challenged rats is $\rho = 0.759$ ($P < 0.001$).

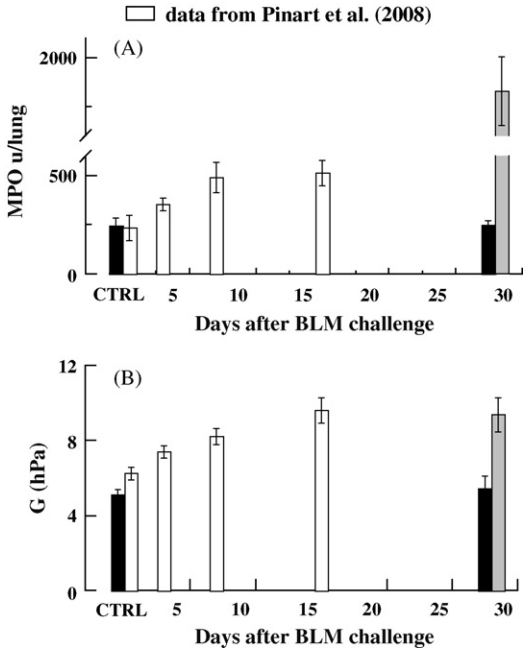

Fig. 4. Composition plots of data from the present study (dark bars) and the previous one (white bars) by Pinart et al. (2008). Values of MPO (U/lung) (plot A) and *G* (hPa) (plot B) obtained in both control groups and at days 3, 7, 15 and 28 days (SD: black, and RD: grey). Observe the parallelism between both parameters.

increase of MPO_L, an index of inflammatory cell infiltration, at days 7 and 15 with no changes at day 28.

Two recent studies in rats (Dolhnikoff et al., 1999; Ebihara et al., 2000) have demonstrated a positive correlation between the volume proportion of collagen fibre and *in vitro* tissue resistance and elastance. Conversely, in our study, we observed a non-significant increase in *G* and *H* 28 days after a single instillation of bleomycin, although there was an increase in collagen fibre content. The differences among these studies could be attributed to the dose of bleomycin used. In our study we used a dose of 2.5 U/kg, which represents half the dose used in Dolhnikoff's and Ebihara's studies. The collagen–elastin–proteoglycan matrix is believed to play a major role in determining the viscoelastic behaviour of the parenchyma tissues and is potentially responsible for tissue resistance (Fredberg and Stamenovic, 1989; Mijailovich et al., 1993). It has been suggested that the increase in collagen fibres is important in determining changes in lung tissue mechanics (Dolhnikoff et al., 1999). Although animals from the RD group showed a significant increase in *G*, *H* and collagen, SD rats presented an increase in collagen fibre with no significant changes in *G* or *H*. Lung mechanical changes may be related to collagen fibre stiffness and the type of cross-linking between molecules and fibrils, as well as the number of fibrils (Suki et al., 2005). Therefore, both quantitative and qualitative factors would influence the relationship between remodelling and biomechanical changes. According to Cavalcante et al. (2005), for a given volume fraction of collagen fibres in the alveolar walls, a lower limit of collagen fibre stiffness in the alveolar wall can be estimated. Therefore, it is feasible to suppose that the amount of collagen would or would not reach the critical limit of stiffness yielding lung mechanical changes. It is also reasonable to think that lung remodelling in the process of healing or recovery (organizing pneumonitis after acute injury) would lead to different mechanical changes than the disregulated remodelling that characterizes fibrosis (Strieter, 2008). In this latter case the dynamic composition and interactions between ECM components may lead to progressive changes in biomechanics.

The increase in LI may be accounted for by cellular components, ECM components and lung water embedded in the ground substance. According to Pinart et al. (2008), bleomycin-induced lung injury induces a thickening of alveolar wall and tissue oedema contributing to the increase in resistance. The same correlation holds in our present results (Fig. 3), supporting the idea that changes in the components of ground substance may play a substantial role in determining internal frictions between fibrilar components of ECM and ground substance (Suki et al., 2005).

In conclusion, single and repeat doses of bleomycin led to different inflammatory and fibrogenic behaviour resulting in distinct lung biomechanical changes 28 days after challenge. The model of three repeated doses of bleomycin simulated the key events in some human interstitial diseases (non-specific interstitial pneumonia, desquamative interstitial pneumonitis, hypersensitivity pneumonitis, etc.) characterised by inflammation, aberrant epithelial repair, deregulated fibrosis activity and progressive tissue scarring. Although longer trials are required, the present experimental model of repeated sub-lethal doses of bleomycin and the evaluation of lung damage by studying lung tissue strip biomechanics may be a promising method for testing antifibrotic drugs and for providing new insights into ILD pathophysiology.

Acknowledgements

(a) We would like to express our gratitude to Mrs. Anna Bachs for her skilful technical assistance.
(b) This study was supported by FISS (PI 04/0671) Spain, Mariona Pinart is granted by a Research Scholarship of IDIBELL.

References

Bowden, D.H., 1984. Unraveling pulmonary fibrosis: the bleomycin model. Lab. Invest. 50, 487–488.
Brown, R.F., Drawbaugh, R.B., Marrs, T.C., 1988. An investigation of possible models for the production of progressive pulmonary fibrosis in the rat. The effects of repeated intratracheal instillation of bleomycin. Toxicology 51, 101–110.
Cavalcante, F.S., Ito, S., Brewer, K., Sakai, H., Alencar, A.M., Almeida, M.P., Andrade J.S.Jr., Majumdar, A., Ingenito, E.P., Suki, B., 2005. Mechanical interactions between collagen and proteoglycans: implications for the stability of lung tissue. J. Appl. Physiol. 98, 672–679.
Chapman, H.A., 2004. Disorders of lung matrix remodeling. J. Clin. Invest. 113, 148–157.
Chua, F., Gauldie, J., Laurent, G.J., 2005. Pulmonary fibrosis: searching for model answers. Am. J. Respir. Cell. Mol. Biol. 33, 9–13.
Dolhnikoff, M., Mauad, T., Ludwig, M.S., 1999. Extracellular matrix and oscillatory mechanics of rat lung parenchyma in bleomycin-induced fibrosis. Am. J. Respir. Crit. Care Med. 160, 1750–1757.
Duchaine, C., Israel-Assayag, E., Fournier, M., Cormier, Y., 1996. Proinflammatory effect of *Pediococcus pentosaceus*, a bacterium used as hay preservative. Eur. Respir. J. 9, 2508–2512.
Ebihara, T., Venkatesan, N., Tanaka, R., Ludwig, M.S., 2000. Changes in extracellular matrix and tissue viscoelasticity in bleomycin-induced lung fibrosis. Temporal aspects. Am. J. Respir. Crit. Care Med. 162, 1569–1576.
Folch, E., Closa, D., Prats, N., Gelpí, E., Rosselló-Catafau, J., 1998. Leukotriene generation and neutrophil infiltration after experimental acute pancreatitis. Inflammation 22, 83–93.
Fredberg, J.J., Stamenovic, D., 1989. On the imperfect elasticity of lung tissue. J. Appl. Physiol. 67, 2408–2419.
Gharaee-Kermani, M., Hatano, K., Nozaki, Y., Phan, S.H., 2005. Gender-based differences in bleomycin-induced pulmonary fibrosis. Am. J. Pathol. 166, 1593–1606.
Hantos, Z., Adamicza, A., Govaerts, E., Daróczy, B., 1992. Mechanical impedances of lungs and chest wall in the cat. J. Appl. Physiol. 73, 427–433.
Ito, S., Ingenito, E.P., Arold, S.P., Parameswaran, H., Tgavalekos, N.T., Lutchen, K.R., Suki, B., 2004. Tissue heterogeneity in the mouse lung: effects of elastase treatment. J. Appl. Physiol. 97, 204–212.
Lopez-Aguilar, J., Romero, P.V., 1998. Effect of elastase pretreatment on rat lung strip induced constriction. Respir. Physiol. 113, 239–246.
Mijailovich, S.M., Stamenović, D., Fredberg, J.J., 1993. Toward a kinetic theory of connective tissue micromechanics. J. Appl. Physiol. 74, 665–681.
Moeller, A., Ask, K., Warburton, D., Gauldie, J., Kolb, M., 2008. The bleomycin animal model: a useful tool to investigate treatment options for idiopathic pulmonary fibrosis? Int. J. Biochem. Cell. Biol. 40, 362–382.
Molina-Molina, M., Serrano-Mollar, A., Bulbena, O., Fernandez-Zabalegui, L., Closa, D., Marin-Arguedas, A., Torrego, A., Mullol, J., Picado, C., Xaubet, A., 2006. Losar-

tan attenuates bleomycin induced lung fibrosis by increasing prostaglandin E2 synthesis. Thorax 61, 604–610.
Molina-Molina, M., Pereda, J., Xaubet, A., 2007. Experimental models for the study of pulmonary fibrosis: current usefulness and future promise. Arch. Bronconeumol. 43, 501–507.
Moore, B.B., Hogaboam, C.M., 2008. Murine models of pulmonary fibrosis. Am. J. Physiol. Lung Cell. Mol. Physiol. 294, L152–160.
Moore, V.L., Mondloch, V.M., Pedersen, G.M., Schrier, D.J., Allen, E.M., 1981. Strain variation in BCG-induced chronic pulmonary inflammation in mice: control by a cyclophosphamide-sensitive thymus-derived suppressor cell. J. Immunol. 127, 339–342.
Phan, S.H., Armstrong, G., Sulavik, M.C., Schrier, D., Johnson, K.J., Ward, P.A., 1983. A comparative study of pulmonary fibrosis induced by bleomycin and an O_2 metabolite producing enzyme system. Chest 83, 44S–45S.
Pinart, M., Serrano-Mollar, A., Negri, E.M., Cabrera, R., Rocco, P.R., Romero, P.V., 2008. Inflammatory related changes in lung tissue mechanics after bleomycin-induced lung injury. Respir. Physiol. Neurobiol. 160, 196–203.
Romero, P.V., Zin, W.A., Lopez-Aguilar, J., 2001. Frequency characteristics of lung tissue during passive stretch and induced pneumoconstriction. J. Appl. Physiol. 91, 882–890.
Serrano-Mollar, A., Closa, D., Cortijo, J., Morcillo, E.J., Prats, N., Gironella, M., Panes, J., Rosello-Catafau, J., Bulbena, O., 2002. P-selectin upregulation in bleomycin induced lung injury in rats: effect of N-acetyl-L-cysteine. Thorax 57, 629–634.
Strieter, R.M., 2008. What differentiates normal lung repair and fibrosis? Inflammation, resolution of repair, and fibrosis. Proc. Am. Thorac. Soc. 5, 305–310.
Suki, B., Ito, S., Stamenovic, D., Lutchen, K.R., Ingenito, E.P., 2005. Biomechanics of the lung parenchyma: critical roles of collagen and mechanical forces. J. Appl. Physiol. 98, 1892–1899.
Trush, M.A., Egner, P.A., Kensler, T.W., 1994. Myeloperoxidase as a biomarker of skin irritation and inflammation. Food. Chem. Toxic. 32, 143–147.
Yuan, H., Kononov, S., Cavalcante, F.S., Lutchen, K.R., Ingenito, E.P., Suki, B., 2000. Effects of collagenase and elastase on the mechanical properties of lung tissue strips. J. Appl. Physiol. 89, 3–14.

V. DISCUSSION

V.1 Mechanical behaviour in rats intratracheally instilled with BLM: a two-week model of BLM

We studied the mechanical behaviour in a two-week model of lung injury elicited by intratracheal instillation of BLM in rats. For these studies, measurements of enzyme activities are performed such as MPO as a marker of neutrophil influx in the early inflammatory stages. Additional parametres such as weight and LI are not always but frequently assessed. For the assessment of fibrosis several common methods are used such as quantification of HP and/or collagen content (**Moeller et al., 2008**).

The main findings in our first study suggest that this model provides new evidence concerning the pathophysiology of BLM-induced lung injury and the relationship between inflammatory changes and lung tissue mechanics. Lung tissue dissipative parametres showed significant changes after BLM injury. Both R0 and η0 were correlated with MPO_L, lung water and LI. HP_L showed no significant correlation with mechanical parametres, but elastin was strongly correlated with hysteresivity and alveolar wall thickness.

BLM causes oxidant-induced inflammatory and fibrotic lesions in the lung (**Hay et al., 1991; Dolhnikoff et al., 1999; Iraz et al., 2006**). Lung damage in the BLM model is characterised by the presence of alveolitis (**Dolhnikoff et al., 1999**). A key characteristic feature of alveolitis is neutrophilic infiltration (**Hunninghake et al., 1981**). The activity of MPO, present in the azurophilic granules of neutrophils, in the lung provides an index of intrapulmonary sequestration of neutrophils. Giri and colleagues (**Giri et al., 1997**) showed an increase in lung MPO and HP content in the BLM compared to control group in hamsters. The increase in HP content was related to multifocal fibrosis and the increase of MPO to the accumulation of mononuclear inflammatory cells and granulocytes. Genovese and colleagues (**Genovese et al., 2005**) found extensive inflammatory infiltration by neutrophils and an increase in MPO activity in lung histological sections of BLM-treated mice. In our study we observed an increase of the MPO activity and HP content in the BLM group since day 7. These results are similar to those of previous authors (**Mata et al., 2003; El-Medany et al., 2005; Iraz et al., 2006**).

For many authors, after BLM injury two processes with different time courses develop: the first process is inflammatory in nature and has a maximal intensity around the first

week after challenge, switching to fibrosis between the second and third week post-instillation (**Izbicki et al., 2002; Selman et al., 2002; Chaudhary et al., 2006**). The second process, overlapping with inflammation, is characterised by lung remodelling with a first phase of fibrinolysis followed by neofibrinogenesis (**Izbicki et al., 2002**). This remodelling process begins shortly after challenge and increases progressively in intensity, especially after the first week. In our results the evolution of HP contents agrees with the described sequence of the remodelling process. Therefore, changes in elastic properties of the lung, in our setting, would be attributable to lung shrinkage due to inflammatory interstitial and alveolar changes, rather than fibrotic changes.

If fibrosis were a relevant mechanism of the pressure-volume changes, we would expect to observe significant relationships between HP contents and the elastance modulus (**Suki et al., 2005**). Although we cannot exclude elastogenesis and proteoglycan synthesis, processes involved in lung remodelling after acute lung injury (**Venkatesan et al., 2000; Rocco et al., 2001; Santos et al., 2006**), we can accept that, in our setting, the mechanical repercussion of PF is mainly due to the inflammatory component.

Furthermore, elastogenesis seems to affect the coupling between elastic and dissipative processes within the tissue. The mechanisms that govern viscoelastic properties of intraparenchymal connective tissues are not yet elucidated. Many authors have hypothesised about the origin of the dissipation in connective tissues, which may occur: at the microstructural level, by contact phenomena (coulomb) friction, between stress-bearing connective tissue fibres (**Fredberg and Stamenovic, 1989**), or by shearing of the proteoglycan ground substance between fibres at the molecular level, or it could occur at surfaces of direct fibre–fibre sliding contact (**Suki et al., 1994**).

Correlations between lung mechanical properties and changes related to inflammation (W_L, LI, MPO_L) may be connected to changes in the composition of the ground substance related to the inflammatory process. In this line, previous studies have found an increase in proteoglycans in the histologic samples obtained at 7 and 14 days after administration of BLM, when inflammation was prominent, and diminished at day 28, when much of the inflammatory response had resolved, and heterogeneous distribution of fibrosis was observed (**Westergren-Thorsson et al., 1993; Venkatesan et al., 2000**). However, the fact that there is no correlation between hydroxyproline and the biomechanical parametres does not mean that fibrogenesis is absent in a 2-week

model of PF, but the amount of collagen fibres is not sufficient to have a significant impact upon tissue mechanics (**Cavalcante et al., 2005**).

The increase in lung water content might arise from two sources: the alveolar exudation, a main feature of alveolitis, and/or the increase of water imbedded by the deposition of hygroscopic molecules (hyaluronan and other proteoglycan) in the ECM (**Nettelbladt et al., 1989; Venkatesan et al., 2000**). Thus, the increase in lung water content observed in BLM animals has been taken as an indicator of the amount of lung parenchymal damage after BLM challenge.

Many authors presented theories to explain the relationship between the water embedded in the lung after lung injury, and mechanical properties of the lung (**Flemmer et al., 2000; Venkatesan et al., 2000; Cavalcante et al., 2005**). They are all focused on the role of proteoglycans, making it reasonable to think that the relationship between LI or lung water and lung tissue viscoelastic properties may be related to proteoglycan mechanical dysfunction in the ECM (**Dolhnikoff et al., 1999**). In fact, versicana, one family of proteoglicans, plays a critical role in determining the water content or turgor of ECM, influencing tissue viscoelastic behaviour as well as cell migration and proliferation (**Pelosi and Rocco, 2008**). The increase of η0 prior to the increase in MPO and elastic fibres in the alveolar septa supports this hypothesis. ECM fibres (elastin and collagen) account for most of the viscoelastic mechanical properties of lung tissue strips (**Rocco et al., 2001**). Once ECM composition is altered, either because of the direct injury or cellular remodelling, there are corresponding changes in the biomechanical properties of the matrix and consequently of the alveolar wall (**Suki et al., 2005**).

Many authors found a significant increase in R and E (**Verbeken et al., 1994; Dolhnikoff et al., 1999; Ebihara et al., 2000**). The maximal increase in R and E occurred at 14 days post-BLM instillation. Discrepancies existed between the behaviour of η. In our study, we observed a maximal increase in R and E, although it was only significant in R. As above mentioned, hysteresivity was related to MPO_L in our study. To our knowledge, this was the first study to show a correlation between an intrinsic property of lung tissue, hysteresivity, and a marker of inflammation (MPO_L). We interpreted this correlation as an indicator of the dependence of tissue biomechanics on the underlying structural changes induced by inflammation. Whether the correlation between MPO_L and biomechanical parametres indicates a direct effect of oxidative stress on ECM or not remains in the field of speculation.

V.2 Mechanical behaviour in rats intratracheally instilled with BLM: a comparison between a four-week single dose model and a four-week after three repeated doses

In general, the multiple dose, longer term models, produce a persistent fibrosis preceded by a gradual progression of contributing events as is typical of interstitial PF in humans. The shorter the duration, single dose models less effectively replicate human interstitial pulmonary fibrosis, but are useful for rapidly screening antifibrotic agents. Thus the duration of the BLM model used for screening potential therapeutic agents maybe important (**Wild et al., 1994**).

In this study, the model of three repeated doses of BLM induced inflammatory cell infiltration, an increase in myeloperoxidase, collagen fibre deposition, and fibroblast focus augmenting both elastic modulus (H) and tissue damping (G) 28 days after the last challenge. In contrast, a single dose of BLM resulted in an increase in collagen fibre content with no significant changes in lung mechanics.

It has been established that PF resulting from BLM injury is due to an increase in the rate of collagen synthesis and a decrease in collagen degradation (**Laurent and McAnulty, 1983**). Previous studies in rats, have shown that biochemical and histological changes suggestive of PF are maximal between 14 and 28 days after single BLM challenge, with peak response around day 21 (**Moore and Hogaboam, 2008**). After this time point, fibroblastic activity decreases and fibrosis begin to resolve (**Phan et al., 1983; Gharaee-Kermani et al., 2005**). Our results are in agreement with these reports: collagen fibre content was augmented at day 28 in SD, but lung tissue biomechanics was similar to controls.

In 1988, Brown et al. developed a multiple BLM dose model for lung fibrosis in rats but the model was only characterised in a histological fashion. They concluded that a model of three repeated doses a week apart is sufficient to observe the features of progressive PF both in extent and severity. Soon after, nine studies developed another three-dose model in hamsters (see Annex). The first of these nine studies, which were all performed in the same laboratory, established the most appropriate doses (2.5U, 2.0 U and 1.5 U/5ml/kg one dose per week) to recreate the progressive PF pattern with the minimum mortality, and characterised the model using biochemical, histological and morphometric techniques. Afterwards, they used the model of three consecutive doses to screen drugs for their potential antifibrotic effect.

In these studies, animals sacrificed four weeks after the third instillation, showed diffuse and interstitial fibrosis, with increased HP content and increased inflammatory cells, MPO, MDAE and SOD activity. Neutrophil sequestration within the pulmonary microvasculature is known to contribute to pathogenic process of acute lung injury by way of releasing ROS, proteases and MPO (**Iyer et al., 1998**). Similar results were observed in our study. After 28 days, lung collagen deposition was augmented and inflammation was still relevant. In some studies (see Annex) neutrophils persisted 4 weeks after the last challenge but in others their increase was maximal at day 7. All studies that counted the macrophages agreed that they remained increased 4 weeks after the last challenge. Macrophages are stimulators of neutrophils, and this may explain why MPO activity, a marker of neutrophilic infiltration, remains significantly increased after 4 weeks.

Moreover, macrophages produce TGF-β especially when stimulated by BLM treatment (**Wang et al., 1992**). The mechanisms for the fibrogenic effect of TGF-β lie in its ability to stimulate procollagen gene expression, inhibit matrix-degrading proteinases and stimulate the production of tissue inhibitor of metalloproteinase. These effects of TGF-β eventually lead to an aberrant and excess deposition of ECM, a hallmark of fibrosis (**Wang et al., 2002**). It has been shown that TGF-β increases collagen synthesis by human lung fibroblasts (**Raghu et al., 1989**). These changes reflected the progression of the fibrotic process in the lung. However in some studies that used a single intratracheal instillation of BLM (**Lindenschmidt et al., 1986; Giri and Hyde 1988**) the magnitude of increases (157-167% respective to control) in lung collagen accumulation at 30 days was comparable to a three-dose model of BLM (**Zia et al., 1992**). In our study, collagen significantly increased in both SD and RD group at 30 days after BLM treatment.

Nonetheless, it appears that acute lung injury and mortality associated with BLM treatment is not attributed to an increase in the accumulation of collagen in the lung but to the vascular and epithelial damage which results in pulmonary oedema, the main cause of death (**Zia et al., 1992**). Zia et al. (**1992**) hypothesised that BLM can enhance vascular permeability at a low dose, producing mild vascular endothelial damage and pulmonary oedema that does not lead to death. They based their hypothesis on the fact that they found similar elevation in protein content in the BALF supernatant of hamsters treated with either 6 U BLM/kg or 7.5 U BLM/kg. Despite the not yet known mechanism of BLM-induced vascular permeability it has been reported that a low dose of BLM is required to inhibit serotonin clearance, a function of endothelial cells

(**Catravas et al., 1983**). It is hypothesised that the increase in vascular permeability after low multiple doses of BLM treatment can be attributed to an increased accumulation of serotonin, which is known to cause vascular permeability during inflammation in the lung due to endothelial cell dysfunction.

Brown et al. (**1988**) reported a maximal increase in PMN and macrophage infiltration 14 days after the single dose of BLM receding at day 30. In our previous study, a single dose of BLM led to maximal MPO_L concentration at day 14, and in the current study no increase in MPO_L was observed at day 28. In this line, Moeller et al. (**2008**) reported that a single dose of BLM resulted in a significant increase of MPO_L, an index of inflammatory cell infiltration, at days 7 and 15 with no changes at day 28. In contrast, lung MPO activity and HP in the BLM-treated group was significantly increased at day 21 (**Iyer et al., 1995**). In our study, MPO activity was similar to the control group at day 28, whereas HP significantly increased. LI, a marker of inflammation and lung damage, augmented significantly in both BLM groups. This increase may be due to cellular components, ECM components and lung water embedded in the ground substance. In our previous study, BLM-induced lung injury induces a thickening of alveolar wall and tissue oedema contributing to the increase in resistance. Seemingly, in our present study, we show the same correlation supporting the idea that changes in the components of ground substance may play a substantial role in determining internal frictions between fibrilar components of ECM and ground substance (**Suki et al., 2005**).

Fibrosis in laboratory animals induced with a single IT instillation of BLM is usually associated with an increase in collagen deposition between 2-3 weeks post-instillation that begin to resolve and collagen deposition diminishes after 4 weeks of treatment (**Zia et al., 1992**). In our study, we observed an increase in G and H albeit non-significant and a significant increase in collagen content after a single instillation of BLM. However, two recent studies in rats (**Dolhnikoff et al., 1999; Ebihara et al., 2000**) have demonstrated a positive correlation between the volume proportion of collagen fibre and “in vitro” tissue resistance and elastance. These discrepancies could be attributed to the dose employed to yield fibrosis. Whilst we used a BLM dose of 2.5 U/kg, Dolhnikoff et al. and Ebihara et al. doubled the dose. The collagen-elastin-proteoglycan matrix is believed to play a major role in determining the viscoelastic behaviour of the parenchyma tissues and is potentially responsible for tissue resistance (**Fredberg and Stamenovic, 1989; Mijailovich et al., 1993**). It has been suggested that the increase in collagen fibres is important in determining changes in lung tissue

mechanics (**Dolhnikoff et al., 1999**). Our results showed that animals from the RD group showed a significant increase in G, H and collagen. Conversely, SD rats presented an increase in collagen fibre with no significant changes in G or H.

Lung mechanical changes may be related to collagen fibre stiffness and the type of cross-linking between molecules and fibrils, as well as the number of fibrils (**Suki et al., 2005**). Therefore, both quantitative and qualitative factors would influence the relationship between remodelling and biomechanical changes. According to Cavalcante et al. (**2005**), for a given volume fraction of collagen fibres in the alveolar walls, a lower limit of collagen fibre stiffness in the alveolar wall can be estimated. Therefore, it is feasible to suppose that the amount of collagen would or would not reach the critical limit of stiffness yielding lung mechanical changes. It is also reasonable to think that lung remodelling in the process of healing or recovery (organizing pneumonitis after acute injury) would lead to different mechanical changes than the disregulated remodelling that characterises fibrosis (**Strieter, 2008**). In this latter case the dynamic composition and interactions between ECM components may lead to progressive changes in biomechanics.

V.3 Strengths and weaknesses of the BLM model

Hitherto, animal models are indispensable in driving high-quality hypothesis-based studies, given that the ideal experimental model of PF is not yet described, or rather it simply does not exist. Additionally, if the characteristics of an animal model are well understood, and the results are interpreted within the limits of the specific model, animal studies can provide focused tests of key elements of the lung injury response in humans (**Matute-Bello et al., 2008**).

Bleomycin has been shown to induce lung injury and fibrosis in a wide variety of experimental animals including mice, rats, hamsters, rabbits, guinea pigs, dogs and primates over a range of doses induced via intraperitoneal, intravenous, subcutaneous, or intratracheal delivery (**Muggia et al., 1983**). The latter, has the advantage that fibrosis can be induced with lower doses, with consequently reduced toxicity to other organs. In addition, when compared to systemic routes, the intratracheal instillation of BLM has provided a convenient and reproducible method to expose the lung to high concentrations of BLM. Since similar lung injury and repair occur following administration of BLM through both routes, the intratrcheal models have proved useful

in studying the mechanisms of BLM-induced lung fibrosis (**Zia et al., 1992**). Furthermore, according to previous authors, this is the most appropriate model to mimic human PF because it replicates some of the major structural findings, such as patchy parenchymal inflammation of variable intensity (**Kaminski et al., 2000**), epithelial cell injury with reactive hyperplasia, basement membrane damage, fibroblast proliferation and ECM deposition (**Snider et al., 1978; Bowden, 1984**). However, high mortality, high morbidity and overwhelming inflammation are usually associated with a single intratracheal instillation (**Zia et al., 1992**).

Nonetheless, the importance of early inflammatory components in the pathogenesis of PF has been extensively debated (**Strieter et al., 2002; Lagente et al., 2005**). Thus, arguments in favour or against the role of acute and chronic inflammation have been reported on the basis of the data of numerous studies. Early in this century, Selman and Pardo (**2002**) proposed two routes for developing diffuse PF. One of these is the "inflammatory route", represented by almost all the non-IPF interstitial lung diseases (idiopathic interstitial pneumonias with no histological features of UIP) where there is an early, clearly distinguishable phase of alveolitis and a late fibrotic phase. The other is the "epithelial/fibroblastic route" represented by IPF. It has been proposed that a "fibrogenic microenvironment" including some tissue remodelling mediators interacting with the ECM could suffice to launch the fibrogenic process (**Gauldie et al., 2002**).

It seems that the early inflammatory response is critical for the development of BLM-induced fibrosis. Therefore, BLM-induced PF mimics those processes based on inflammatory-related remodelling or fibrosis, but perhaps not IPF (or usual interstitial pneumonia) where inflammatory changes are less significant (**Selman and Pardo, 2006; Cabrera, 2008**). Furthermore, caution is needed when interpreting data derived from the BLM model and extrapolating them to human PF, especially because the fibrosis induced by BLM starts with an inflammatory reaction and the cessation of BLM-induced injury may reverse or diminish the previously induced fibrotic changes, an event not seen in human lung fibrosis (**Chua et al., 2005b**). Single doses of BLM induce subchronic lesions, but more lasting fibrosis can result from repeated drug dosing (**Thrall et al., 1995**).

For this last reason we wanted to compare the single-dose model elongated up to four weeks *versus* a model of repeat doses. Biochemical and histological changes suggestive of PF can be observed since day 14 after single BLM challenge, with maximal responses generally noted around day 21 (**Janick-Buckner et al., 1989;**

Izbicki et al., 2002; Moore and Hogaboam, 2008). Beyond this point fibrosis can either progress for 60-90 days (**Starcher et al., 1978; Thrall et al., 1979; Goldstein et al., 1979**) or begin to resolve (**Phan et al., 1983; Gharaee-Kermani et al., 2005; Lawson et al., 2005**). Our results agree with the latter reports: although collagen content was augmented, lung tissue biomechanics of the rats from the single-dose group were similar to controls. Thus, choosing the correct end point in the BLM model is critical, especially as it has been shown that the standard outcome parametres are highly variable after day 21 and may even return to normal baseline (histomorphometry and hydroxyproline lung content) (**Izbicki et al., 2002**).

In 1988, Brown et al. showed that fibrotic score peaked two weeks after a single dosis of BLM (0.5 U/animal) regressing thereafter, albeit remaining higher than controls at day 30. According to these authors, to induce a progressive fibrosis, both in extent and severity, a minimum of three doses of BLM have to be given a week apart. Indeed, single doses of BLM induce subchronic lesions, but more lasting fibrosis results from repeated drug dosing (**Chua et al., 2005b**). Using the same dose of BLM (0.25 U/100g for animals weighting 200-250 g), we obtained similar results. Furthermore, Brown et al. (**1988**) showed a maximal increase in polymorphonuclear leucocyte (PMN) and macrophage infiltration at day 14 in the single dose group reverting at day 30. In our previous study, maximal neutrophilic infiltration was also seen at day 14 (**Pinart et al., 2008**), regressing at day 28 according to the current study. MPO_L, an index of inflammatory cell infiltration (**Moeller et al., 2008**), increased significantly at days 7 and 15 compared to control, but not at day 28 in the animals that received a single dose of BLM. Conversely, in the group that received repeated doses, MPO activity augmented compared to control. These results can be related with previously observed histological changes (**Brown et al., 1988; Borzone et al., 2001**). Moreover, fibroblast foci, characterised by the presence of fibroblasts and myofibroblasts, and collagen deposition reflecting the fibrogenic activity (**Izbicki et al., 2002**) were observed in the RD group.

VI. FINAL CONCLUSIONS

1. In the 2-week model, the inflammatory process triggered by the BLM challenge leads to changes in biomechanical parametres related to tissue damping such as resistance and hysteresivity. Therefore, tissue biomechanics is altered by the underlying structural changes induced by inflammation.

2. Inflammation and elastogenesis are the main determinants for hysteretic changes observed in the first 15 days after BLM challenge in rats.

3. Single and repeat doses of BLM led to different inflammatory and fibrogenic behaviour resulting in distinct lung biomechanical changes 28 days after challenge.

4. In agreement with other studies, the BLM model of lung fibrosis induced with single intratracheal instillations do not duplicate the clinical process of lung fibrosis seen with BLM therapy in patients.

5. The model of three repeated doses of BLM simulated the key events in some human interstitial diseases (non specific interstitial pneumonia, desquamative interstitial pneumonitis, hypersensitivity pneumonitis, etc) characterised by inflammation, aberrant epithelial repair, deregulated fibrosis activity and progressive tissue scarring.

6. The present experimental model of repeated sublethal doses of BLM and the evaluation of lung damage by studying lung tissue strip biomechanics may be a promising method for testing antifibrotic drugs and for providing new insights into ILD pathophysiology.

VII. REFERENCES

Adamson, I.Y., Bowden, D.H., 1974. The type 2 cell as progenitor of alveolar epithelial regeneration. A cytodynamic study in mice after exposure to oxygen. Lab. Invest. 30, 35-42.

Adamson, I.Y., Young, L., Bowden, D.H., 1988. Relationship of alveolar epithelial injury and repair to the induction of pulmonary fibrosis. Am. J. Pathol. 130, 377-383.

Ahuja, S.S., Paliogianni, F., Yamada, H., Balow, J.E., Boumpas, D.T., 1993. Effect of transforming growth factor-beta on early and late activation events in human T cells. J. Immunol. 150, 3109-3118.

Albertine, K.H., Soulier, M.F., Wang, Z., Ishizaka, A., Hashimoto, S., Zimmerman, G.A., Matthay, M.A., Ware, L.B., 2002. Fas and fas ligand are up-regulated in pulmonary oedema fluid and lung tissue of patients with acute lung injury and the acute respiratory distress syndrome. Am. J. Pathol. 161, 1783-1796.

Alexander, C.M., Werb, Z., 1991. Extracellular matrix degradation. In : Hay ED, ed. Cell biology of Extracellular Matrix. 2nd ed. New York, NY: Plenum Press; 11-146.

Allen, J., Cooper, D.Jr., 2000. Pulmonary fibrosis: pathways are slowly coming into light. Am. J. Respir. Cell. Mol. Biol. 22, 520-523.

Allen, J.T., Spiteri, M.A., 2002. Growth factors in idiopathic pulmonary fibrosis: relative roles. Respir. Res. 3:13.

American Thoracic Society; European Respiratory Society. American Thoracic Society/European Respiratory Society International Multidisciplinary Consensus Classification of the Idiopathic Interstitial Pneumonias., 2002. Am. J. Respir. Crit. Care. Med. 165, 277-304.

Ando, K., Hirata, Y., Shichiri, M., Emori, T., Marumo, F., 1989. Presence of immunoreactive endothelin in human plasma. FEBS. Lett. 245, 164-166.

Antoniades, H.N., Bravo, M.A., Avila, R.E., Galanopoulos, T., Neville-Golden, J., Maxwell, M., Selman, M., 1990. Platelet-derived growth factor in idiopathic pulmonary fibrosis. J. Clin. Invest. 86, 1055-1064.

Antoniades, H.N., Galanopoulos, T., Neville-Golden, J., Kiritsy, C.P., Lynch, S.E., 1994. p53 expression during normal tissue regeneration in response to acute cutaneous injury in swine. J. Clin. Invest. 93, 2206-2214.

Arai, T., Abe, K., Matsuoka, H., Yoshida, M., Mori, M., Goya, S., Kida, H., Nishino, K., Osaki, T., Tachibana, I., Kaneda, Y., Hayashi, S., 2000. Introduction of the interleukin-10 gene into mice inhibited bleomycin-induced lung injury “in vivo”. Am. J. Physiol. Lung. Cell. Mol. Physiol. 278, L914-922.

Asakura, S., Colby, T.V., Limper, A.H., 1996. Tissue localization of transforming growth factor-beta1 in pulmonary eosinophilic granuloma. Am. J. Respir. Crit. Care. Med. 154, 1525-1530.

Ask, K., Martin, G.E., Kolb, M., Gauldie, J., 2006. Targeting genes for treatment in idiopathic pulmonary fibrosis: challenges and opportunities, promises and pitfalls. Proc. Am. Thorac. Soc. 3, 389-393.

Avery, N.C., Bailey, A.J., 2005. Enzymic and non-enzymic cross-linking mechanisms in relation to turnover of collagen: relevance to aging and exercise. Scand. J. Med. Sci. Sports. 15, 231-240.

Azambuja, E., Fleck, J.F., Batista, R.G., Menna Barreto, S.S., 2005. Bleomycin lung toxicity: who are the patients with increased risk? Pulm. Pharmacol. Ther. 18, 363-366.

Bachofen, H., Hildebrandt, J., Bachofen, M., 1970. Pressure-volume curves of air- and liquid-filled excised lungs-surface tension in situ. J. Appl. Physiol. 29, 422-431.

Bartram, U., Speer, C.P., 2004. The role of transforming growth factor beta in lung development and disease. Chest. 125, 754-765.

Basset, F., Ferrans, V.J., Soler, P., Takemura, T., Fukuda, Y., Cristal, R., 1986. Intraluminal fibrosis in interstitial lung disorders. Am. J. Pathol. 122, 443-461.

Bates, J.H.T., Allen, G.B., 2006. The estimation of lung mechanics parametres in the presence of pathology: a theoretical analysis. Ann. Biomed. Eng. 34, 384-392.

Bates, J.H., 2007. A recruitment model of quasi-linear power-law stress adaptation in lung tissue. Ann. Biomed. Eng. 35, 1165-1174.

Belvisi, M.G., Saunders, M., Yacoub, M., Mitchell, J.A., 1998. Expression of cyclo-oxygenase-2 in human airway smooth muscle is associated with profound reductions in cell growth. Br. J. Pharmacol. 125, 1102-1108.

Benjamin, R.C., Gill, D.M., 1980. Poly(ADP-ribose) synthesis “in vitro” programmed by damaged DNA. A comparison of DNA molecules containing different types of strand breaks. J. Biol. Chem. 255, 10502-10508.

Bitterman, P.B., Wewers, M.D., Rennard, S.I., Adelberg, S., Crystal, R.G., 1986. Modulation of alveolar macrophage-driven fibroblast proliferation by alternative macrophage mediators. J. Clin. Invest. 77, 700-708.

Blaisdell, R.J., Schiedt, M.J., Giri, S.N., 1994. Dietary supplementation with taurine and niacin prevents the increase in lung collagen cross-links in the multidose bleomycin hamster model of pulmonary fibrosis. J. Biochem. Toxicol. 9, 79-86.

Blaisdell, R.J., Giri, S.N., 1995. Mechanism of antifibrotic effect of taurine and niacin in the multidose bleomycin-hamster model of lung fibrosis: inhibition of lysyl oxidase and collagenase. J. Biochem. Toxicol. 10, 203-210.

Bonner, J.C., Badgett, A., Lindroos, P.M., Osornio-Vargas, A.R., 1995. Transforming growth factor beta 1 downregulates the platelet-derived growth factor alpha-receptor subtype on human lung fibroblasts “in vitro”. Am. J. Respir. Cell. Mol. Biol. 13, 496-505.

Border, W.A., Ruoslahti, E., 1992. Transforming growth factor-beta in disease: the dark side of tissue repair. J. Clin. Invest. 90, 1-7.

Borok, Z., Gillissen, A., Buhl, R., Hoyt, R.F., Hubbard, R.C., Ozaki, T., Rennard, S.I., Crystal, R.G., 1991. Augmentation of functional prostaglandin E levels on the respiratory epithelial surface by aerosol administration of prostaglandin E. Am. Rev. Respir. Dis. 144, 1080-1084.

Borok. Z., Danto, S.I., Lubman, R.L., Cao, Y., Williams, M.C., Crandall, E.D., 1998a. Modulation of t1alpha expression with alveolar epithelial cell phenotype “in vitro”. Am. J. Physiol. 275, L155-L164.

Borok, Z., Lubman, R.L., Danto, S.I., Zhang, X.L., Zabski, S.M., King, L.S., Lee, D.M., Agre, P., Crandall, E.D., 1998b. Keratinocyte growth factor modulates alveolar epithelial cell phenotype “in vitro”: expression of aquaporin 5. Am. J. Respir. Cell. Mol. Biol. 18, 554-561.

Borzone, G., Moreno, R., Urrea, R., Meneses, M., Oyarzún, M., Lisboa, C., 2001. Bleomycin-induced chronic lung damage does not resemble human idiopathic pulmonary fibrosis. Am. J. Respir. Crit. Care. Med. 163, 1648-1653.

Bowden, D.H., 1984. Unraveling pulmonary fibrosis: the bleomycin model. Lab. Invest. 50, 487-488.

Boyaci, H., Maral, H., Turan, G., Basyigit, I., Dillioglugil, M.O., Yildiz, F., Tugay, M., Pala, A., Ercin, C., 2006. Effects of erdosteine on bleomycininduced lung fibrosis in rats. Mol. Cell. Biochem. 281, 129-137.

Brennan, M.L., Penn, M.S., Van Lente, F., Nambi, V., Shishehbor, M.H., Aviles, R.J., Goormastic, M., Pepoy, M.L., McErlean, E.S., Topol, E.J., Nissen, S.E., Hazen, S.L., 2003. Prognostic value of myeloperoxidase in patients with chest pain. N. Engl. J. Med. 349, 1595-1604.

Brewster, C.E., Howarth, P.H., Djukanovic, R., Wilson, J., Holgate, S.T., Roche, W.R., 1990. Myofibroblasts and subepithelial fibrosis in bronchial asthma. Am. J. Respir. Cell. Mol. Biol. 3, 507-511.

Brinckerhoff, C.E., Matrisian, L.M., 2002. Matrix metalloproteinases: a tail of a frog that became a prince. Nat. Rev. Mol. Cell. Biol. 3, 207-214.

Broekelmann, T.J., Limper, A.H., Colby, T.V., McDonald, J.A., 1991. Transforming growth factor beta 1 is present at sites of extracellular matrix gene expression in human pulmonary fibrosis. Proc. Natl. Acad. Sci. USA. 88, 6642-6646.

Brown, R.F., Drawbaugh, R.B., Marrs, T.C., 1988. An investigation of possible models for the production of progressive pulmonary fibrosis in the rat. The effects of repeated intratracheal instillation of bleomycin. Toxicology. 51, 101-110.

Cabrera Beitez, S., 2006. Bleomicina: un modelo de fibrosis pulmonar. Rev. Inst. Nal. Enf. Resp. Mex. 19, 53-61.

Cambrey, A.D., Harrison, N.K., Dawes, K.E., Southcott, A.M., Black, C.M., du Bois, R.M., Laurent, G.J., McAnulty, R.J., 1994. Increased levels of endothelin-1 in bronchoalveolar lavage fluid from patients with systemic sclerosis contribute to fibroblast mitogenic activity “in vitro”. Am. J. Respir. Cell Mol. Biol. 11, 439-445.

Cantin, A.M., North, S.L., Hubbard, R.C., Crystal, R.G., 1987a. Normal alveolar epithelial lining fluid contains high levels of glutathione. J. Appl. Physiol. 63, 152-157.

Cantin, A.M., North, S.L., Fells, G.A., Hubbard, R.C., Crystal, R.G., 1987b. Oxidant-mediated epithelial cell injury in idiopathic pulmonary fibrosis. J. Clin. Invest. 79, 1665-1673.

Catravas, J.D., Lazo, J.S., Dobuler, K.J., Mills, L.R., Gillis, C.N., 1983. Pulmonary endothelial dysfunction in the presence and absence ofinterstitial injury induced by intratracheally injected bleomycin in rabbits. Am. Rev. Respir. Dis. 128, 740-746.

Cavalcante, F.S., Ito, S., Brewer, K., Sakai, H., Alencar, A.M., Almeida, M.P., Andrade Jr.J.S., Majumdar, A., Ingenito, E.P., Suki, B., 2005. Mechanical interactions between collagen and proteoglycans: implications for the stability of lung tissue. J. Appl. Physiol. 98, 672-679.

Chandler, D.B., Hyde, D.M., Giri, S.N., 1983. Morphometric estimates of infiltrative cellular changes during the development of bleomycin-induced pulmonary fibrosis in hamsters. Am. J. Pathol. 112, 170-177.

Chanson, M., Derouette, J.P., Roth, I., Foglia, B., Scerri, I., Dudez, T., Kwak, B.R., 2005. Gap junctional communication in tissue inflammation and repair. Biochim. Biophys. Acta. 1711, 197-207.

Chapman, H.A., 1999. A Fas pathway to pulmonary fibrosis. J. Clin. Invest. 104, 1-2.

Chapman, H.A., 2004. Disorders of lung matrix remodelling. J. Clin. Invest. 113, 148-157.

Chaudhary, N.I., Schnapp, A., Park, J.E., 2006. Pharmacologic differentiation of inflammation and fibrosis in the rat Bleomycin model. Am. J. Respir. Crit. Care. Med. 173, 769-776.

Chauncey, J.B., Peters-Golden, M., Simon, R.H., 1988. Arachidonic acid metabolism by rat alveolar epithelial cells. Lab. Invest. 58, 133-140.

Cheek, J.M., Evans, M.J., Crandall, E.D., 1989. Type I cell-like morphology in tight alveolar epithelial monolayers. Exp. Cell. Res. 184, 375-387.

Chen, J.J., Sun, Y., Nabel, G.J., 1998. Regulation of the proinflammatory effects of Fas ligand (CD95L). Science. 282, 1714-1717.

Chen, J., Stubbe, J., 2005. Bleomycins: towards better therapeutics. Nat. Rev. Cancer. 5, 102-112.

Chua, F., Sly, P.D., Laurent, G.J., 2005a. Pediatric lung disease: from proteinases to pulmonary fibrosis. Pediatr. Pulmonol. 39, 392-401.

Chua, F., Gauldie, J., Laurent, G.J., 2005b. Pulmonary fibrosis: searching for model answers. Am. J. Respir. Cell. Mol. Biol. 33, 9-13.

Clark, J.G., Overton, J.E., Marino, B.A., Uitto, J., Starcher, B.C., 1980. Collagen biosynthesis in bleomycin-induced pulmonary fibrosis in hamsters. J. Lab. Clin. Med. 96, 943-953.

Coker, R.K., Laurent, G.J., Shahzeidi, S., Lympany, P.A., du Bois, R.M., Jeffery, P.K., McAnulty, R.J., 1997. Transforming growth factors-beta 1, -beta 2, and -beta 3 stimulate fibroblast procollagen production “in vitro” but are differentially expressed during bleomycin-induced lung fibrosis. Am. J. Pathol. 150, 981-991.

Cooper, J.A.Jr., 2000. Pulmonary fibrosis: pathways are slowly coming into light. Am. J. Respir. Cell. Mol. Biol. 22, 520-523.

Corbel, M., Belleguic, C., Boichot, E., Lagente, V., 2002. Involvement of gelatinases (MMP-2 and MMP-9) in the development of airway inflammation and pulmonary fibrosis. Cell. Biol. Toxicol. 18, 51-61.

Cosi, C., Marien, M., 1999. Implication of poly (ADP-ribose) polymerase (PARP) in neurodegeneration and brain energy metabolism. Decreases in mouse brain NAD+ and ATP caused by MPTP are prevented by the PARP inhibitor benzamide. Ann. N. Y. Acad. Sci. 890, 227-239.

Cox, G., Kable, E., Jones, A., Fraser, I., Manconi, F., Gorrell, M.D., 2003. 3-dimensional imaging of collagen using second harmonic generation. J. Struct. Biol. 141, 53-62.

Culav, E.M., Clark, C.H., Merrilees, M.J., 1999. Connective tissues: matrix composition and its relevance to physical therapy. Phys Ther. 79, 308-319.

Cushley, M.J., Davison, A.G., du Bois, R.M., Egan, J., Flower, C.D., Gibson, G.J., Greening, A.P., Ibrahim, N.B., Johnston, I.D., Mitchell, D.M., 1999. The diagnosis, assessment and treatment of diffuse parenchymal lung disease in adults. Thorax. 54, S1- S30.

Cuzzocrea, S., Genovese, T., Failla, M., Vecchio, G., Fruciano, M., Mazzon, E., Di Paola, R., Muia, C., La Rosa, C., Crimi, N., Rizzarelli, E., Vancheri, C., 2007. Protective effect of orally administered carnosine on bleomycin-induced lung injury. Am. J. Physiol. Lung. Cell. Mol. Physiol. 295, L1905-L1104.

Damsky, C.H., Werb, Z., 1992. Signal transduction by integrin receptors for extracellular matrix: cooperative processing of extracellular information. Curr. Opin. Cell. Biol. 4, 772-781.

Dawes, K.E., Cambrey, A.D., Campa, J.S., Bishop, J.E., McAnulty, R.J., Peacock, A.J., Laurent, G.J., 1996. Changes in collagen metabolism in response to endothelin-1: evidence for fibroblast heterogeneity. Int. J. Biochem. Cell. Biol. 28, 229-238.

Day, B.J., 2008. Antioxidants as potential therapeutics for lung fibrosis. Antiox. Redox. Signal. 10, 355-370.

Dempsey, O.J., 2006. Clinical review: idiopathic pulmonary fibrosis-past, present and future. Respir. Med. 100, 1871-1885.

Desmouliere, A., Chaponnier, C., Gabbiani, G., 2005. Tissue repair, contraction, and the myofibroblast. Wound. Repair. Regen. 13, 7-12.

Dolhnikoff, M., Mauad, T., Ludwig, M.S., 1999. Extracellular matrix and oscillatory mechanics of rat lung parenchyma in bleomycin-induced fibrosis. Am. J. Respir. Crit. Care. Med. 160, 1750-1757.

Doucet, C., Brouty-Boye, D., Pottin-Clemenceau, C., Jasmin, C., Canonica, G.W., Azzarone, B., 1998. IL-4 and IL-13 specifically increase adhesion molecule and inflammatory cytokine expression in human lung fibroblasts. Int. Immunol. 10, 1421-1433.

du Bois, R.M., Wells, A.U., 2001. Cryptogenic fibrosing alveolitis/idiopathic pulmonary fibrosis. Eur. Respir. J. Suppl. 32, 43s-55s.

Dunsmore, S.E., Shapiro, S.D., 2004. The bone marrow leaves its scar: new concepts in pulmonary fibrosis. J. Clin. Invest. 113, 180-182.

Ebihara, T., Venkatesan, N., Tanaka, R., Ludwig, M.S., 2000. Changes in extra-cellularmatrix and tissue viscoelasticity in bleomycin-induced lung fibrosis. Temporal aspects. Am. J. Respir. Crit. Care. Med. 162, 1569-1576.

El Kebir, D., József, L., Pan, W., Filep, J.G., 2008. Myeloperoxidase delays neutrophil apoptosis through CD11b/CD18 integrins and prolongs inflammation. Circ. Res. 103, 352-359.

El-Medany, A., Hagar, H.H., Moursi, M., At Muhammed, R., El-Rakhawy, F.I., El-Medany, G., 2005. Attenuation of bleomycin-induced lung fibrosis in rats by mesna. Eur. J. Pharmacol. 509, 61-70.

Elssner, A., Jaumann, F., Dobmann, S., Behr, J., Schwaiblmair, M., Reichenspurner, H., Furst, H., Briegel, J., Vogelmeier, C., 2000. Elevated levels of interleukin-8 and transforming growth factor-beta in bronchoalveolar lavage fluid from patients with

bronchiolitis obliterans syndrome: proinflammatory role of bronchial epithelial cells. Transplantation. 70, 362-367.

Eyden, B., 2001. The fibronexus in reactive and tumoral myofibroblasts: further characterisation by electron microscopy. Histol. Histopathol. 16, 57-70.

Faffe, D.S., Silva, G.H., Kurtz, P.M., Negri, E.M., Capelozzi, V.L., Rocco, P.R., Zin, W.A., 2001. Lung tissue mechanics and extracellular matrix composition in a murine model of silicosis. J. Appl. Physiol. 90, 1400-1406.

Filderman, A.E., Genovese, L.A., Lazo, J.S., 1988. Alterations in pulmonary protective enzymes following systemic bleomycin treatment in mice. Biochem. Pharmacol. 37, 1111-1116.

Fint, M.H., 1990. Connective tissue biology. In: Mc Farlane RM, McCrouther DA, Flint MH, eds. Dupuytren's Disease. Edinburgh, Scotland: Churchill Livingstone; 13-24.

Fireman, E., Vardinon, N., Burke, M., Spizer, S., Levin, S., Endler, A., Stav, D., Topilsky, M., Mann, A., Schwarz, Y., Kivity, S., Greif, J., 1998. Predictive value of response to treatment of T-lymphocyte subpopulations in idiopathic pulmonary fibrosis. Eur. Respir. J. 11, 706-711.

Fleischman, R.W., Baker, J.R., Thompson, G.R., Schaeppi, U.H., Illievski, V.R., Cooney, D.A., Davis, R.D., 1971. Bleomycin-induced interstitial pneumonia in dogs. Thorax. 26, 675-682.

Flemmer, A., Simbruner, G., Muenzer, S., Proquitte, H., Haberl, C., Nicolai, T., Leiderer, R., 2000. Effect of lung water content, manipulated by intra-traqueal furosemide, surfactant, or a mixture of both, on compliance and viscoelastic tissue forces in lung-lavaged newborn piglets. Crit. Care. Med. 28, 1911-1917.

Fredberg, J.J., Keefe, D.H., Glass, G.M., Castile R.G., Frantz, D.3rd., 1984. Alveolar pressure nonhomogeneity during small-amplitude hi-frequency oscillation. J. Appl. Physiol: Respirat. Environ. Exercise Physiol. 57, 788-800.

Fredberg, J.J., Stamenovic, D., 1989. On the imperfect elasticity of lung tissue. J. Appl. Physiol. 67, 2408-2419.

Fukaya, H., Martin, C.J., Young, A.C., Katsura, S., 1968. Mechanical properties of alveolar walls. J. Appl. Physiol. 25, 689-695.

Fukuda, Y., Ferrans, V.J., 1988. Pulmonary elastic fibre degradation in paraquat toxicity. An electron microscopic immunohistochemical study. J. Submicrosc. Cytol. Pathol. 20, 15-23.

Fukuda, Y., Basset, F., Soler, P., Ferrans, V.J., Masugi, Y., Crystal, R.G., 1990. Intraluminal fibrosis and elastic fibre degradation lead to lung remodelling in pulmonary Langerhans cell granulomatosis (histiocytosis X). Am. J. Pathol. 137, 415-424.

Fukuda, Y., Ishizaki, M., Kudoh, S., Kitaichi, M., Yamanaka, N., 1998. Localization of matrix metalloproteinases-1, -2, and -9 and tissue inhibitor of metalloproteinase-2 in interstitial lung diseases. Lab. Invest. 78, 687-698.

Fung, Y.C., 1993. Biomechanics: Mechanical properties of living tissues. Springer-Verlag, New York.

Gadek, J.E., Fells, G.A., Zimmerman, R.L., Crystal, R.G., 1984. Role of connective tissue proteases in the pathogenesis of chronic inflammatory lung disease. Environ. Health. Perspect. 55, 297-306.

Gauldie, J., Kolb, M., Sime, P.J., 2002. A new direction in the pathogenesis of idiopathic pulmonary fibrosis? Respir. Res. 3:1.

Geiser, T., 2003. Idiopathic pulmonary fibrosis- a disorder of alveolar wound repair? Swiss. Med. Wkly. 133, 405-411.

Genovese, T., Mazzon, E., Di Paola, R., Muià, C., Threadgill, M.D., Caputi, A.P., Thiemermann, C., Cuzzocrea, S., 2005. Inhibitors of poly(ADP-ribose) polymerase modulate signal transduction pathways and the development of bleomycin-induced lung injury. J. Pharmacol. Exp. Ther. 313, 529-538.

Gharaee-Kermani, M., Denholm, E.M., Phan, S.H., 1996. Costimulation of fibroblast collagen and transforming growth factor beta1 gene expression by monocyte chemoattractant protein-1 via specific receptors. J. Biol. Chem. 271, 17779-17784.

Gharaee-Kermani, M., Nozaki, Y., Hatano, K., Phan, S.H., 2001. Lung interleukin-4 gene expression in a murine model of bleomycin-induced pulmonary fibrosis. Cytokine. 15, 138-147.

Gharaee-Kermani, M., Phan, S.H., 2005a. Molecular mechanisms of and possible treatment strategies for idiopathic pulmonary fibrosis. Curr. Pharm. Des. 11, 3943-3971.

Gharaee-Kermani, M., Hatano, K., Nozaki, Y., Phan, SH., 2005b. Gender-based differences in bleomycin-induced pulmonary fibrosis. Am. J. Pathol. 166, 1593-1606.

Giaid, A., Michel, R.P., Stewart, D.J., Sheppard, M., Corrin, B., Hamid, Q., 1993. Expression of endothelin-1 in lungs of patients with cryptogenic fibrosing alveolitis. Lancet. 341, 1550-1554.

Gilroy, D.W., Lawrence, T., Perretti, M., Rossi, A.G., 2004. Inflammatory resolution: new opportunities for drug discovery. Nat. Rev. Drug. Discov. 3, 401-416.

Giri, S.N., Hyde, D.A., 1988. Ameliorating effects of an interferon inducer polyinosinic-polycytidylic acid on bleomycin-induced lung fibrosis in hamsters. Am. J. Pathol. 153, 525-536.

Giri, S.N., Hyde, D.M., Braun, R.K., Gaarde, W., Harper, J.R., Pierschbacher, M.D., 1997. Antifibrotic effect of decorin in a bleomycin hamster model of lung fibrosis. Biochem. Pharmacol. 54, 1205-1216.

Global Initiative for Asthma (GINA), National Heart, Lung and Blood Institute (NHLBI). Global strategy for asthma management and prevention. Bethesda (MD): Global Initiative for Asthma (GINA), National Heart, Lung and Blood Institute (NHLBI); 2007. 92 p.

Goldstein, R.H., Lucey, E.C., Franzblau, C., Snider, G.L., 1979. Failure of mechanical properties to parallel changes in lung connective tissue composition in bleomycin-induced pulmonary fibrosis in hamsters. Am. Rev. Respir. Dis. 120, 67-73.

Goldstein, R.H., Polgar, P., 1982. The effect and interaction of bradykinin and prostaglandins on protein and collagen production by lung fibroblasts. J. Biol. Chem. 257, 8630-8633.

Grande, J.P., 1997. Role of transforming growth factor-beta in tissue injury and repair. Proc. Soc. Exp. Biol. Med. 214, 27-40.

Gruber, R., Pforte, A., Beer, B., Riethmuller, G., 1996. Determination of gamma/delta and other T-lymphocyte subsets in bronchoalveolar lavage fluid and peripheral blood from patients with sarcoidosis and idiopathic fibrosis in the lung. A.P.M.I.S. 104, 199-205.

Gutiérrez-Ruíz, M.C., Robles-Díaz, G., Kershenobich, D., 2002. Emerging concepts in inflammation and fibrosis. Arch. Med. Res. 33, 595-599.

Hafstrom, I., Ringertz, B., Lundeberg, T., Palmblad, J., 1993. The effect of endothelin, neuropeptide Y, calcitonin gene-related peptide and substance P on neutrophil functions. Acta. Physiol. Scand. 148, 341-346.

Halim, A., Kanayama, N., el Maradny, E., Maehara, K., Terao, T., 1995. Activated neutrophil by endothelin-1 caused tissue damage in human umbilical cord. Thromb. Res. 77, 321-327.

Hance, A.J., Crystal, R.G., 1975. The connective tissue of lung. Am. Rev. Respir. Dis. 112, 657-711.

Hantos, Z., Suki, B., Csendes, T., Daroczy, B., 1987. Constant-phase modeling of pulmonary tissue impedance. Bull. Eur. Physiopathol. Respir. 23, S326.

Hantos, Z., Adamicza, A., Govaerts, E., Daróczy, B., 1992. Mechanical impedances of lungs and chest wall in the cat. J. Appl. Physiol. 73, 427-433.

Hantos, Z., Peták, F., Adamicza, A., Daróczy, B., Fredberg, J.J., 1995. Differential responses of global airway, terminal airway, and tissue impedances to histamine. J. Appl. Physiol. 79, 1440-1448.

Harari, S., Caminati, A., 2005. Idiopathic pulmonary fibrosis. Allergy. 60, 421-435.

Hardingham, T.E., Fosang, A.J., 1992. Proteoglycans: many forms and many functions. FASEB. J. 6, 861-870.

Harkness, R.D., 1980. Mechanical properties of connective tisúes in relation to function. In: Parry DAD, Creamer LK, eds. Fibrous Proteins: Scientific, Industrial, and Medical Aspects. London, England: Academic Press; 207-230.

Harrison, J.H.Jr, Lazo, J.S., 1987. High dose continuous infusion of bleomycin in mice: a new model for drug-induced pulmonary fibrosis. J. Pharmacol. Exp. Ther. 243, 1185-1194.

Hashimoto, N., Jin, H., Liu, T., Chensue, S.W., Phan, S.H., 2004. Bone marrow-derived progenitor cells in pulmonary fibrosis. J. Clin. Invest. 113, 243-252.

Hay, J.G., Haslam, P.L., Dewar, A., Addis, B., Turner-Warwick, M., Laurent, G.J., 1987. Development of acute lung injury after the combination of intravenous bleomycin and exposure to hyperoxia in rats. Thorax. 42, 374-382.

Hay, J., Shahzeidi, S., Laurent, G., 1991. Mechanisms of bleomycin-induced lung damage. Arch. Toxicol. 65, 81-94.

Heinegard, D., Oldberg, A., 1993. Glycosylated matrix proteins. In: Royce PM, Steinmann B, eds. Connective Tissue and its Heritable Disorders: Molecular, Genetic, and Medical Aspects. New York, NY: Wiley-Liss; 189-209.

Heusinger-Ribeiro, J., Eberlein, M., Wahab, N.A., Goppelt-Struebe, M., 2001. Expression of connective tissue growth factor in human renal fibroblasts: regulatory roles of RhoA and cAMP. J. Am. Soc. Nephrol. 12, 1853-1861.

Hildebrandt. J., 1969. Comparison of mathematical models for cat lung and viscoelastic balloon derived by Laplace transform methods from pressure-volume data. Bull. Math. Biophys. 31, 651-667.

Holgate, S.T., Peters-Golden, M., Panettieri, R.A., Henderson, W.R. Jr., 2003. Roles of cysteinyl leukotrienes in airway inflammation, smooth muscle function, and remodelling. J. Allergy. Clin. Immunol. 111, S18-S36.

Hoppin, F.G.Jr., Lee, G.C., Dawson, S.V., 1975. Properties of lung parenchyma in distortion. J. Appl. Physiol. 39, 742-751.

Horwitz, A.L., Crystal, R.C., 1975. Content and synthesis of glycosaminoglycans in the developing lung. J. Clin. Invest. 56, 1312-1318.

Hoshino, M., Nakamura, Y., Sim, J., Shimojo, J., Isogai, S., 1998. Bronchial subepithelial fibrosis and expression of matrix metalloproteinase-9 in asthmatic airway inflammation. J. Allergy. Clin. Immunol. 102, 783-788.

Hu, B., Wu, Z., Phan, S.H., 2003. Smad3 mediates transforming growth factor-beta-induced alpha-smooth muscle actin expression. Am. J. Respir. Cell. Mol. Biol. 29, 397-404.

Hubbard, A.K., Timblin, C.R., Shukla, A., Rincon, M., Mossman, B.T., 2002. Activation of NF-kappaB-dependent gene expression by silica in lungs of luciferase reporter mice. Am. J. Physiol. Lung. Cell. Mol. Physiol. 282, L968-L975.

Hunninghake, G.W., Gadek, J.E., Lawley, T.J., Crystal, R.G., 1981. Mechanisms of neutrophil accumulation in the lungs of patients with idiopathic pulmonary fibrosis. J. Clin. Invest. 68, 259-269.

Ignotz, R.A., Massague, J., 1986. Transforming growth factor-beta stimulates the expression of fibronectin and collagen and their incorporation into the extracellular matrix. J. Biol. Chem. 261, 4337-4345.

Imokawa, S., Sato, A., Hayakawa, H., Kotani, M., Urano, T., Takada, A., 1997. Tissue factor expression and fibrin deposition in the lungs of patients with idiopathic pulmonary fibrosis and systemic sclerosis. Am. J. Respir. Crit. Care. Med. 156, 631-636.

Iraz, M., Erdogan, H., Kotuk, M., Yagmurca, M., Kilic, T., Ermis, H., Fadillioglu, E., Yildirim, Z., 2006. Ginkgo biloba inhibits bleomycin-induced lung fibrosis in rats. Pharmacol. Res. 53, 310-316.

Ito, S., Ingenito, E.P., Arold, S.P., Parameswaran, H., Tgavalekos, N.T., Lutchen, K.R., Suki, B., 2004. Tissue heterogeneity in the mouse lung: effects of elastase treatment. J. Appl. Physiol. 97, 204-212.

Iyer, S.N., Wild, J.S., Schiedt, M.J., Hyde, D.M., Margolin, S.B., Giri, S.N., 1995. Dietary intake of pirfenidone ameliorates bleomycin-induced lung fibrosis in hamsters. J. Lab. Clin. Med. 125, 779-785.

Iyer, S.N., Margolin, S.B., Hyde, D.M., Giri, S.N., 1998. Lung fibrosis is ameliorated by pirfenidone in diet after the second dose in a three-dose bleomycin hamster model. Exp. Lung. Res. 24, 119-132.

Izbicki, G., Segel, M.J., Christensen, T.G., Conner, M.W., Breuer, R., 2002. Time course of bleomycin-induced lung fibrosis. Int. J. Exp. Pathol. 83, 111-119.

Janick-Buckner, D., Ranges, G.E., Hacker, M.P., Alteration of bronchoalveolar lavage cell populations following bleomycin treatment in mice. Toxicol. Appl. Pharmacol. 100, 465-473.

Janoff, A., White, R., Carp, H., Harel, S., Dearing, R., Lee, D., 1979. Lung injury induced by leukocytic proteases. Am. J. Pathol. 97, 111-136.

Jones, A.W., Reeve, N.L., 1978. Ultrastructural study of bleomycin-induced pulmonary changes in mice. J. Pathol. 124, 227-233.

Kahaleh, M.B., 1991. Endothelin, an endothelial-dependent vasoconstrictor in scleroderma: enhanced production and profibrotic action. Arthritis. Rheum. 34, 978-983.

Kaminski, N., Allard, J.D., Pittet, J.F., Zuo, F., Griffiths, M.J., Morris, D., Huang, X., Sheppard, D., Heller, R.A., 2000. Global analysis of gene expression in pulmonary fibrosis reveals distinct programs regulating lung inflammation and fibrosis. Proc. Natl. Acad. Sci. USA. 97, 1778-1783.

Kapanci, Y., Assimacopoulos, A., Irle, C., Zwahlen, A., Gabbiani, G., 1974. "Contractile interstitial cells" in pulmonary alveolar septa: a possible regulator of ventilation-perfusion ratio? Ultrastructural, immunofluorescence, and in vitro studies. J. Cell. Biol. 60, 375-392.

Kapanci, Y., Desmouliere, A., Pache, J.C., Redard, M., Gabbiani, G., 1995. Cytoskeletal protein modulation in pulmonary alveolar myofibroblasts during idiopathic

pulmonary fibrosis. Possible role of transforming growth factor beta and tumor necrosis factor alpha. Am. J. Respir. Crit. Care. Med. 152, 2163-2169.

Kasper, M., Gunthert, U., Dall, P., Kayser, K., Schuh, D., Haroske, G., Muller, M., 1995. Distinct expression patterns of CD44 isoforms during human lung development and in pulmonary fibrosis. Am. J. Respir. Cell. Mol. Biol. 13, 648-656.

Kasper, M., Haroske, G., 1996. Alterations in the alveolar epithelium after injury leading to pulmonary fibrosis. Histol. Histopathol. 11. 463-483.

Kassel, O., de Blay, F., Duvernelle, C., Olgart, C., Israel-Biet, D., Krieger, P., Moreau, L., Muller, C., Pauli, G., Frossard, N., 2001. Local increase in the number of mast cells and expression of nerve growth factor in the bronchus of asthmatic patients after repeated inhalation of allergen at low-dose. Clin. Exp. Allergy. 31, 1432-1440.

Katzenstein, A.L., Myers, J.L., 1998. Idiopathic pulmonary fibrosis: clinical relevance of pathologic classification. Am. J. Respir. Crit. Care. Med. 157, 1301-1315.

Keerthisingam, C.B., Jenkins, R.G., Harrison, N.K., Hernandez-Rodriguez, N.A., Booth, H., Laurent, G.J., Hart, S.L., Foster, M.L., McAnulty, R.J., 2001. Cyclooxygenase-2 deficiency results in a loss of the anti-proliferative response to transforming growth factor-beta in human fibrotic lung fibroblasts and promotes bleomycin-induced pulmonary fibrosis in mice. Am. J. Pathol. 158, 1411-1422.

Khalil, N., Bereznay, O., Sporn, M., Greenberg, A.H., 1989. Macrophage production of transforming growth factor beta and fibroblast collagen synthesis in chronic pulmonary inflammation. J. Exp. Med. 170, 727-737.

Khalil, N., O'Connor, R.N., Unruh, H.W., Warren, P.W., Flanders, K.C., Kemp, A., Bereznay, O.H., Greenberg, A.H., 1991. Increased production and immunohistochemical localization of transforming growth factor-beta in idiopathic pulmonary fibrosis. Am. J. Respir. Cell. Mol. Biol. 5, 155-162.

Kim, D.S., Collard, H.R., King, T.E.Jr., 2006. Classification and natural history of the idiopathic interstitial pneumonias. Proc. Am. Thorac. Soc. 3, 285-292.

Kinnula, V.L., Fattman, C.L., Tan, R.J., Oury, T.D., 2005. Oxidative stress in pulmonary fibrosis: a possible role for redox modulatory therapy. Am. J. Respir. Crit. Care. Med. 172, 417-422.

Kinnula, V.L., Myllarniemi, M., 2008. Oxidant-antioxidant imbalance as a potential contributor to the progression of human pulmonary fibrosis. Antiox. Redox. Signal. 10, 727-738.

Klebanoff, S.J., 2005. Myeloperoxidase: friend and foe. J. Leukoc. Biol. 77, 598-625.

Knight, D., 2001. Epithelium-fibroblast interactions in response to airway inflammation. Immunol. Cell. Biol. 79, 160-164.

Koeller, R.C., 1984. Applications of fractional calculus to the theory of viscoelasticity. J. Appl. Mech. 51, 299-307.

Kohyama, T., Ertl, R.F., Valenti, V., Spurzem, J., Kawamoto, M., Nakamura, Y., Veys, T., Allegra, L., Romberger, D., Rennard, S.I., 2001. Prostaglandin E(2) inhibits fibroblast chemotaxis. Am. J. Physiol. Lung. Cell. Mol. Physiol. 281, L1257-L1263.

Kotani, I., Sato, A., Hayakawa, H., Urano, T., Takada, Y., Takada, A., 1995. Increased procoagulant and antifibrinolytic activities in the lungs with idiopathic pulmonary fibrosis. Thromb. Res. 77, 493-504.

Krishna, G., Liu, K., Shigemitsu, H., Gao, M., Raffin, T.A., Rosen, G.D., 2001. PG490-88, a derivative of triptolide, blocks bleomycin-induced lung fibrosis. Am. J. Pathol. 158, 997-1004.

Kuhn, C., Boldt, J., King, T.E.Jr., Crouch, E., Vartio, T., McDonald, J.A., 1989. An immunohistochemical study of architectural remodelling and connective tissue synthesis in pulmonary fibrosis. Am. Rev. Respir. Dis. 140, 1693-1703.

Kuhn, .C, McDonald, J.A., 1991. The roles of the myofibroblast in idiopathic pulmonary fibrosis. Ultrastructural and immunohistochemical features of sites of active extracellular matrix synthesis. Am. J. Pathol. 138, 1257-1265.

Kuroki, S., Ohta, A., Sueoka, N., Katoh, O., Yamada, H., Yamaguchi, M., 1995. Determination of various cytokines and type III procollagen aminopeptide levels in bronchoalveolar lavage fluid of the patients with pulmonary fibrosis: inverse correlation between type III procollagen aminopeptide and interferon-gamma in progressive patients. Br. J. Rheumatol. 34, 31-36.

Kuwano, K., Maeyama, T., Inoshima, I., Ninomiya, K., Hagimoto, N., Yoshimi, M., Fujita, M., Nakamura, N., Shirakawa, K., Hara, N., 2002. Increased circulating levels of soluble Fas ligand are correlated with disease activity in patients with fibrosing lung diseases. Respirology. 7, 15-21.

Kuwano, K., Hagimoto, N., Nakanishi, Y., 2004. The role of apoptosis in pulmonary fibrosis. Histol. Histopathol. 19, 867-881.

Kwong, K.Y., Literat, A., Zhu, N.L., Huang, H.H., Li, C., Jones, C.A., Minoo, P., 2004. Expression of transforming growth factor beta (TGF-beta1) in human epithelial alveolar cells: a pro-inflammatory mediator independent pathway. Life. Sci. 74, 2941-2957.

Lagente, V., Manoury, B., Nénan, S., Le Quément, C., Martin-Chouly, C., Boichot, E., 2005. Role of matrix metalloproteinases in the development of airway inflammation and remodelling. Braz. J. Med. Biol. Res. 38, 1521-1530.

Lama, V., Moore, B.B., Christensen, P., Toews, G.B., Peters-Golden, M., 2002. Prostaglandin E2 synthesis and suppression of fibroblast proliferation by alveolar epithelial cells is cyclooxygenase-2-dependent. Am. J. Respir. Cell. Mol. Biol. 27, 752-758.

Lau, D., Mollnau, H., Eiserich, J.P., Freeman, B.A., Daiber, A., Gehling, U.M., Brümmer, J., Rudolph, V., Münzel, T., Heitzer, T., Meinertz, T., Baldus, S., 2005. Myeloperoxidase mediates neutrophil activation by association with CD11b/CD18 integrins. Proc. Natl. Acad. Sci. USA. 102, 431-436.

Laurent, G.J., McAnulty, J.C., 1983. Protein metabolism during bleomycin-induced pulmonary fibrosis in rabbits. “in vivo” evidence for collagen accumulation because of increased synthesis and decreased degradation of the newly synthethised collagen. Am. Rev. Respir. Dis. 128, 82-88.

Laurent, G.J., Chambers, R.C., Hill, M.R., McAnulty, R.J., 2007. Regulation of matrix turnover: fibroblasts, forces, factors and fibrosis. Biochem. Soc. Trans. 35, 647-651.

Lawson, W.E., Polosukhin, V.V., Stathopoulos, G.T., Zoia, O., Han, W., Lane, K.B., Li, B., Donnelly, E.F., Holburn, G.E., Lewis, K.G., Collins, R.D., Hull, W.M., Glasser, S.W., Whitsett, J.A., Blackwell, T.S., 2005. Increased and prolonged pulmonary fibrosis in surfactant protein C-deficient mice following intratracheal bleomycin. Am. J. Pathol. 167, 1267-1277.

Lee, A., Whyte, M.K.B., Haslett, C., 1993. Inhibition of apoptosis and prolongation of neutrophil functional longevity by inflammatory mediators. J. Leukoc. Biol. 54, 283-288.

Leite-Júnior, J.H., Rocco, P.R., Faffe, D.S., Romero, P.V., Zin, W.A., 2003. On the preparation of lung strip for tissue mechanics measurement. Respir. Physiol. Neurobiol. 134, 255-262.

Li, Q., Park, P.W., Wilson, C.L., Parks, W.C., 2002. Matrilysin shedding of syndecan-1 regulates chemokine mobilization and transepithelial efflux of neutrophils in acute lung injury. Cell. 111, 635-646.

Liebow, A.A., Carrington, D.B., 1969. The interstitial pneumonias. In: Simon M, Potchen EJ, LeMay M, editors. Frontiers of pulmonary radiology. New York: Grune & Stratteon; 102-141.

Limper, A.H., Broekelmann, T.J., Colby, T.V., Malizia, G., McDonald, J.A., 1991. Analysis of local mRNA expression for extracellular matrix proteins and growth factors using in situ hybridization in fibroproliferative lung disorders. Chest. 99, 55S-56S.

Lindenschmidt, R.C., Tryka, A.F., Godfrey, G.A., Frome, E.L., Witchi, H., 1986. Intratracheal versus intravenous administration of bleomycin in mice: Acute effects. Toxicol. Appl. Pharmacol. 85, 69-77.

Liu, S.H., Yang, R.S., al-Shaikh, R., Lane, J.M., 1995. Collagen in tendon, ligament, and bone healing. A current review. Clin. Orthop. Relat. Res. 318, 265-278.

Lopez-Aguilar, J., Romero, P.V., 1998. Effect of elastase pretreatment on rat lung strip induced constriction. Respir. Physiol. 113, 239-246.

Lu, Q., Harrington, E.O., Rounds, S., 2005. Apoptosis and lung injury. Keio. J. Med. 54, 184-189.

Ludwig, M.S., Robatto, F.M., Sly, P.D., Browman, M., Bates, J.H., Romero, P.V., 1991. Histamine-induced constriction of canine peripheral lung: an airway or tissue response? J. Appl. Physiol. 71, 287-293.

Lutchen, K.R., Yang, K., Kaczka, D.W., Suki, B., 1993. Optimal ventilation waveforms for estimating low-frequency respiratory impedance. J. Appl. Physiol. 75, 478-488.

Lutchen, K.R., Suki, B., Zhang, Q., Petak, F., Daroczy, B., Hantos, Z., 1994. Airway and tissue mechanics during physiological breathing and bronchoconstriction in dogs. J. Appl. Physiol. 77, 373-385.

Lypmany, P.A., du Bois, R.M., 1997. Diffuse lung disease: product of genetic susceptibility and environmental encounters. Thorax. 52, 92-94.

Madtes, D.K., Elston, A.L., Kaback, L.A., Clark, J.G., 2001. Selective induction of tissue inhibitor of metalloproteinase-1 in bleomycin-induced pulmonary fibrosis. Am. J. Respir. Cell. Mol. Biol. 24, 599-607.

Magnan, A., Mege, J.L., Escallier, J.C., Brisse, J., Capo, C., Reynaud, M., Thomas, P., Meric, B., Garbe, L., Badier, M., Viard, L., Bongrand, P., Giudicelli, R., Metras, D., Fuentes, P., Vervloet, D., Noirclerc, M., 1996. Balance between alveolar macrophage IL-6 and TGF-beta in lung-transplant recipients. Am. J. Respir. Crit. Care. Med. 153, 1431-1436.

Marikovsky, M., Breuing, K., Liu, P.Y., Eriksson, E., Higashiyama, S., Farber, P., Abraham, J., Klagsbrun, M., 1993. Appearance of heparin-binding EGF-like growth factor in wound fluid as a response to injury. Proc. Natl. Acad. Sci. USA. 90, 3889-3893.

Marshall, R.P., McAnulty, R.J., Laurent, G.J., 2000. Angiotensin II is mitogenic for human lung fibroblasts via activation of the type 1 receptor. Am. J. Respir. Crit. Care. Med. 161, 1999-2004.

Marshall, R.P., Gohlke, P., Chambers, R.C., Howell, D.C., Bottoms, S.E., Unger, T., McAnulty, R.J., Laurent, G.J., 2004. Angiotensin II and the fibroproliferative response to acute lung injury. Am. J. Physiol. Lung. Cell. Mol. Physiol. 286, L156-L164.

Martin, P., 1997. Wound healing--aiming for perfect skin regeneration. Science. 276, 75-81.

Martinet, Y., Menard, O., Vaillant, P., Vignaud, J.M., Martinet, N., 1996. Cytokines in human lung fibrosis. Arch. Toxicol. Suppl. 18,127-139.

Mason, R.J., Schwarz, M.I., Hunninghake, G.W., Musson, R.A., 1999. NHLBI Workshop Summary. Pharmacological therapy for idiopathic pulmonary fibrosis. Past, present, and future. Am. J. Respir. Crit. Care. Med. 160, 1771-1777.

Mata, M., Ruíz, A., Cerdá, M., Martinez-Losa, M., Cortijo, J., Santangelo, F., Serrano-Mollar, A., Llombart-Bosch, A., Morcillo, E.J., 2003. Oral N-acetylcysteine reduces bleomycin-induced lung damage and mucin Muc5ac expression in rats. Eur. Respir. J. 22, 900-905.

Mattoli, S., Soloperto, M., Marini, M., Fasoli, A., 1991. Levels of endothelin in the bronchoalveolar lavage fluid of patients with symptomatic asthma and reversible airflow obstruction. J. Allergy Clin. Immunol. 88, 376-384.

Matute-Bello, G., Liles, W.C., Radella, F.2nd, Steinberg, K.P., Ruzinski, J.T., Jonas, M., Chi, E.Y., Hudson, L.D., Martin, T.R, 1997. Neutrophil apoptosis in the acute respiratory distress syndrome. Am. J. Respir. Crit. Care. Med. 156, 1969-1977.

Matute-Bello, G., Frevert, C.W., Martin, T.R., 2008. Animal models of acute lung injury. Am. J. Physiol. Lung. Cell. Mol. Physiol. 295, L379-L399.

McGrouther, D.A., 1994. Hypertrophic or keloid scars? Eye. 8, 200-203.

McIntyre, J.O., Matrisian, L.M., 2003. Molecular imaging of proteolytic activity in cancer. J. Cell. Biochem. 90, 1087-1097.

Menezes, S.L., Bozza, P.T., Neto, H.C., Laranjeira, A.P., Negri, E.M., Capelozzi, V.L., Zin, W.A., Rocco, P.R., 2005. Pulmonary and extrapulmonary acute lung injury: inflammatory and ultrastructural analyses. J. Appl. Physiol. 98, 1777-1783.

Mercer, R.R., Crapo, J.D., 1990. Spatial distribution of collagen and elastin fibres in the lungs. J. Appl. Physiol. 69, 756-765.

Micera, A., Vigneti, E., Pickholtz, D., Reich, R., Pappo, O., Bonini, S., Maquart, F.X., Aloe, L., Levi-Schaffer, F., 2001. Nerve growth factor displays stimulatory effects on human skin and lung fibroblasts, demonstrating a direct role for this factor in tissue repair. Proc. Natl. Acad. Sci. USA. 98, 6162-6167.

Mignatti, P., Rifkin, D.B., Welgus, H.G., Parks, W.C., 1996. Proteinases and tissue remodelling. In The Molcwdar cmd Cellukrr Biolog!. of Wound Rrpcrir. Second Edition. (Ed. Clark R. A. F.). Plenum Press, New York. pp 427.-474.

Mijailovich, S.M., Stamenović, D., Fredberg, J.J., 1993. Toward a kinetic theory of connective tissue micromechanics. J. Appl. Physiol. 74, 665-681.

Mishra, A., Doyle, N.A., Martin, W.J.2nd., 2000. Bleomycin-mediated pulmonary toxicity: evidence for a p53-mediated response. Am. J. Respir. Cell. Mol. Biol. 22, 543-549.

Moeller, A., Ask, K., Warburton, D., Gauldie, J., Kolb, M., 2008. The bleomycin animal model: a useful tool to investigate treatment options for idiopathic pulmonary fibrosis? Int. J. Biochem. Cell. Biol. 40, 362-382.

Molina-Molina, M., Serrano-Mollar, A., Bulbena, O., Fernandez-Zabalegui, L., Closa, D., Marin-Arguedas, A., Torrego, A., Mullol, J., Picado, C., Xaubet, A., 2006. Losartan attenuates bleomycin induced lung fibrosis by increasing prostaglandin E2 synthesis. Thorax. 61, 604-610.

Molina-Molina, M., Pereda, J., Xaubet, A., 2007. Experimental models for the study of pulmonary fibrosis: current usefulness and future promise Arch. Bronconeumol. 43, 501-507.

Molina-Molina, M., Xaubet, A., Li, X., Abdul-Hafez, A., Friderici, K., Jernigan, K., Fu, W., Ding, Q., Pereda, J., Serrano-Mollar, A., Casanova, A., Rodríguez-Becerra, E., Morell, F., Ancochea, J., Picado, C., Uhal, B.D., 2008. Angiotensinogen gene G-6A polymorphism influences idiopathic pulmonary fibrosis disease progression. Eur. Respir. J. 32, 1004-1008.

Montes, G.S., 1996. Structural biology of the fibres of the collagenous and elastic systems. Cell. Biol. Int. 20, 15-27.

Moore, B.B., Hogaboam, C.M., 2008. Murine models of pulmonary fibrosis. Am. J. Physiol. Lung. Cell. Mol. Physiol. 294, L152-L160.

Muggia, F.M., Louie, A.C., Sikic, B.I., 1983. Pulmonary toxicity of antitumor agents. Cancer. Treat. Rev. 10, 221-243.

Muller, M., Strand, S., Hug, H., Heinemann, E.M., Walczak, H., Hofmann, W.J., Stremmel, W., Krammer, P.H., Galle, P.R., 1997. Drug-induced apoptosis in hepatoma cells is mediated by the CD95 (APO-1/Fas) receptor/ligand system and involves activation of wild-type p53. J. Clin. Invest. 99, 403-413.

Murrell, G.A., Francis, M.J., Bromley, L., 1990. Modulation of fibroblast proliferation by oxygen free radicals. Biochem. J. 265, 659-665.

Murphy, G., Docherty, A.J., 1992. The matrix metalloproteinases and their inhibitors. Am. J. Respir. Cell. Mol. Biol. 7, 120-125.

Mutsaers, S.E., Bishop, J.E., McGrouther, G., Laurent, G.J., 1997. Mechanisms of tissue repair: from wound healing to fibrosis. Int. J. Biochem. Cell. Biol. 29, 5-17.

Mutsaers, S. E., Foster, M.L., Chambers, R.C., Laurent, G.J., McAnulty, R.J., 1998a. Increased endothelin-1 and its localization during the development of bleomycin-induced pulmonary fibrosis in rats. Am. J. Respir. Cell Mol. Biol. 18, 611-619.

Mutsaers, S.E., Marshall, R.P., Goldsack, N.R., Laurent, G.J., McAnulty, R.J., 1998b. Effect of endothelin receptor antagonists (BQ-485, Ro 47-0203) on collagen deposition during the development of bleomycin- induced pulmonary fibrosis in rats. Pulm. Pharmacol. Ther. 11, 221-225.

Nagaoka, I., Trapnell, B.C., Crystal, R.G., 1990. Upregulation of platelet-derived growth factor-A and –B gene expression in alveolar macrophages of individuals with idiopathic pulmonary fibrosis. J. Clin. Invest. 85, 2023-2027.

Nagase, T., Ludwig, M.S., 1998. Antigen-induced responses in lung parenchymal strips during sinusoidal oscillation. Can. J. Physiol. Pharmacol. 76, 176-181.

Nathan, C., 2002. Points of control of inflammation. Nature. 420, 846-852.

Navajas, D., Maksym, G.N., Bates, J.H., 1995. Dynamic viscoelastic nonlinearity of lung parenchymal tissue. J. Appl. Physiol. 79, 348-356.

Nettelbladt, O., Bergh, J., Schenholm, M., Tengblad, A., Hallgren, R., 1989. Accumulation of hyaluronic acid in the alveolar interstitial tissue in bleomycin-induced alveolitis. Am. Rev. Respir. Dis. 139, 759-762.

Nicholls, S.J., Hazen, S.L., 2005. Myeloperoxidase and cardiovascular disease. Arterioscler. Thromb. Vasc. Biol. 25, 1102-1111.

Nissen, N.N., Polverini, P.J., Koch, A.E., Volin, M.V., Gamelli, R.L., Di Pietro, L.A., 1998. Vascular endothelial growth factor mediates angiogenic activity during the proliferative phase of wound healing. Am. J. Pathol. 152, 1445-1452.

Okudela, K., Ito, T., Mitsui, H., Hayashi, H., Udaka, N., Kanisawa, M., Kitamura, H., 1999. The role of p53 in bleomycin-induced DNA damage in the lung. A comparative study with the small intestine. Am. J. Pathol. 155, 1341-1351.

O'Neill, C.A., Giri, S.N., Wang, Q., Perricone, M.A., Hyde, D.M., 1992. Effects of dibutyrylcyclic adenosine monophosphate on bleomycin-induced lung toxicity in hamsters. J. Appl. Toxicol. 12, 97-111.

Ortiz, L.A., Lasky, J., Hamilton, R.F.Jr., Holian, A., Hoyle, G.W., Banks, W., Peschon, J.J., Brody, A.R., Lungarella, G., Friedman, M., 1998. Expression of TNF and the necessity of TNF receptors in bleomycin-induced lung injury in mice. Exp. Lung. Res. 24, 721-743.

Ozaki, T., Moriguchi, H., Nakamura, Y., Kamei, T., Yasuoka, S., Ogura, T., 1990. Regulatory effect of prostaglandin E2 on fibronectin release from human alveolar macrophages. Am. Rev. Respir. Dis. 141, 965-969.

Pan, T., Mason, R.J., Westcott, J.Y., Shannon, J.M., 2001. Rat alveolar type II cells inhibit lung fibroblast proliferation “in vitro”. Am. J. Respir. Cell. Mol. Biol. 25, 353-361.

Papp, M., Li, X., Zhuang, J., Wang, R., Uhal, B.D., 2002. Angiotensin receptor subtype AT(1) mediates alveolar epithelial cell apoptosis in response to ANG II. Am. J. Physiol. Lung. Cell. Mol. Physiol. 282, L713-L718.

Pardo, A., Selman, M., 2002. Idiopathic pulmonary fibrosis: new insights in its pathogenesis. Int. J. Biochem. Cell. Biol. 34, 1534-1538.

Pardo, A., Gibson, K., Cisneros, J., Richards, T.J., Yang, Y., Becerril, C., Yousem, S., Herrera, I., Ruiz, V., Selman, M., Kaminski, N., 2005. Up-regulation and profibrotic role of osteopontin in human idiopathic pulmonary fibrosis. PLoS. Med. 2, e251.

Pardo, A., Selman, M., 2005b. MMP-1: the elder of the family. Int. J. Biochem. Cell. Biol. 37, 283-288.

Park, D.R., Thomsen, A.R., Frevert, C.W., Pham, U., Skerrett, S.J., Kiener, P.A., Liles, W.C., 2003. Fas (CD95) induces proinflammatory cytokine responses by human monocytes and monocyte-derived macrophages. J. Immunol. 170, 6209-6216.

Park, S.H., Saleh, D., Giaid, A., Michel R.P., 1997. Increased endothelin-1 in bleomycin-induced pulmonary fibrosis and the effect of an endothelin receptor antagonist. Am. J. Respir. Crit. Care Med. 156, 600-608.

Peacock, A.J., Dawes, K.E., Shock, A., Gray, A.J., Reeves, J.T., Laurent, G.J., 1992. Endothelin-1 and endothelin-3 induce chemotaxis and replication of pulmonary artery fibroblasts. Am. J. Respir. Cell Mol. Biol. 7, 492-499.

Pelosi, P., Rocco, P.R., 2008. Effects of mechanical ventilation on the extracellular matrix. Intensive. Care. Med. 34, 631-639.

Peták, F., Hantos, Z., Adamicza, A., Daroczy, B., 1993. Partitioning of pulmonary impedance: modeling vs. alveolar capsule approach. J. Appl. Physiol. 75, 513-521.

Peták, F., Hantos, Z., Adamicza, A., Asztalos, T., Sly, P.D., 1997. Methacholine-induced bronchoconstriction in rats: effects of intravenous vs. aerosol delivery. J. Appl. Physiol. 82, 1479-1487.

Phan, S.H., Armstrong, G., Sulavik, M.C., Schrier, D., Johnson, K.J., Ward, P.A., 1983. A comparative study of pulmonary fibrosis induced by bleomycin and an O_2 metabolite producing enzyme system. Chest. 83, 44S-45S.

Phan, S.H., 2002. The myofibroblast in pulmonary fibrosis. Chest. 122, 286S-289S.

Pinart, M., Serrano-Mollar, A., Negri, E.M., Cabrera, R., Rocco, P.R., Romero, P.V., 2008. Inflammatory related changes in lung tissue mechanics after bleomycin-induced lung injury. Respir. Physiol. Neurobiol. 160, 196-203.

Postlethwaite, A.E., Keski-Oja, J., Moses, H.L., Kang, A.H., 1987. Stimulation of the chemotactic migration of human fibroblasts by transforming growth factor beta. J. Exp. Med. 165, 251-256.

Pron, G., Belehradek, J.Jr., Orlowski, S., Mir, L.M., 1994. Involvement of membrane bleomycin-binding sites in bleomycin cytotoxicity. Biochem. Pharmacol. 48, 301-310.

Radford, E.P., 1957. Recent studies of the mechanical properties of mammalian lungs. In: Tissue elasticity, edited by J.W. Remington. Washington, DC: Am. Physiol. SOC. p. 177- 190.

Raghu, G., Masta, S., Meyers, D., Narayanan, A.S., 1989. Collagen synthesis by normal and fibrotic human lung fibroblasts and the effect of transforming growth factor-beta. Am. Rev. Respir. Dis. 140, 95-100.

Ramotar, D., Wang, H., 2003. Protective mechanisms against the antitumor agent bleomycin: lessons from Saccharomyces cerevisiae. Curr. Genet. 43, 213-224.

Razzaque, M.S., Taguchi, T., 1999. The possible role of colligin/HSP47, a collagen-binding protein, in the pathogenesis of human and experimental fibrotic diseases. Histol. Histopathol. 14, 1199-1212.

Razzaque, M.S., Taguchi, T., 2003. Pulmonary fibrosis: cellular and molecular events. Pathol. Int. 53, 133-145.

Redaelli, A., Vesentini, S., Soncini, M., Vena, P., Mantero, S., Montevecchi, F.M., 2003. Possible role of decorin glycosaminoglycans in fibril to fibril force transfer in relative mature tendons-a computational study from molecular to microstructural level. J. Biomech. 36, 1555-1569.

Rennard, S.I., Ferrans, V.J., Bradley, K.H., Crystal, R.G., 1980. Lung connective tissue. In: Mechanisms in Respiratory Toxicology, Vol. 2 (H. Witchi, Ed.), CRC Press.

Rocco, P.R.M., Negri, E.M., Kurtz, P.M., Vasconcellos, F.P., Silva, G.H., Capelozzi, V.L., Romero, P.V., Zin, W.A., 2001. Lung tissue mechanics and extracellular matrix remodelling in acute lung injury. Am. J. Respir. Crit. Care Med. 164, 1067-1071.

Rocco, P.R., Souza, A.B., Faffe, D.S., Pássaro, C.P., Santos, F.B., Negri, E.M., Lima, J.G., Contador, R.S., Capelozzi, V.L., Zin, W.A., 2003. Effect of corticosteroid on lung parenchyma remodelling at an early phase of acute lung injury. Am. J. Respir. Crit. Care. Med. 168, 677-684.

Rockey, D.C., Chung, J.J., 1996. Endothelin antagonism in experimental hepatic fibrosis: implications for endothelin in the pathogenesis of wound healing. J. Clin. Invest. 98, 1381-1388.

Romero, P.V., Rodriguez, B., Lopez-Aguilar, J., Manresa, F., 1998. Parallel airways inhomogeneity and lung tissue mechanics in transition to constricted state in rabbits. J. Appl. Physiol. 84, 1040-1047.

Romero, P.V., Zin, W.A., Lopez-Aguilar, J., 2001. Frequency characteristics of lung tissue during passive stretch and induced pneumoconstriction. J. Appl. Physiol. 91, 882-890.

Rozin, G.F., Gomes, M.M., Parra, E.R., Kairalla, R.A., de Carvalho, C.R., Capelozzi, V.L., 2005. Collagen and elastic system in the remodelling process of major types of idiopathic interstitial pneumonias (IIP). Histopathology. 46, 413-421.

Rube, C.E., Uthe, D., Schmid, K.W., Richter, K.D., Wessel, J., Schuck, A., Willich, N., Rube, C., 2000. Dose-dependent induction of transforming growth factor beta (TGF-beta) in the lung tissue of fibrosis-prone mice after thoracic irradiation. Int. J. Radiat. Oncol. Biol. Phys. 47, 1033-1042.

Sakai, H., Ingenito, E.P., Mora, R., Abbay, S., Cavalcante, F.S., Lutchen, K.R., Suki, B., 2001. Hysteresivity of the lung and tissue strip in the normal rat: effects of heterogeneities. J. Appl. Physiol. 91, 737-747.

Salez, F., Gosset, P., Copin, M.C., Lamblin Degros, C., Tonnel, A.B., Wallaert, B., 1998. Transforming growth factor-beta1 in sarcoidosis. Eur. Respir. J. 12, 913-919.

Santana, A., Saxena, B., Noble, N.A., Gold, L.I., Marshall, B.C., 1995. Increased expression of transforming growth factor beta isoforms (beta 1, beta 2, beta 3) in bleomycin-induced pulmonary fibrosis. Am. J. Respir. Cell. Mol. Biol. 13, 34-44.

Santos, F.B., Nagato, L.K., Boechem, N.M., Negri, E.M., Guimarães, A., Capelozzi, V.L., Faffe, D.S., Zin, W.A., Rocco, P.R., 2006. Time course of lung parenchyma remodelling in pulmonary and extrapulmonary acute lung injury. J. Appl. Physiol. 100, 98-106.

Savill, J., Hogg, N., Ren, Y., Haslett, C., 1992. Thrombospondin cooperates with CD36 and the vitronectin receptor in macrophage recognition of neutrophils undergoing apoptosis. J. Clin. Invest. 90, 1513-1522.

Schurch, W., Seemayer, T.A., Gabbiani, G., 1998. The myofibroblast: a quarter century after its discovery. Am. J. Surg. Pathol. 22, 141-147.

Selman, M., Ruiz, V., Cabrera, S., Segura, L., Ramirez, R., Barrios, R., Pardo A., 2000. TIMP-1 –2 –3, and –4 in idiopathic pulmonary fibrosis. A prevailing nondegradative lung microenvironment? Am. J. Physiol. Lung. Cell. Mol. Physiol. 279, L562-L574.

Selman, M., King, T.E., Pardo, A.; 2001. American Thoracic Society; European Respiratory Society; American College of Chest Physicians. Idiopathic pulmonary fibrosis: prevailing and evolving hypotheses about its pathogenesis and implications for therapy. Ann. Intern. Med. 134, 136-151.

Selman, M., Pardo, A., 2002. Idiopathic pulmonary fibrosis: an epithelial /fibroblastic cross-talk disorder. Respir. Res. 3:3.

Selman, M., Pardo, A., 2003. The epithelial/fibroblastic pathway in the pathogenesis of idiopathic pulmonary fibrosis. Am. J. Respir. Cell. Mol. Biol. 29, S93-S97.

Selman, M., Thannickal, V.J., Pardo, A., Zisman, D.A., Martinez, F.J., Lynch, III.J.P., 2004. Idiopathic pulmonary fibrosis: pathogenesis and therapeutic approaches. Drugs. 64, 405-430.

Selman, M., Pardo, A., 2006. Role of epithelial cells in idiopathic pulmonary fibrosis: from innocent targets to serial killers. Proc. Am. Thorac. Soc. 3, 364-372.

Seppa, H., Grotendorst, G., Seppa, S., Schiffmann, E., Martin, G.R., 1982. Platelet-derived growth factor in chemotactic for fibroblasts. J. Cell. Biol. 92, 584-588.

Seyer, J.M., 1978. Basement membrane associated collagens of human lung. Fed. Proc. 37, 1527.

Shahar, I., Fireman, E., Topilsky, M., Grief, J., Schwarz, Y., Kivity, S., Ben-Efraim, S., Spirer, Z., 1999. Effect of endothelin-1 on alpha-smooth muscle actin expression and on alveolar fibroblast proliferation in interstitial lung diseases. Int. J. Immunopharmacol. 21, 759-775.

Silva, P.L., Garcia, C.S., Maronas, P.A., Cagido, V.R., Negri, E.M., Damaceno-Rodrigues, N.R., Ventura, G.M., Bozza, P.T., Zin, W.A., Capelozzi, V.L., Pelosi, P., Rocco, P.R., 2009. Early short-term versus prolonged low-dose methylprednisolone therapy in acute lung injury. Eur. Respir. J. 33, 634-645.

Sime, P.J., Marr, R.A., Gauldie, D., Xing, Z., Hewlett, B.R., Graham, F.L., Gauldie, J., 1998. Transfer of tumor necrosis factor-alpha to rat lung induces severe pulmonary inflammation and patchy interstitial fibrogenesis with induction of transforming growth factor-beta1 and myofibroblasts. Am. J. Pathol. 153, 825-832.

Sime, P.J., O'Reilly, K.M., 2001. Fibrosis of the lung and other tissues: new concepts in pathogenesis and treatment. Clin. Immunol. 99, 308-319.

Simon, H.U., 2003. Neutrophil apoptosis pathways and their modifications in inflammation. Immunol. Rev. 193,101-110.

Singer, A.J., Clark, R.A., 1999. Cutaneous wound healing. N. Engl. J. Med. 341, 738-746.

Sirianni, F.E., Chu, F.S., Walker, D.C., 2003. Human alveolar wall fibroblasts directly link epithelial type 2 cells to capillary endothelium. Am. J. Respir. Crit. Care. Med. 168, 1532-1537.

Sly, P.D., Collins, R.A., Thamrin, C., Turner, D.J., Hantos, Z., 2003. Volume dependence of airway and tissue impedances in mice. J. Appl. Physiol. 94, 1460-1466.

Smaldone, G.C., Mitzner, W., Itoh, H., 1983. Role of alveolar recruitment in lung inflation: influence on pressure-volume hysteresis. J. Appl. Physiol. 55, 1321-1332.

Snider, G.L., Celli, B.R., Goldstein, R.H., O'Brien, J.J., Luey, E.C., 1978. Chronic interstitial pulmonary fibrosis produced in hamsters by endotracheal bleomycin. Lung volumes, volume-pressure relations, carbon monoxide uptake, and arterial blood gas studied. Am. Rev. Respir. Dis. 117, 289-297.

Sogut, S., Ozyurt, H., Armutcu, F., Kart, L., Iraz, M., Akyol, O., Ozen, S., Kaplan, S., Temel, I., Yildirim, Z., 2004. Erdosteine prevents bleomycin-induced pulmonary fibrosis in rats. Eur. J. Pharmacol. 494, 213-220.

Souza-Fernandes, A.B., Pelosi, P., Rocco, P.R., 2006. Bench-to-bedside review: the role of glycosaminoglycans in respiratory disease. Crit. Care. 10, 237.

Specks, U., Nerlich, A., Colby, T.V., Wiest, I., Timpl, R., 1995. Increased expression of type VI collagen in lung fibrosis. Am. J. Respir. Crit. Care. Med. 151, 1956-1964.

Sporn, M.B., Roberts, A.B., 1992. Transforming growth factor-β: recent progress and new challenges. J. Cell. Biol. 119, 1017-1021.

Starcher, B.C., Kuhn, C., Overton, J.E., 1978. Increased elastin and collagen content in the lungs of hamsters receiving an intratracheal injection of bleomycin. Am. Rev. Respir. Dis. 117, 299-305.

Strieter, R.M., 2002. Con: Inflammatory mechanisms are not a minor component of the pathogenesis of idiopathic pulmonary fibrosis. Am. J. Respir. Crit. Care. Med. 165, 1206-1207; discussion 1207-1208.

Strieter, R.M., Belperio, J.A., Keane, M.P., 2002. CXC chemokines in angiogenesis related to pulmonary fibrosis. Chest. 122, 298S-301S.

Sugihara, T., Martin, C.J., Hildebrandt, J., 1971. Length-tension properties of alveolar wall in man. J. Appl. Physiol. 30, 874-878.

Sugihara, T., Hildebrandt, J., Martin, C.J., 1972. Viscoelastic properties of alveolar wall. J. Appl. Physiol. 33, 93-98.

Suki, B., Varabais, A.L., Lutchen, K.R., 1994. Lung tissue viscoelasticity: a mathematical framework and its molecular basis. J. Appl. Physiol. 76, 2749.2759.

Suki, B., Ito, S., Stamenovic, D., Lutchen, K.R., Ingenito, E.P., 2005. Biomechanics of the lung parenchyma: critical roles of collagen and mechanical forces. J. Appl. Physiol. 98, 1892-1899.

Suki, B., Bates, J.H., 2008. Extracellular matrix mechanics in lung parenchymal diseases. Respir. Physiol. Neurobiol. 163, 33-43.

Suwa, N., Fukasawa, H., Fujimoto, R., Kawakami, M., 1966. Strain and stress of pulmonary tissues. Tohoku. J. Exper. Med. 90, 61-75.

Suzuki, T., Chow, C.W., Downey, G.P., 2008. Role of innate immune cells and their products in lung immunopathology. Int. J. Biochem. Cell. Biol. 40, 1348-1361.

Tai, R.C., Lee, G.C., 1981. Isotropy and homogeneity of lung tissue deformation. J. Biomech. 14, 243-252.

Takehara, K., 2000. Growth regulation of skin fibroblasts. J. Dermatol. Sci. 24, S70-S77.

Tetley, T.D., 1993. New perspectives on basic mechanisms in lung disease. 6. Proteinase imbalance: its role in lung disease. Thorax. 48, 560-565.

Thannickal, V.J., Horowitz, J.C., 2006. Evolving concepts of apoptosis in idiopathic pulmonary fibrosis. Proc. Am. Thorac. Soc. 3, 350-356.

Thomas, P.E., Peters-Golden, M., White, E.S., Thannickal, V.J., Moore, B.B., 2007. PGE(2) inhibition of TGF-beta1-induced myofibroblast differentiation is Smad-independent but involves cell shape and adhesion-dependent signaling. Am. J. Physiol. Lung. Cell. Mol. Physiol. 293, L417-L428.

Thrall, R.S., McCormick, J.R., Jack, R.M., McReynolds, R.A., Ward, P.A., 1979. Bleomycin-induced pulmonary fibrosis in the rat: inhibition by indomethacin. Am. J. Pathol. 95, 117-130.

Thrall, R.S., Scalise, P.J., 1995. Bleomycin. In: ThrallRS, Phan SM, editors. Pulmonary fibrosis. New York: Marcel Dekker Inc. pp. 230–292.

Tomasek, J.J., Gabbiani, G., Hinz, B., Chaponnier, C., Brown, R.A., 2002. Myofibroblasts and mechano-regulation of connective tissue remodelling. Nat. Rev. Mol. Cell. Biol. 3, 349-363.

Tonnesen, M.G., Feng, X., Clark, R.A., 2000. Angiogenesis in wound healing. J. Invest. Dermatol. Symp. Proc. 5, 40-46.

Toti, P., Buonocore, G., Tanganelli, P., Catella, A.M., Palmeri, M.L., Vatti, R., Seemayer, T.A., 1997. Bronchopulmonary dysplasia of the premature baby: an immunohistochemical study. Pediatr. Pulmonol. 24, 22-28.

Tschopp, J., Irmler, M., Thome, M., 1998. Inhibition of fas death signals by FLIPs. Curr. Opin. Immunol. 10, 552-558.

Uchida, Y., Ninomiya, H., Sakamoto, T., Lee, J.Y., Endo, T., Nombra, A., Hasegawa, S., Hirata, F., 1992. ET-1 released histamine from guinea pig pulmonary but not peritoneal mast cells. Biochem. Biophys. Res. Comm. 189, 1196-1201.

Uguccioni, M.L., Pulsatelli, B., Grigolo, A., Facchini, L., Fasano, C., Cinti, M., Fabbri, G., Gasbarrini, Meliconi, R. 1995. Endothelin-1 in idiopathic pulmonary fibrosis. J. Clin. Pathol. 48, 330-334.

Umezawa, H., Maeda, K., Takeuchi, T., Okami, Y., 1966. New antibiotics, bleomycin A and B. J. Antibiot. (Tokyo). 19, 200-209.

Venkatesan, N., Ebihara, T., Roughley, P.J., Ludwig, M.S., 2000. Alterations in large and small proteoglycans in bleomycin-induced pulmonary fibrosis in rats. Am. J. Respir. Crit. Care. Med. 161, 2066-2073.

Verbeken, E.K., Cauberghs, M., Lauweryns, J.M., Van de Woestijne, K.P., 1994. Structure and function in fibrosing alveolitis. J. Appl. Physiol. 76, 731-742.

Visscher, D.W., Myers, J.L., 2006. Histologic spectrum of idiopathic interstitial pneumonias. Proc. Am. Torac. Soc. 3, 322-329.

Waghray, M., Cui, Z., Horowitz, J.C., Subramanian, I.M., Martinez, F.J., Toews, G.B., Thannickal, V.J., 2005. Hydrogen peroxide is a diffusable paracrine signal for the induction of epithelial cell death by activated myofibroblasts. FASEB. J. 19, 854-856.

Wagner, B.A., Buettner, G.R., Oberley, L.W., Darby, C.J., Burns, P.C., 2000. Myeloperoxidase is involved in H2 O2 -induced apoptosis of HL-60 human leukemia cells. J. Biol. Chem. 275, 22461-22469.

Wang, Q., Hyde, D.M., Giri, S.N., 1992. Abatement of bleomycin-induced increases in vascular permeability, inflammatory cell infiltration, and fibrotic lesions in hamster lungs by combined treatment with taurine and niacin. Lab. Invest. 67, 234-242.

Wang, Q., Hyde, D.M., Gotwals, P.J., Giri, S.N., 2002. Effects of delayed treatment with transforming growth factor-beta soluble receptor in a three-dose bleomycin model of lung fibrosis in hamsters. Exp. Lung. Res. 28, 405-417.

Wang, R., Zagariya, A., Ang, E., Ibarra-Sunga, O., Uhal, B.D., 1999, Fas-induced apoptosis of alveolar epithelial cells requires ANG II generation and receptor interaction. Am. J. Physiol. 277, L1245-L1250.

Weibel, E.R., Gil, J., 1977. Structure-function relationships at the alveolar level. In: Bioengineering aspects of the lung, edited by J. B. West. New York: Marcel- Dekker, Inc. p. 1-81.

Westergren-Thorsson, G., Hernnäs, J., Särnstrand, B., Oldberg, A., Heinegård, D., Malmström, A., 1993. Altered expression of small proteoglycans, collagen, and transforming growth factor-beta 1 in developing bleomycin-induced pulmonary fibrosis in rats. J. Clin. Invest. 92, 632-637.

Wilborn, J., Crofford, L.J., Burdick, M.D., Kunkel, S.L., Strieter, R.M., Peters-Golden, M., 1995. Cultured lung fibroblasts isolated from patients with idiopathic pulmonary fibrosis have a diminished capacity to synthesize prostaglandin E2 and to express cyclooxygenase-2. J. Clin. Invest. 95, 1861-1868.

Wild, J.S., Hyde, D.M., Giri, S.N., 1994. Dose and regimen effects of poly ICLC, an interferon inducer, in a multi-dose bleomycin model of interstitial pulmonary fibrosis. Pharmacol. Toxicol. 75, 42-48.

Willis, B.C., du Bois, R.M., Borok, Z., 2006. Epithelial origin of myofibroblasts during fibrosis in the lung. Proc. Am. Thorac. Soc. 3, 377-382.

Wilson, M.S., Wynn, T.A., 2009. Pulmonary fibrosis: pathogenesis, etiology and regulation. Mucosal Immunol. 2, 103-121.

Winkler, M.K., Fowlkes, J.L., 2002. Metalloproteinase and growth factor interactions: do they play a role in pulmonary fibrosis? Am. J. Physiol. Lung. Cell. Mol. Physiol. 283, L1-L11.

Wolf, G., Cristal, R.G., 1997. Biology of pulmonary fibrosis. In: Crystal RG, West JB, Weibel ER & Barnes PJ (ed) The Lung. Scientific foundations. Lippincott-Raven, Philadelphia, pp 2509-2524.

Xaubet, A., Roca-Ferrer, J., Pujols, L., Ramirez, J., Mullol, J., Marin-Arguedas, A., Torrego, A., Gimferrer, J.M., Picado, C., 2004. Cyclooxygenase-2 is up-regulated in lung parenchyma of chronic obstructive pulmonary disease and down-regulated in idiopathic pulmonary fibrosis. Sarcoidosis. Vasc. Diffuse. Lung. Dis. 21, 35-42.

Xu, Y.D., Hua, J., Mui, A., O'Connor, R., Grotendorst, G., Khalil, N., 2003. Release of biologically active TGF-beta1 by alveolar epithelial cells results in pulmonary fibrosis. Am. J. Physiol. Lung. Cell. Mol. Physiol. 285, L527-L539.

Yaguchi, T., Fukuda, Y., Ishizaki, M., Yamanaka, N., 1998. Immunohistochemical and gelatin zymography studies for matrix metalloproteinases in bleomycin-induced pulmonary fibrosis. Pathol. Int. 48, 954-963.

Yamauchi, M., Mechanic, G.L., 1988. Cross-linking of collagen. In Collagen. Vol I. Biochemistry, (Ed. Nimni M. E.), CRC Press, Boca Raton.

Yao, H.W., Zhu, J.P., Zhao, M.H., Lu, Y., 2006. Losartan attenuates bleomycin induced pulmonary fibrosis in rats. Respiration. 73, 236-242.

Ye, Q., Chen, B., Tong, Z., Nakamura, S., Sarria, R., Costabel, U., Guzman, J., 2006. Thalidomide reduces IL-18, IL-8 and TNF-alpha release from alveolar macrophages in interstitial lung disease. Eur. Respir. J. 28, 824-831.

Yi, E.S., Salgado, M., Williams, S., Kim, S.J., Masliah, E., Yin, S., Ulich, T.R., 1998. Keratinocyte growth factor decreases pulmonary oedema, transforming growth factor-beta and platelet-derived growth factor-BB expression, and alveolar type II cell loss in bleomycin-induced lung injury. Inflammation. 22, 315-325.

Yuan, H., Ingenito, E., Suki, B., 1997. Dynamic properties of lung parenchyma: mechanical contributions of fibre network and interstitial cells. J. Appl. Physiol. 83, 1420-1431.

Yuan, H., Kononov, S., Cavalcante, F.S., Lutchen, K.R., Ingenito, E.P., Suki, B., 2000. Effects of collagenase and elastase on the mechanical properties of lung tissue strips. J. Appl. Physiol. 89, 3-14.

Zavadil, J., Bottinger, E.P., 2005. TGF-beta and epithelial-to-mesenchymal transitions. Oncogene. 24, 5764-5774.

Zhang, H.Y., Phan, S.H., 1999. Inhibition of myofibroblast apoptosis by transforming growth factor beta(1). Am. J. Respir. Cell. Mol. Biol. 21, 658-665.

Zhang, K., Gharaee-Kermani, M., Mc Garry, B., Phan, S.H., 1994. In situ hybridization analysis of rat lung alpha 1 (I) and alpha (2) (I) collagen gene expression in pulmonary fibrosis induced by endotracheal bleomycin injection. Lab. Invest. 70, 192-202.

Zhang, K., Flanders, K.C., Phan, S.H., 1995. Cellular localization of transforming growth factor-beta expression in bleomycin-induced pulmonary fibrosis. Am. J. Pathol. 147, 352-361.

Zia, S., Hyde, D.M., Giri, S.N., 1992. Development of a bleomycin hamster model of subchronic lung fibrosis. Pathology. 24, 155-163.

Zuo, F., Kaminski, N., Eugui, E., Allard, J., Yakhini, Z., Ben-Dor, A., Lollini, L., Morris, D., Kim, Y., DeLustro, B., Sheppard, D., Pardo, A., Selman, M., Heller, R.A., 2002. Gene expression analysis reveals matrilysin as a key regulator of pulmonary fibrosis in mice and humans. Proc. Natl. Acad. Sci. USA. 99, 6292-6297.

VIII. ANNEX

Summary of studies retrieved from the literature that used a model of repeated doses of bleomycin

Study reference	Dosage	Animal	Inflammation	Fibrosis
Wang et al. (2002)	3 doses (2.5U, 2.0 U and 1.5 U/4ml/kg) one dose per week. Sacrificed 21 days after the last challenge.	♂ golden Syrian hamsters (120-130 g)	MDAE and macrophages significantly increased. Neutrophils were increased although not significantly.	HP_L significantly increased. Patchy alveolitis and multifocal interstitial fibrosis containing an accumulation of extracellular fibres. They had also thickened interalveolar septa and inflammatory cells in adjacent airspaces.
Iyer et al. (1998)	3 doses (2.5U, 2.0 U and 1.5 U/3.75ml/kg) one dose per week. Sacrificed 28 after the last challenge.	♂ golden Syrian hamsters (90-110 g)	MPO_L, MDAE and SOD significantly increased.	HP_L significantly increased. Multifocal lesions containing an accumulation of extracellular fibres and a cellular infiltrate of predominantly mononuclear cells.
Giri et al. (1997)	3 doses (2.5U, 2.0 U and 1.5 U/4ml/kg) weekly. Sacrificed 30 days after the first challenge.	♂ golden Syrian hamsters (115-130 g)	Neutrophils and MPO_L dramatically increased. MDAE and SOD increased significantly.	HP_L significantly increased. High immunostaining intensity for EDA-fibronectin and collagen type I.

Blaisdell and Giri, (1995)	3 doses (2.5U, 2.0 U and 1.5 U/5ml/kg) one dose per week. Sacrificed 1, 4 and 8 weeks after the third challenge.	♂ golden Syrian hamsters (~ 100-110 g)		HP_L was significantly increased throughout the experiment. The collagenase activity (Type I) was significantly increased at week 1 and 4. At week 8, the activity between control and BLM groups were similar.
Blaisdell et al. (1994)	3 doses (2.5U, 2.0 U and 1.5 U/5ml/kg) one dose per week. Sacrificed 1, 4 and 8 weeks after the third challenge.	♂ golden Syrian hamsters (~ 110 g)		HP_L was significantly increased throughout the experiment. DHLNL content pero mole of lung collagen was only significantly increased at 4 weeks. OHP content per mole of lung collagen was only significantly increased at 8 weeks.
Wild et al. (1994)	3 doses (2.5U, 2.0 U and 1.5 U/5ml/kg) one dose per week. Sacrificed 20 days after the third challenge.	♂ golden Syrian hamsters	SOD significantly increased. MDAE significantly increased.	HP_L significantly increased.

O'Neill et al. (1992)	3 doses (2.5U, 2.0 U and 1.5 U/5ml/kg) one dose per week. Sacrificed at 7, 14 and 20 days after the third challenge.	♂ golden Syrian hamsters (90-110g)	SOD was maximal at day 20. Neutrophils were elevated at all time points being maximal at day 7.	HP_L was maximal at day 20
Wang et al. (1992)	3 doses (2.5U, 2.0 U and 1.5 U/5ml/kg) one dose per week. Sacrificed 20 days after the third challenge.	♂ golden Syrian hamsters	Patchy alveolitis observed. Had thickened interalveolar septa and inflammatory cells in adjacent airspaces. Neutrophils were significantly increased at day 20.	In ½ of the hamsters, foci of fibrotic consolidation were observed. In diffuse lesions, alveolar airspaces were often obliterated by highly organised connective tissue. These fibrotic regions contained abundant fibroblasts, and numerous inflammatory cells (mononuclear phagocytes and neutrophils) and were usually adjacent to necrotic epithelial cells.
Zia et al. (1992)	3 doses (2.5U, 2.0 U and 1.5 U/5ml/kg) one dose per week. Sacrificed at periods up to	♂ golden Syrian hamsters (80-100g)	The increase of macrophages occurred at 20, 30 and 60 days. The total number of neutrophils was higher than	Induced a moderate level of lung fibrosis. HP_L was maximal 30 days after the third dose and remained elevated throughout the experiment.

	periods up to 90 days.		was higher than controls at all time points but was significant only at 10 days.	the experiment. Collagen was found to be more diffuse and more intense at 20 and 30 days than at later times.
Brown et al. (1983)	0.5U/animal with a dose volume of 0.5ml/animal. Single, 2, 3, 4 doses a week apart. Sacrificed at periods up to 90 days.	♂ Porton Wistar-derived rats (200-250 g)	Single, 2 and 3 doses: maximal increase in PMN leucocytes and macrophages at day 14 receding at day 30. 4 doses: lymphocitic infiltration increased throughout the experiment.	Pulmonary fibrosis was mainly interstitial in distribution. Single dose: interstitial fibrosis was maximal at day 14 and decreased thereafter. 3-4 doses: severity of fibrosis was increased throughout the experiment.

Abbreviations: BLM: bleomycin; MPO: myeloperoxidase; HP: hydroxyproline; SOD: superoxide dismutase activity was measured as an indirect indicator of oxygen free radical production); MDAE: malonilaldehyde measured as an index if lipid peroxidation; DHLNL: dihydroxylysinoroleucine is the spontaneously reversibly formed product of the spontaneous Schiff base reaction between hydroxyallysine and hydroxylisine; OHP: hydroxypyridinium is a mature stable cross-link in the lung covalently binding three molecules of collagen together.